

Doctoral Thesis

**Molecular studies on the formation of silica layer in
bacterial spores and its application**

〔細菌孢子におけるシリカ層の形成に関する分子生物学的研
究とその応用〕

Mohamed Abdeltawab Abdallah Abdelhamid

Graduate School of Advanced Sciences of Matter

Hiroshima University

March 2016

Table of Contents

1. Main Thesis

Molecular studies on the formation of silica layer in bacterial spores and its application

(細菌孢子におけるシリカ層の形成に関する分子生物学的研究とその応用)

2. Articles

- 1) The C-terminal zwitterionic sequence of CotB1 is essential for biosilicification of the *Bacillus cereus* spore coat

Kei Motomura, Takeshi Ikeda, Satoshi Matsuyama, Mohamed A. A. Abdelhamid, Tatsuya Tanaka, Takenori Ishida, Ryuichi Hirota, and Akio Kuroda

Journal of Bacteriology, 198: 276-282 (2016).

- 2) Affinity purification of recombinant proteins using a novel silica-binding peptide as a fusion tag

Mohamed A. A. Abdelhamid, Kei Motomura, Takeshi Ikeda, Takenori Ishida, Ryuichi Hirota, and Akio Kuroda

Applied Microbiology and Biotechnology, 98:5677-5684 (2014).

Main Thesis

Contents	Page
Chapter 1. General introduction	
1.1 Introduction.....	2
1.2 Biosilicification in eukaryotes.....	3
1.3 Biosilicification in prokaryotes.....	5
1.4 Biotechnological applications of silica-precipitating proteins/peptides.....	7
1.5 Research purpose of this thesis.....	9
Chapter 2. Biosilicification of <i>Bacillus cereus</i> spore coat	
2.1 Introduction.....	12
2.2 Materials and Methods	
2.2.1 In silico screening for silica-forming proteins.....	13
2.2.2 Bacterial strains and growth conditions.....	13
2.2.3 Mutant construction.....	14
2.2.4 Extraction of spore coat proteins.....	18
2.2.5 Silicate uptake assay.....	18
2.2.6 Acid resistance assay.....	19
2.2.7 Plasmid construction and transformation.....	19
2.2.8 Microscopy.....	21
2.3 Results and Discussion	
2.3.1 Silacidin-like sequence in the C-terminal of CotB1.....	22
2.3.2 CotB1 is involved in the biosilicification of <i>B. cereus</i> spores.....	25
2.3.3 A C-terminal zwitterionic sequence is essential for biosilicification	31
2.3.4 Expression and localization of CotB1.....	33
2.3.5 CotB1 may be the founding member of a subset of prokaryotic proteins that stimulate biosilicification.....	37
Chapter 3. Affinity purification of recombinant proteins using a novel silica-binding peptide as a fusion tag	
3.1 Introduction.....	41
3.2 Materials and Methods	
3.2.1 Materials.....	43
3.2.2 Construction of expression plasmids for green fluorescent protein GFP-CotB1 and GFP-CotB1p fusions.....	43
3.2.3 Expression and purification of GFP-CotB1 and GFP-CotB1p.....	45
3.2.4 Determination of the dissociation constant (K_d) values for GFP-	

	CotB1 and GFP-CotB1p.....	46
3.2.5	Construction of expression plasmids for CotB1-SUMO-mCherry (CotB1-SC) and CotB1p-SUMO-mCherry (CotB1p-SC) fusions...	47
3.2.6	Expression of CotB1-SC and CotB1p-SC.....	51
3.2.7	Optimization of silica-binding conditions.....	51
3.2.8	Affinity purification of mCherry using CotB1/CotB1p as a silica-binding tag.....	52
3.2.9	Nucleotide sequence data.....	53
3.3	Results and Discussion	
3.3.1	Binding of GFP-CotB1 and GFP-CotB1p to silica particles.....	54
3.3.2	Optimization of silica-binding conditions.....	57
3.3.3	Affinity purification of mCherry using CotB1/CotB1p as a silica-binding tag.....	60
3.3.4	Discussion.....	65
Chapter 4. Application of volcanic ash particles for protein affinity purification with a minimized silica-binding tag		
4.1	Introduction.....	70
4.2	Materials and Methods	
4.2.1	Materials.....	72
4.2.2	Construction of expression plasmids.....	72
4.2.3	Expression of recombinant proteins.....	75
4.2.4	Silica-binding assay of recombinant proteins.....	75
4.2.5	Affinity purification of SB7-tagged proteins using silica or Shirasu particles as the adsorbent.....	76
4.2.6	Protein assay.....	77
4.3	Results and Discussion	
4.3.1	Minimization of the silica-binding CotB1p tag.....	78
4.3.2	Alanine scanning mutagenesis of the SB7 peptide.....	80
4.3.3	L-Arginine as an efficient eluent for silica-bound SB7 tag.....	80
4.3.4	Affinity purification of SB7-tagged proteins by using natural silica-containing particles as an adsorbent.....	83
4.3.5	Discussion.....	91
Chapter 5. General conclusion.....		
		95

References	100
Acknowledgments	115

Chapter 1

General introduction

1.1 Introduction

Silicon, the second most abundant element in the Earth's crust, is an important mineral for living organisms. It is also the basic raw material for semiconductors and many advanced materials. In several eukaryotes such as diatoms, radiolarians, siliceous sponges and higher plants (*e.g.* horsetail and rice), silicon is taken up as silicic acid, then deposited as biogenic silica through natural process, named biosilicification (1). The molecular mechanisms underlying eukaryotic biosilicification, as well as the genes and proteins responsible for transport/accumulation of silicon, have been intensively investigated. The biosilica nanoparticles are produced under milder conditions (pH, temperature and pressure) than synthetic ones. Those particles have been used in numerous biotechnological applications that include biocatalysis, drug delivery, biosensors, and hybrid materials (2). Recently, Hirota et al. demonstrated that a *Bacillus cereus* group and its close relatives accumulate silica in and around a spore coat layer and that the silica-containing layer enhances acid resistance of the spores (3). Another group identified an extracellular protein of a thermophilic bacterium involved in silica-scale formation (4). However, the molecular mechanisms of biosilicification in prokaryotes are still obscure. Understanding the molecular mechanisms and discovering the genes and proteins that control the biosilicification process in prokaryotes will not only provide a novel fundamental knowledge about this process, but could also widen biotechnological

applications of silica materials. Therefore, in the work described in this thesis, the first insights of the fundamental basis of the biosilicification process in prokaryotes have been studied.

In this chapter, the author provides a brief overview of the molecular mechanisms of eukaryotic biosilicification, followed by a discussion of biosilification in prokaryotes. Finally, the objectives of this thesis will be addressed.

1.2 Biosilicification in eukaryotes

Silicon (Si) acts as the main component of structural skeletons of diatoms, radiolaria, and siliceous sponges (1). It is also utilized by some plants (e.g., rice and cucumber) to protect against biotic and abiotic stresses (5). In Si-accumulating organisms, Si is taken up from the environment as soluble silicate ($\text{Si}[\text{OH}]_4$), a biologically available form of Si in nature, which is then polymerized and accumulated as insoluble silica (SiO_2). Such silica biomineralization (biosilicification) in eukaryotes is under genetic control, which in turn implies the existence of specific gene products guiding biosilicification.

The best-known example of biosilicification occurs in diatoms, which are eukaryotic unicellular algae that possess silica walls with species-specific micro- and nano-patternings (6). To date, several peptides and proteins involved in diatom

biosilicification have been identified, including silaffins, silacidins, and silaffin-like cingulins (7-9). The silaffins are short peptides that undergo extensive post-translational modifications such as phosphorylation and polyamine conjugation. Due to a zwitterionic character imparted by negative charges of the phosphate groups and positive charges of the polyamines, silaffins easily self-assemble into supramolecular aggregates, which serve as templates for silica formation (7, 10-12). The negatively charged silacidin peptides also form supramolecular aggregates with positively charged long-chain polyamines, and act as templates for silica formation (8, 13). These facts indicate the importance of combining positive and negative charges in order to direct biosilicification.

1.3 Biosilicification in prokaryotes

The presence of Si in bacterial spores was first noted several decades ago (14, 15). Until recently, however, there have been no reports on the precise localization of Si and its biological function in prokaryotes. Recently, Hirota et al. reported that some bacterial isolates take up silicon when cultivated in a nutrient medium supplemented with silicate and accumulate it in and around their spore coat layer (Fig. 1.1) (3). Those isolates belong to *Bacillus cereus* group, a very homogenous cluster of six species, *B. cereus*, *B. thuringiensis*, *B. anthracis*, *B. mycoides*, *B. pseudomycoides*, and *B. weihenstephanesis*. The strain with the highest silicon uptake was designated as *Bacillus cereus* YH64. Moreover, it was observed that silicon uptake occurs during the sporulation phase. As the bacterial mother cells take up the silicate from the medium, the silica layer formed within the spore coat. Furthermore, it was determined that the silica layer formation enhances the acid resistance of the bacterial spores.

These findings were the first insights about silicon uptake by prokaryotes. However, the mechanisms of silicate uptake and silica layer formation in the bacteria and their physiological functions are not sufficiently understood. Moreover, no proteins or peptides involved in prokaryotic biosilicification have been identified thus far.

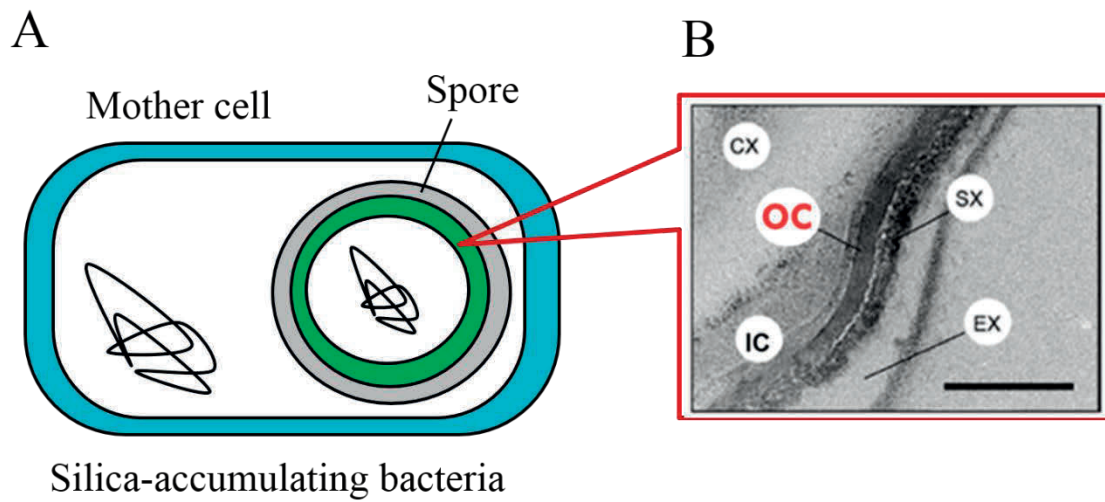


Fig. 1.1 Silica layer formation in spore coat of *B. cereus*. A. Schematic illustration of silica-precipitating bacteria. B. TEM image of Silica localization in the *B. cereus* spore coat. Scale bar, 100 nm. CX, cortex; IC, inner coat; OC, outer coat; EX, exosporium; SX, silica layer. Silica is deposited in OC and SX layers. Adapted from research originally published in Reference 3, copyright ©American Society for Microbiology.

1.4 Biotechnological applications of silica-precipitating proteins/peptides

Silica particles are attractive support materials for protein purification and immobilization due to their wide range of well-defined surface areas, particle sizes and pore sizes as well as their commercial availability at low cost. Silaffins, the well-characterized silica-precipitating peptides, have been used for biotechnological applications (e.g. enzyme immobilization on silica surfaces for biocatalysis and biosensors applications) (16). These peptides are rich in serine and positively charged (arginine and lysine) residues which enable them to interact with negatively charged silica surfaces. Recently, several proteins and peptides sharing the main features of silaffins have been used as silica-binding proteins/peptides for protein immobilization and purification using silica particles as an adsorbent. An example of silica-binding tag is bacterial ribosomal protein L2 (also known as Si-tag; 273 amino acids) (17, 18). Si-tag has been utilized for an affinity purification method with inexpensive commercial silica (SiO_2) particles serving as the specific adsorbent (19, 20). The purity and yield achieved with this method are comparable to conventional affinity purification methods (21) while the cost is lower (20). Si-tag affinity purification can be used even under denaturing conditions (i.e., 8 M urea), enabling purification of inclusion body proteins (19). However, the large size of the Si-tag (273 amino acids [aa]) and high concentration of divalent

cations (e.g., 2 M MgCl₂) required to elute Si-tagged fusion proteins may negatively affect the intrinsic properties and function of the fusion partner. Another potential disadvantage of the large protein affinity tag is that it wastes more metabolic energy during overproduction than do small tags (22, 23). These drawbacks motivated the author to develop an improved silica-based affinity purification method utilizing shorter silica-binding tags and milder elution conditions.

1.5 Research purpose of this thesis

Although the mechanisms underlying eukaryotic biosilicification have been intensively investigated, prokaryotic biosilicification has not been studied until recently. Previously, Hirota et al. demonstrated that biosilicification occurs in *Bacillus cereus* and its close relatives and the accumulated silica is deposited in and around a spore coat layer as a protective coating against acid. Therefore, building upon this research, the author seeks to address the following objectives:

- Identifying and characterizing protein (s) involved in prokaryotic biosilicification.
- Harnessing this fundamental knowledge for biotechnological applications such as engineering silica-binding peptides for protein immobilization and purification.

The first topic is discussed in Chapter 2. The author discovered the role of *B. cereus* spore coat protein CotB1 and its C-terminal zwitterionic sequence in silica biomineralization. This is the first report of a prokaryotic protein involved in biosilicification.

The second topic is discussed in Chapter 3. A novel silica-binding tags have been engineered for silica-based protein purification. The developed silica-based affinity method enables purification of tagless proteins with high purity and yield. This method is also useful for therapeutic applications as it enables removal of the affinity tag, producing

native recombinant proteins.

In Chapter 4, the author described a newly developed method utilizing an even shorter silica-binding tag and mild elution conditions for silica-based affinity purification.

Furthermore, the binding mechanism of silica-binding tag has been determined.

Finally, Chapter 5 provides a summary of the results and discusses the implications of this work.

Chapter 2

Biosilicification of *Bacillus cereus* spore coat

2.1 Introduction

Biosilicification in prokaryotes is poorly understood. Previously, it was demonstrated that *Bacillus cereus* isolates take up silicate during spore formation and form silica layer on and around their spores (3). Furthermore, the formation of silica layer was associated with the increased acid resistance of *Bacillus* spores (3). Spores of *Bacillus* species are highly resilient dormant cell types that can withstand extremes of temperature, radiation, and chemical assault (24). These spore properties are attributable to the physical and chemical composition of the structures that encase the spore (25, 26). The outermost portion of *Bacillus* spores consists of cortex, spore coat, and, in some species, exosporium. The spore coat, where silica is deposited in *B. cereus*, is composed of more than 50 proteins (27). Silica accumulation in and around the *B. cereus* spore coat strongly suggests that spore coat proteins play an important role in biosilicification. Here the author reports that one of the spore coat proteins, CotB1, carries a negatively charged silacidin-like sequence on its C-terminus, followed by a positively charged arginine-rich sequence. The author demonstrates that the zwitterionic C-terminus of CotB1 plays an essential role in prokaryotic biosilicification.

2.2 Materials and Methods

2.2.1 In silico screening for silica-forming proteins

A database of *B. cereus* spore coat protein sequences (as reported by Henriques *et al.* [27]) was constructed with the sequences obtained from the NCBI website (<http://www.ncbi.nlm.nih.gov/>). Previously characterized silica-forming peptides (silaffin-1A₁, -1A₂, and -1B of *Cylindrotheca fusiformis* [7, 28] and silacidin A, B, and C of *Thalassiosira pseudonana* [9]) were used as query sequences. Searching for spore coat proteins with significant similarity to the silica-forming peptides was conducted using the BLAST program obtained from the NCBI FTP server (<ftp://ftp.ncbi.nih.gov/blast/>) with an E-value of 10 as a threshold.

2.2.2 Bacterial strains and growth conditions

B. cereus strain NBRC 15305, which corresponds to strain ATCC 14579 (29), was obtained from the NITE Biological Resource Center (NBRC; Chiba, Japan) and used as the wild-type strain in this study. The wild-type and mutant strains of *B. cereus* were routinely grown at 28°C in LB medium (30). Sporulation was induced at 28°C by nutrient exhaustion in mR2A medium (an R2A medium [31] supplemented with 0.6 mM CaCl₂, 0.03 mM MnCl₂, 0.05 mM ZnCl₂, and 0.05 mM FeSO₄). The author notes that the

concentrations of CaCl₂ and MnCl₂ in the medium are three times higher compared to the previous report (3) in order to induce efficient sporulation for *B. cereus*. Spore development was monitored by bright-field microscopy, and the timing of entry into sporulation was defined as the end of the exponential growth phase (32). *Escherichia coli* JM109 was used as a host for cloning and was grown at 37°C in 2× YT medium (30). When necessary, spectinomycin (250 µg ml⁻¹ for *B. cereus*), erythromycin (10 µg ml⁻¹ for *B. cereus*), and carbenicillin (50 µg ml⁻¹ for *E. coli*) were added to the medium.

2.2.3 Mutant construction

The *cotB1B2* deletion mutant was constructed by using the allelic replacement method described by Arnaud *et al.* (33). DNA fragments (approximately 1 kb each) corresponding to the up- and downstream regions of *cotB1B2* were amplified from the chromosomal DNA of *B. cereus* using the primer pairs cotB1-F1/cotB1-R1 and cotB2-F1/cotB2-R1 (nucleotide sequences are given in Table 2.1), and then treated with *Bg/II* and *SalI*, respectively. A spectinomycin resistance (Sp^r) cassette was amplified from pIC333 (34) with the primers spc-F1 and spc-R1 and was digested with *Bg/II* and *SalI*. These three fragments were ligated by T4 DNA ligase, and the resultant fragment was amplified by PCR with primers cotB1-F1 and cotB2-R1. The PCR fragment was digested

Table 2.1. Plasmids used in this study

Primer	Sequence (5' to 3') ^a
Mutant construction	
spc-F1	GGAGATCTGTATAATAAAGAATAATTATTAATC
spc-R1	ATTGGTCGACTAAATTAAGTAATAAAGCGTTCTC
cotB1-F1	ACGGACGCGTTTTGTAAGATGACCTTG
cotB1-R1	AAAGATCTGAGAAAACCCCTTCCATTAA
cotB2-F1	AGATGTCGACTGTTTAATAAATAAGAGGGGCATT
cotB2-R1	TATAACGCGTITAGCTCGTACACAATGTTTATAAG
cotG-F1	ATCTACGCGTTAACGTATTATACCCTTGAATGCG
cotG-R1	CGAGATCTAGAAATCCTCCTTATCATGTATTAAG
cotG-F2	TAACGTCGACTTTTTATAACCCAAAAAAGGC
cotG-R2	AATTACGCGTAATGGCCCAATCACATTAGTTG
Mutant screening	
spc-F2	GTGATGATAAGTGGGAAGGACTAT
spc-R2	TTGCTCATGATTCACCTCGTTG
cotB1-F2	AAATGGCATATTTAGTATAGAAGCAATATACTGTT
cotB2-R2	TAATTGATAACGAATTCGGAAACTGCTC
cotG-F3	TCGGCCTCATAAACGAAACTGTGAA
cotG-R3	TAAGCGAATGAGTTCTGCACCAGAA
Plasmid construction	
cotB1-F3	GCGAGAGGATCCAAAGACGAAGATTAAACTA
cotB2-R3	TCAGGTGAATTCATATCCTCCTTCCCTACGAA
cotB1-F4	TTATCTTCTCTACTTGATTGTC
cotB1-R2	TGTTTAATAAATAAGAGGGGCAT
cotB2-F2	GAGAAAACCCCTTCCATTAATTT
cotB2-R4	TTGGAGAATGTATTATGCTGTGA
cotB1-F5	TGCTAAAGCATTATAGTTAACACTTTTAA
cotB1-R3	TAATGTTTAATAAATAAGAGGGGC
cotB1-F6	ATTATCGCTACTTTCCTTACTATCG
cotB1-R4	TCAGGTCGTGCTCGTGCAAA
cotB1-R5	AGTTTATTTTATTGTGATTTTTTGAAAGAC
gfp-F1 ^b	ATGAGTAAAGGAGAAGAAGACTTTTCAC
gfp-R1 ^b	TTTGTAGAGCTCATCCATGCCATG
gfp-R2 ^b	TTATTTGTAGAGCTCATCCATGCCA

^a Underlined sequences indicate restriction sites.

^b These primers were phosphorylated at the 5' end.

with *Mlu*I and inserted into the *Mlu*I site of the pMAD vector (33), which was obtained from the Pasteur Institute (Paris, France), yielding pMAD Δ *cotB1B2* (Table 2.2). The plasmid was then introduced into the *B. cereus* wild-type strain by electroporation (35), and the transformants were selected at 30°C on LB agar plates with 250 μ g ml⁻¹ spectinomycin and 50 μ g ml⁻¹ X-Gal. Integration and excision of pMAD Δ *cotB1B2* were performed as described by Arnaud *et al.* (33) with slight modifications: the double-crossover deletion mutants were screened by blue/white screening on LB agar plates without spectinomycin, because they showed unexpectedly low spectinomycin resistance when the Sp^r cassette was inserted into the *cotB1B2* locus. The insufficient resistance can be ascribed to the incomplete promoter sequence of the Sp^r cassette (36) and the upstream *cotB1B2* promoter, which is not active in vegetative cells (see Results and Discussion). These weak promoters could not support sufficient expression of the Sp^r cassette, although the cassette works appropriately when inserted into the *tetB* locus of the wild-type strain (33). Disruption of *cotB1B2* was confirmed by PCR amplification with the primer pairs cotB1-F2/spc-R2 and cotB2-R2/spc-F2.

The *cotG* deletion mutant was constructed in a similar way by replacing the primers cotB1-F1, cotB1-R1, cotB2-F1, and cotB2-R1 with cotG-F1, cotG-R1, cotG-F2, and cotG-R2, respectively, to yield pMAD Δ *cotG*. Disruption of *cotG* was confirmed by

Table 2.2 Plasmids used in this study

Plasmid	Description	Source or reference
pIC333	Source of an Sp ^r cassette	(34)
pMAD	Thermosensitive shuttle vector for allelic replacement; Amp ^r in <i>E. coli</i> , Em ^r in <i>B. cereus</i>	(33)
pMAD Δ <i>cotB1B2</i>	pMAD carrying up- and downstream regions of <i>cotB1B2</i> with an inserted Sp ^r cassette	This study
pMAD Δ <i>cotG</i>	pMAD carrying up- and downstream regions of <i>cotG</i> with an inserted Sp ^r cassette	This study
pHT304	Shuttle vector; Amp ^r in <i>E. coli</i> , Em ^r in <i>B. cereus</i>	(39)
pHT-cotB1B2	pHT304 carrying <i>cotB1</i> and <i>cotB2</i> with the promoter region of <i>cotB1B2</i>	This study
pHT-cotB1	pHT304 carrying <i>cotB1</i> with the promoter region of <i>cotB1B2</i>	This study
pHT-cotB2	pHT304 carrying <i>cotB2</i> with the promoter region of <i>cotB1B2</i>	This study
pHT-cotB1-141	pHT-cotB1 lacking silacidin-like and arginine-rich sequences	This study
pHT-cotB1-157	pHT-cotB1 lacking arginine-rich sequence	This study
pHT-cotB1-142/157	pHT-cotB1 lacking silacidin-like sequence	This study
pGFPuv	Source of <i>gfp</i> gene	Clontech Laboratories
pHT-gfp-cotB1	pHT304 carrying <i>gfp</i> -fused <i>cotB1</i>	This study
pHT-gfp	pHT304 carrying <i>gfp</i>	This study

Amp^r, ampicillin resistance; Em^r erythromycin resistance; Sp^r, spectinomycin resistance

PCR amplification with the primer pairs cotG-F3/spc-R2 and cotG-R3/spc-F2.

2.2.4 Extraction of spore coat proteins

Spores were prepared by growing *B. cereus* strains in mR2A medium supplemented with 100 $\mu\text{g ml}^{-1}$ silicate at 28°C for 48 h, and were harvested by centrifugation. The pellets were sonicated in buffer containing 25 mM Tris-HCl (pH 7.5), 1 mM EDTA, 15% glycerol, 0.1 M NaCl and protease inhibitor cocktail (Nacalai Tesque, Kyoto, Japan) to disrupt residual mother cells, and then the spores were separated from the suspension by centrifugation as reported by Isticato *et al.* (37). Spore coat proteins were extracted from the spores with SDS gel-loading buffer (30) containing 50 mM Tris-HCl (pH 6.8), 100 mM dithiothreitol, 10% glycerol, 2% SDS and 0.1% bromophenol blue at 100°C for 10 min. The extracts were immediately fractionated on 12.5% Bis-Tris SDS-PAGE gels with MOPS running buffer (38), and stained with Coomassie brilliant blue R-250.

2.2.5 Silicate uptake assay

B. cereus cells grown overnight with shaking at 28°C in R2A medium were inoculated (5%) into mR2A medium supplemented with 100 $\mu\text{g ml}^{-1}$ silicate. The cultures

were incubated at 28°C with shaking. Samples taken from the cultures at 12-h intervals were centrifuged, and then the silicate concentrations in the supernatants were measured by using a Silicate Test kit (Merck, Darmstadt, Germany) according to the manufacturer's instructions.

2.2.6 Acid resistance assay

Sporulation of *B. cereus* strains was induced in mR2A medium with or without 100 µg ml⁻¹ silicate as described above. After keeping the cultures standing at 4°C for 12 h, the spores were collected by centrifugation at 8,100 × g for 10 min and washed twice with cold sterile distilled water. The purified spores were suspended in distilled water to an optical density of 1.0 at 600 nm. Spores were centrifuged and resuspended in equal volumes of 0.2 N HCl. At the designated times, samples were diluted with cold water and spread on R2A agar plates. Spore viability was determined by counting the colonies after a 24-h incubation at 28°C.

2.2.7 Plasmid construction and transformation

For complementation tests, a DNA fragment containing the *cotBIB2* genes with their putative promoter and terminator regions was amplified by PCR from the

chromosomal DNA of *B. cereus* using the primer pair of cotB1-F3 and cotB2-R3 (Table 2.1). The PCR fragment was digested with *Bam*HI and *Eco*RI and then inserted into the same sites of plasmid pHT304 (39), yielding pHT-cotB1B2. The plasmids carrying either *cotB1* or *cotB2* gene were amplified by inverse PCR using pHT-cotB1B2 as a template with the primer pairs of cotB1-F4/cotB1-R2 and cotB2-F2/cotB2-R4, respectively. The amplified DNA fragments were self-ligated to yield pHT-cotB1 and pHT-cotB2, respectively. To construct the plasmids carrying truncated mutants of *cotB1*, another round of inverse PCR was performed using pHT-cotB1 as a template with the primer pairs of cotB1-F5/cotB1-R3, cotB1-F6/cotB1-R3, and cotB1-F6/cotB1-R4. The amplified DNA fragments were self-ligated to yield pHT-cotB1-141, pHT-cotB1-157, and pHT-cotB1-142/157, respectively. These plasmids were introduced into the Δ *cotB1B2* strain by electroporation as described above, and then the transformants were selected at 28°C on LB agar plates with 10 μ g ml⁻¹ erythromycin. To construct a plasmid expressing green fluorescent protein (GFP)-fused CotB1 under the control of the promoter of *cotB1B2*, the vector backbone was amplified by inverse PCR using pHT-cotB1 as a template with the primer pair of cotB2-F2 and cotB1-R5. A GFP-encoding DNA fragment was amplified by PCR from pGFPuv (Clontech Laboratories, Mountain View, CA) using the phosphorylated primers gfp-F1 and gfp-R1. These PCR products were ligated by T4 DNA

ligase, yielding pHT-gfp-cotB1. As a control, plasmid pHT-gfp, which expresses GFP under the control of the promoter of *cotB1B2*, was prepared by the same procedures using the primer pairs cotB2-F2/cotB1-R2 and gfp-F1/gfp-R2. These plasmids were introduced into the wild-type strain by electroporation as described above.

2.2.8 Microscopy

Sporulating cells and spores grown in mR2A medium supplemented with silicate were harvested at various time points and observed under a BX51 fluorescence microscope equipped with an UPlanApo 100×/1.35 objective lens and a U-MNIBA3 filter (Olympus, Tokyo, Japan). Images were captured using a DP72 cooled charge-coupled device camera (Olympus). For transmission electron microscopy (TEM), spores were prepared without silicate as described above. Ultrathin sections of the spores were prepared and stained as described previously except that spores were initially fixed with 2.5% glutaraldehyde in 0.1 M cacodylate buffer (pH 7.2) containing 0.1% MgSO₄ for 4 h at 4°C followed by postfixation with 1% OsO₄ in 0.2 M cacodylate buffer (pH 7.2) for 10 h at 4°C. The ultrathin sections were observed under a JEM-1400 transmission electron microscope (JEOL, Tokyo, Japan) operating at an accelerating voltage of 80 kV.

2.3 Results and Discussion

2.3.1 Silacidin-like sequence in the C-terminal region of CotB1

To identify the proteins involved in the biosilicification of *B. cereus* spores, the author performed a local BLAST search of spore coat proteins using sequences of previously characterized silica-forming peptides (diatom silaffins and silacidins) as queries. Among the 53 spore coat proteins that have been identified in *B. cereus* to date (37), a C-terminal region of CotB1 (GenBank accession number AAP07429.1) showed significant similarity to silacidin A (50% identity over 16 amino acids, E-value 8.5) (Fig. 2.1, boxed). Silacidin A is a highly acidic peptide of 28 amino acids that is isolated from cell walls of the diatom *T. pseudonana* (9). Interestingly, a gene encoding a CotB1 paralog, namely CotB2 (GenBank accession number AAP07430.1), is located in tandem downstream of the *cotB1* gene on the *B. cereus* genome. The *cotB1* and *cotB2* genes are separated by only 20 bp. The *cotB1* gene is preceded by a putative σ^K promoter (40), which is activated in the mother cell during the late stage of sporulation, whereas no canonical promoter sequence is found in the 500 bp sequence preceding the *cotB2* open reading frame (Fig. 2.2). These facts imply that the *cotB1* and *cotB2* genes are present in a single transcriptional unit.

A

```

CotB1  1  -MSLFHCDFLKDLIGSFVRVNRGGPESQKGTIISVCQDYFVLKNEKGELYYYQLKHLKSI 59
CotB2  1  MENVLCDDQIKCLVGETVKVNLRGPERVVELVSLGKDYLLTQLPHGELVYYQLKHVKSL 60

CotB1  60  TKNKECGSSDCEWEDCACAED-FEALLESFKYCWVKINRGGPEKVEGILQDVSCDFVTL 118
CotB2  61  VKKVKESKCGDCYSSCFCSDEDTFLDILKDLKYKWKINRGGPECVEGLLSEVHHGCITL 120

CotB1  119  IVKEEITLLIAIKHIKSVNYNALACGESDESDDSKESSDNSGRARAQRQSSRGR 171
CotB2  121  VNGDEVLYVIKSHIKSVSQVVKCKKNEDE----- 149

```

B

```

                                     Silacidin-like   Arginine-rich
                                     ┌───────────┬───────────┐
CotB1      137  YNALACGESDESDDSKESSDNSGRARAQRQSSRGR 171
Silacidin A   1  SSSEDSGDSPPSDESEEESEDSVSSEDED----- 28
Silaffin-1A1                SSKKSGSYSGSKGSK

```

Fig. 2.1 Pairwise alignment of *B. cereus* CotB1 and CotB2 and primary structure of *T. pseudonana* silacidin A. Alignments of CotB1 with CotB2 (A) and with silacidin A (B) were performed using the ClustalW program at GenomeNet (<http://www.genome.jp/>) with default parameters. Black-shaded and grey-shaded amino acid residues indicate identity and similarity, respectively. The boxed sequence of CotB1 (CGESDESDDSKESSDN) was identified by a local BLAST search for sequences with significant similarity to silacidin A (SGDSPPSDESEEESEDS). The underlined sequence indicates the arginine-rich region of CotB1. The amino acid sequence of *C. fusiformis* silaffin-1A₁ is given for comparison. Reprinted with permission from “The C-Terminal Zwitterionic Sequence of CotB1 Is Essential for Biosilicification of the *Bacillus cereus* Spore Coat”, Kei Motomura, Takeshi Ikeda, Satoshi Matsuyama, Mohamed A. A. Abdelhamid, Tatsuya Tanaka, Takenori Ishida, Ryuichi Hirota, and Akio Kuroda. *Journal of Bacteriology*, 198: 276-282 (2016), copyright © American Society for Microbiology.

```

1   GTAGTCTACCATGTTAAAAGCATATTTTTTCTAGCTAGGACAAACATAGAGAACGTAAC 60
61  CTGTACAGATACATATACTATCAGTGCAAAAAGCTTATAAATTAATGGAAGGGGTTTTCTC 120
    cotB1
121 GTGGAGTTTATTTTCATTGTGATTTTTTGAAGACTTAATTGGATCTTTTGTGAGAGTAAAC 180
    M S L F H C D F L K D L I G S F V R V N
181  AGGGGTGGTCCAGAATCTCAAAAAGGAACAATAATATCAGTATGTCAGGACTACTTCGTA 240
    R G G P E S Q K G T I I S V C Q D Y F V
241  TTGAAGAATGAAAAGGTGAGCTTTATTACTATCAACTTAAACATCTAAAAAGTATTACA 300
    L K N E K G E L Y Y Y Q L K H L K S I T
301  AAAAATGCGAAAGAATGTGGATCAAGTGATTTGTGAGTGGGAAGATTGCGCCTGTGCAGAA 360
    K N A K E C G S S D C E W E D C A C A E
361  GATTTGAAGCACTACTTGAAGTTTCAAATATTGCTGGGTGAAAATTAATCGCGGGCGGT 420
    D F E A L L E S F K Y C W V K I N R G G
421  CCAGAGAAAGTGGAAAGGCATTTTGCAAGATGTTTCTTGTGACTTCGTAACATTAATCGTA 480
    P E K V E G I L Q D V S C D F V T L I V
481  AAAGAAGAAATTATATTAATTGCAATAAAGCATATTAAGAAGTGTAACTATAATGCTTTA 540
    K E E I I L I A I K H I K S V N Y N A L
541  GCATGCGGAGAGAGTGTATGAGAGCGACGATAGTAAGGAAAGTAGCGATAATTGAGTCTGT 600
    A C G E S D E S D D S K E S S D N S G R
601  GCTCGTGCACAAAGACAATCAAGTAGAGGAAGATAATAAGAAAGGGGATACGAAATTTGG 660
    A R A Q R Q S S R G R *
    cotB2
    M E
661  AGAATGTATTATGCTGTGACCAAATTAATGTTTAGTTGGTGAGACTGTAAAAGTAAACC 720
    N V L C C D Q I K C L V G E T V K V N L
721  TTCGTGGACCAGAAAGTCGAGTTGGTGAGCTCGTATCGTTAGGAAAAGATTATCTAACGT 780
    R G P E S R V G E L V S L G K D Y L T L
781  TACAGTTACCTCATGGTGAATTAGTATATTATCAGTTGAACATGTGAAGAGTCTAGTGA 840
    Q L P H G E L V Y Y Q L K H V K S L V K
841  AGAAAAGTAAAAGAAAGTAAATGTGGCGATTGCTATAGTTCATGTTTCTGCTCTGATGAGG 900
    K V K E S K C G D C Y S S C F C S D E D
901  ATACTTTTTAGATATATTAAGACTTGAAGTATAAGTGGGTAAAATAATCGTGGCG 960
    T F L D I L K D L K Y K W V K I N R G G
961  GTCCAGAGTGTGTGGAAGGTTTATTAAGTGAGGTACACCATGGCTGTATTACACTAGTAA 1020
    P E C V E G L L S E V H H G C I T L V N
1021  ACGGTGATGAAGTTATTTATGTAATTAAGTCTCATATTAAGAGTGTGAGTCAAGTAGTTA 1080
    G D E V I Y V I K S H I K S V S Q V V K
1081  AATGTA AAAAGAATGAAGATGAATAATGTTTAAATAAATAAGAGGGGCATTATGAGGGAAA 1140
    C K K N E D E *

```

Fig. 2.2 Nucleotide sequence of *cotB1B2* genes with its promoter region (retrieved from GenBank accession number AE016877.1; region 368,717–369,856). Consensus sequence of a putative σ_K -specific promoter is underlined, and the initiation codons of *cotB1* and *cotB2* are written in boldface type. The elements in the consensus sequence AC and CATA---TA correspond to the -35 and -10 regions of the promoter, respectively (1). Reprinted with permission from “The C-Terminal Zwitterionic Sequence of CotB1 Is Essential for Biosilicification of the *Bacillus cereus* Spore Coat”, Kei Motomura, Takeshi Ikeda, Satoshi Matsuyama, Mohamed A. A. Abdelhamid, Tatsuya Tanaka, Takenori Ishida, Ryuichi Hirota, and Akio Kuroda. *Journal of Bacteriology*, 198: 276-282 (2016), copyright © American Society for Microbiology.

Although CotB1 and CotB2 are highly similar to each other (49% identity and 66% similarity over 131 amino acids), CotB1 is longer than CotB2 (171 aa vs 149 aa) and contains a characteristic C-terminal extension (Fig. 2.1). The extension overlaps the silacidin A-like sequence identified by the local BLAST search (residues 142 to 157; Fig. 2.1, boxed), which is rich in serine, aspartate, and glutamate residues, as is the case for silacidin A. The downstream region (residues 158 to 171; Fig. 2.1, underlined) is rich in serine and positively charged arginine residues. Such properties are common to diatom silaffins, although the majority of positively charged residues in silaffins are lysines (e.g., silaffin R5: SSKKSGSYSGSKGSKRRIL) (7). The presence of the negatively charged silacidin-like sequence and positively charged arginine-rich sequence would impart a zwitterionic character to the C-terminal extension of CotB1.

2.3.2 CotB1 is involved in the biosilicification of *B. cereus* spores

In order to investigate whether CotB1 and/or CotB2 is involved in the biosilicification, the author constructed a mutant strain of $\Delta cotB1B2$. The mutant contains a chromosomal mutation that replaces the entire *cotB1* and *cotB2* genes with an Sp^f cassette. Another mutant strain $\Delta cotG$ was constructed as a negative control, in which the Sp^f cassette replaces the gene encoding another spore coat protein Cot γ (41) (formerly known as an exosporium protein ExsB [42]; however recent studies showed that most of

this protein is located in spore coat [41, 43]). These mutant strains grew as fast and formed spores at the same rate as the wild type in the mR2A medium with $100 \mu\text{g ml}^{-1}$ silicate (data not shown), suggesting that the *cotB1B2* and *cotG* disruption did not affect vegetative growth or spore formation. Biosilicification of the spores was evaluated by measuring the decrease in silicate concentration in the culture supernatant during incubation, because the previous study indicated most of silicate removed from the culture supernatant is deposited as silica in the spores (3). During early-stationary phase (24 to 36 h after inoculation), the silicate concentration in the culture supernatants of the wild type and $\Delta\textit{cotG}$ mutant dropped from 100 to about $25 \mu\text{g ml}^{-1}$ while that in the $\Delta\textit{cotB1B2}$ culture supernatant decreased to about $75 \mu\text{g ml}^{-1}$ (Fig. 2.3A), indicating that one or both of the *cotB1B2* genes are involved in biosilicification.

Previously Hirota et al. reported that the biosilicification of the spore coat increased spore viability under acidic conditions (3). To investigate whether *cotB1B2* disruption affects acid resistance, the author purified spores from the wild-type and mutant strains, which were produced in mR2A medium with or without silicate, and treated them with 0.2 N HCl. Consistent with the previous results (3), the wild-type spores prepared in the presence of silicate showed higher survival rates than those prepared in

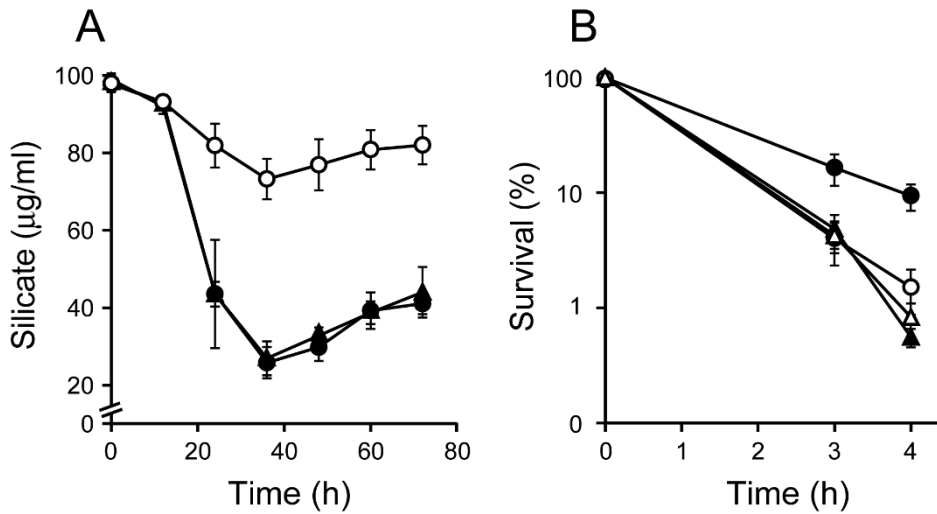


Fig.2.3 Silicate uptake and spore acid resistance of the *B. cereus* wild type, $\Delta cotB1B2$, and $\Delta cotG$ mutants. (A) Silicate concentrations in the culture supernatant of the wild-type (closed circles), $\Delta cotB1B2$ (open circles), and $\Delta cotG$ (closed triangles) strains were measured at the indicated times after inoculation into mR2A medium supplemented with $100 \mu\text{g ml}^{-1}$ silicate. Microscopic observation showed that engulfed forespores formed during the 12–24 h period and that mature spores were gradually released from mother cells after 36 h. (B) Viability of wild-type (circles) and $\Delta cotB1B2$ (triangles) spores in 0.2 N HCl. Spores were produced in the presence (closed symbols) or absence (open symbols) of silicate. Data represent the means and standard deviations of the results of at least three independent experiments. Reprinted with permission from “The C-Terminal Zwitterionic Sequence of CotB1 Is Essential for Biosilicification of the *Bacillus cereus* Spore Coat”, Kei Motomura, Takeshi Ikeda, Satoshi Matsuyama, Mohamed A. A. Abdelhamid, Tatsuya Tanaka, Takenori Ishida, Ryuichi Hirota, and Akio Kuroda. *Journal of Bacteriology*, 198: 276-282 (2016), copyright © American Society for Microbiology.

the absence of silicate (Fig. 2.3B). This was also the case for the $\Delta cotG$ mutant (data not shown). By contrast, and as expected, the presence of silicate did not affect the survival rates of the $\Delta cotB1B2$ spores (Fig. 2.3B). The $\Delta cotB1B2$ spores prepared with and without silicate showed survival rates similar to those of the wild-type spores prepared without silicate (Fig. 2.3B). These data indicate that biosilicification was significantly reduced in the $\Delta cotB1B2$ spores.

In order to exclude the possibility that the decrease in the silicate uptake and acid resistance in the $\Delta cotB1B2$ mutant was caused by incomplete coat assembly, the author observed wild-type and $\Delta cotB1B2$ spores by thin-section TEM and found no measurable difference in spore coat structure (Fig. 2.4). Consistent with this, SDS-PAGE analysis of spore coat proteins from the $\Delta cotB1B2$ mutant showed specific loss of a protein with a molecular mass consistent with that of CotB1 (19.3 kDa) in the $\Delta cotB1B2$ spores (Fig. 2.5, arrowhead). Absence of CotB2 could not be unequivocally identified on the SDS gel because of the overlap with other highly expressed protein bands near the expected molecular mass of CotB2 (16.8 kDa). These results indicate that the disruption of *cotB1B2* genes did not measurably disrupt the overall spore coat assembly, as reported for several other spore coat proteins (44-46). Therefore, the decrease in acid resistance in the $\Delta cotB1B2$ mutant is not due to incomplete coat assembly.

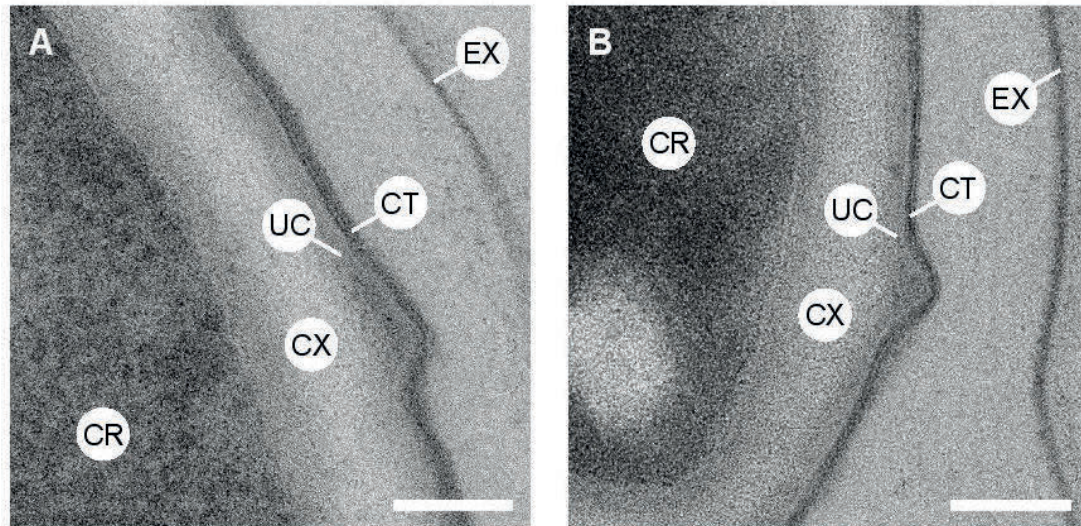


Fig. 2.4 Spore coat structures of the *B. cereus* wild type and $\Delta cotB1B2$ mutant. TEM images of ultrathinsections of the wild-type spores (A) and $\Delta cotB1B2$ spores (B). Dark-staining spore coat (CT) and underlying undercoat (UC) are visible in both images. Scale bar, 100 nm. CR, core; CX, cortex; EX, exosporium. Reprinted with permission from “The C-Terminal Zwitterionic Sequence of CotB1 Is Essential for Biosilicification of the *Bacillus cereus* Spore Coat”, Kei Motomura, Takeshi Ikeda, Satoshi Matsuyama, Mohamed A. A. Abdelhamid, Tatsuya Tanaka, Takenori Ishida, Ryuichi Hirota, and Akio Kuroda. *Journal of Bacteriology*, 198: 276-282 (2016), copyright © American Society for Microbiology.

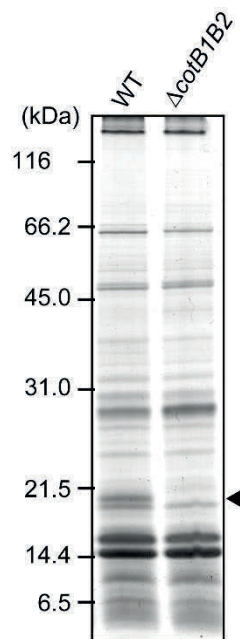


Fig. 2.5 SDS-PAGE analysis (12.5%) of the spore coat proteins. Sporulation of the *B. cereus* wild type (WT) and $\Delta cotB1B2$ mutant strains was induced in mR2A medium supplemented with $100 \mu\text{g ml}^{-1}$ silicate for 48 h. The arrowhead indicates the position corresponding to the expected size of CotB1 (19.3 kDa). Reprinted with permission from “The C-Terminal Zwitterionic Sequence of CotB1 Is Essential for Biosilicification of the *Bacillus cereus* Spore Coat”, Kei Motomura, Takeshi Ikeda, Satoshi Matsuyama, Mohamed A. A. Abdelhamid, Tatsuya Tanaka, Takenori Ishida, Ryuichi Hirota, and Akio Kuroda. *Journal of Bacteriology*, 198: 276-282 (2016), copyright © American Society for Microbiology.

To perform gene complementation analysis, the author constructed plasmids carrying *cotB1*, *cotB2*, or both of these genes with the native promoter region of *cotB1B2*, designated pHT-cotB1, pHT-cotB2, and pHT-cotB1B2, respectively. Wild-type levels of biosilicification were restored by the introduction of either pHT-cotB1 or pHT-cotB1B2 into the Δ *cotB1B2* mutant, whereas this was not the case for pHT-cotB2 (Fig. 2.6A). The reduction in acid resistance caused by *cotB1B2* disruption was also restored by the introduction of pHT-cotB1 and pHT-cotB1B2, but not pHT-cotB2 (data not shown). These results clearly indicate that only CotB1 is involved in the biosilicification.

2.3.3 A C-terminal zwitterionic sequence is essential for biosilicification

As noted above, CotB1 (but not CotB2) has a C-terminal extension consisting of a negatively charged silacidin-like region (residues 142 to 157) and a positively charged arginine-rich region (residues 158 to 171) (Fig. 2.1). To investigate whether the zwitterionic extension is essential for biosilicification, the author constructed three plasmids encoding C-terminally truncated mutants of CotB1: pHT-cotB1-141 encodes CotB1 lacking residues 142 to 171; pHT-cotB1-157 encodes CotB1 lacking residues 158 to 171; pHT-cotB1-142/157 encodes CotB1 lacking the residues between 142 and 157. Introduction of any of these mutant plasmids into the Δ *cotB1B2* did not restore the

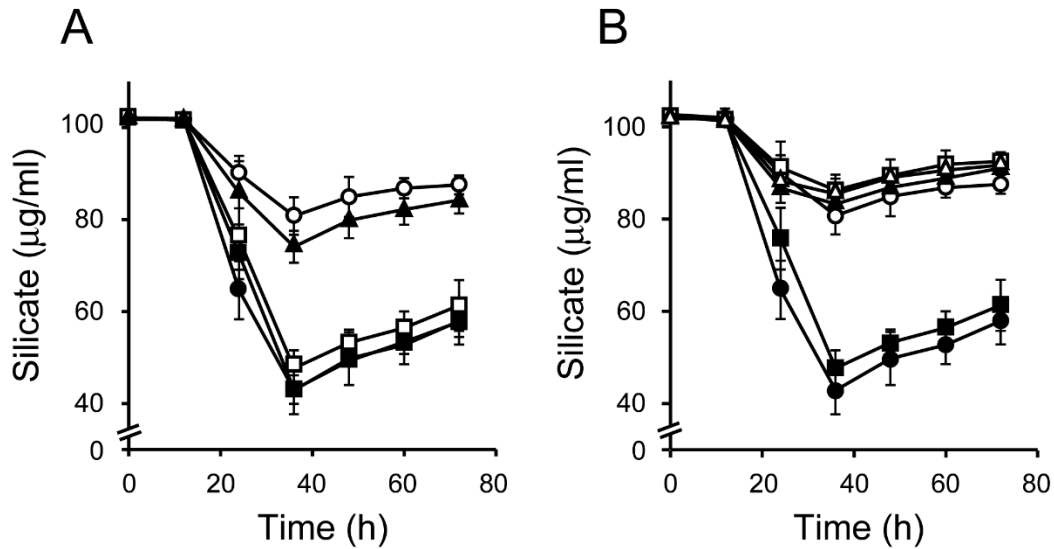


Fig. 2.6 Complementation analysis of $\Delta cotB1B2$. (A) Silicate concentrations in the culture supernatant of the *B. cereus* wild-type strain carrying pHT304 (closed circles), $\Delta cotB1B2$ carrying pHT304 (open circles), pHT-cotB1B2 (closed squares), pHT-cotB1 (open squares), or pHT-cotB2 (closed triangles) were measured at the indicated times after inoculation into mR2A medium supplemented with 100 $\mu\text{g ml}^{-1}$ silicate. (B) The same experiment was performed for the wild-type strain carrying pHT304 (closed circles), $\Delta cotB1B2$ carrying pHT304 (open circles), pHT-cotB1 (closed squares), pHT-cotB1-141 (open squares), pHT-cotB1-157 (closed triangles), or pHT-cotB1-142/157 (open triangles). Data represent the means and standard deviations of the results of at least three independent experiments. Reprinted with permission from “The C-Terminal Zwitterionic Sequence of CotB1 Is Essential for Biosilicification of the *Bacillus cereus* Spore Coat”, Kei Motomura, Takeshi Ikeda, Satoshi Matsuyama, Mohamed A. A. Abdelhamid, Tatsuya Tanaka, Takenori Ishida, Ryuichi Hirota, and Akio Kuroda. *Journal of Bacteriology*, 198: 276-282 (2016), copyright © American Society for Microbiology.

biosilicification (Fig. 2.6B), although comparable amounts of the C-terminally truncated CotB1 proteins were expressed and integrated in the spores (Fig. 2.7). These results strongly suggest that both the silacidin-like and arginine-rich sequences, which would impart a zwitterionic character to the C-terminus of CotB1, are essential for biosilicification.

2.3.4 Expression and localization of CotB1

To further examine the relationship between CotB1 and biosilicification, the time course of expression and subcellular localization of CotB1 were monitored during sporulation. First, the author constructed a plasmid containing the *cotB1B2* promoter region followed by a chimeric gene *gfp-cotB1* that encodes CotB1 with an N-terminal GFP (pHT-gfp-cotB1), and then introduced it into the Δ *cotB1B2* mutant. However, the levels of biosilicification were not completely restored in the transformant (data not shown), implying that the presence of the fused GFP attenuates CotB1 function. Therefore, pHT-gfp-cotB1 was introduced into the wild-type strain, producing a merodiploid strain that contains *gfp-cotB1* fusion on the plasmid in addition to the native *cotB1* chromosomal locus. The transformant grew and sporulated normally in mR2A medium, and its levels of biosilicification were the same as those of the wild-type strain (data not shown).

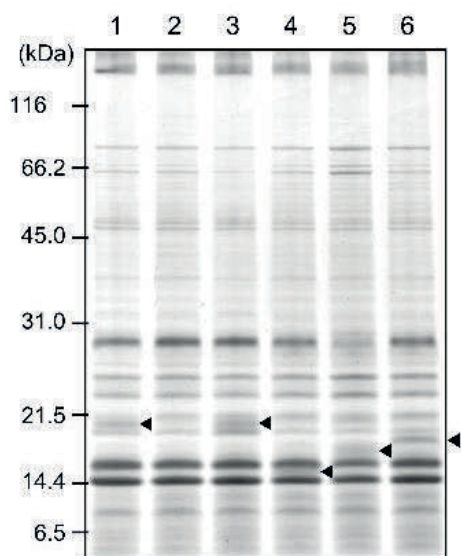


Fig. 2.7 SDS-PAGE analysis (12.5%) of the spore coat proteins of the *B. cereus* $\Delta cotB1B2$ mutant harboring plasmids encoding C-terminally truncated CotB1 proteins. Sporulation was induced in mR2A medium supplemented with $100 \mu\text{g ml}^{-1}$ silicate for 48 h. Lane 1, wild-type strain carrying pHT304; lanes 2–6, $\Delta cotB1B2$ carrying pHT304 (lane 2), pHT-cotB1 (lane 3), pHT-cotB1-141 (lane 4), pHT-cotB1-157 (lane 5), or pHT-cotB1-142/157 (lane 6). The arrowheads indicate the position of the expressed proteins. Reprinted with permission from “The C-Terminal Zwitterionic Sequence of CotB1 Is Essential for Biosilicification of the *Bacillus cereus* Spore Coat”, Kei Motomura, Takeshi Ikeda, Satoshi Matsuyama, Mohamed A. A. Abdelhamid, Tatsuya Tanaka, Takenori Ishida, Ryuichi Hirota, and Akio Kuroda. *Journal of Bacteriology*, 198: 276-282 (2016), copyright © American Society for Microbiology.

In the merodiploid strain, no fluorescence signals were detected under fluorescence microscopy at 12 h after inoculation, which is approximately 2 h after entry into sporulation (Fig. 2.8). At 24 h after inoculation, when the silicate uptake started and the engulfed forespores could be observed by bright-field microscopy, green fluorescence was distributed around the entire forespores (Fig. 2.8). This expression time course agrees well with the presence of a putative σ^K promoter (40) upstream of the *cotB1* gene, which is activated in the mother cell during the late stage of sporulation (Fig. 2.2). Subsequently, GFP fluorescence was consistently associated with the developing spores, and finally formed a complete ring around the mature spores. This fluorescence localization pattern is essentially the same as those of previously reported GFP-fused spore proteins located in the exosporium and/or spore coat (47-49), where silica is deposited in *B. cereus* (3). By contrast, in the wild-type strain carrying pHT-gfp that contains only the *gfp* gene instead of *gfp-cotB1*, GFP fluorescence was dispersed throughout the mother cell cytoplasm and did not localize on the spore. Taken together, the timing of CotB1 expression and its localization agree well with the time course of biosilicification and the location of the deposited silica, supporting the direct involvement of this protein in silica formation.

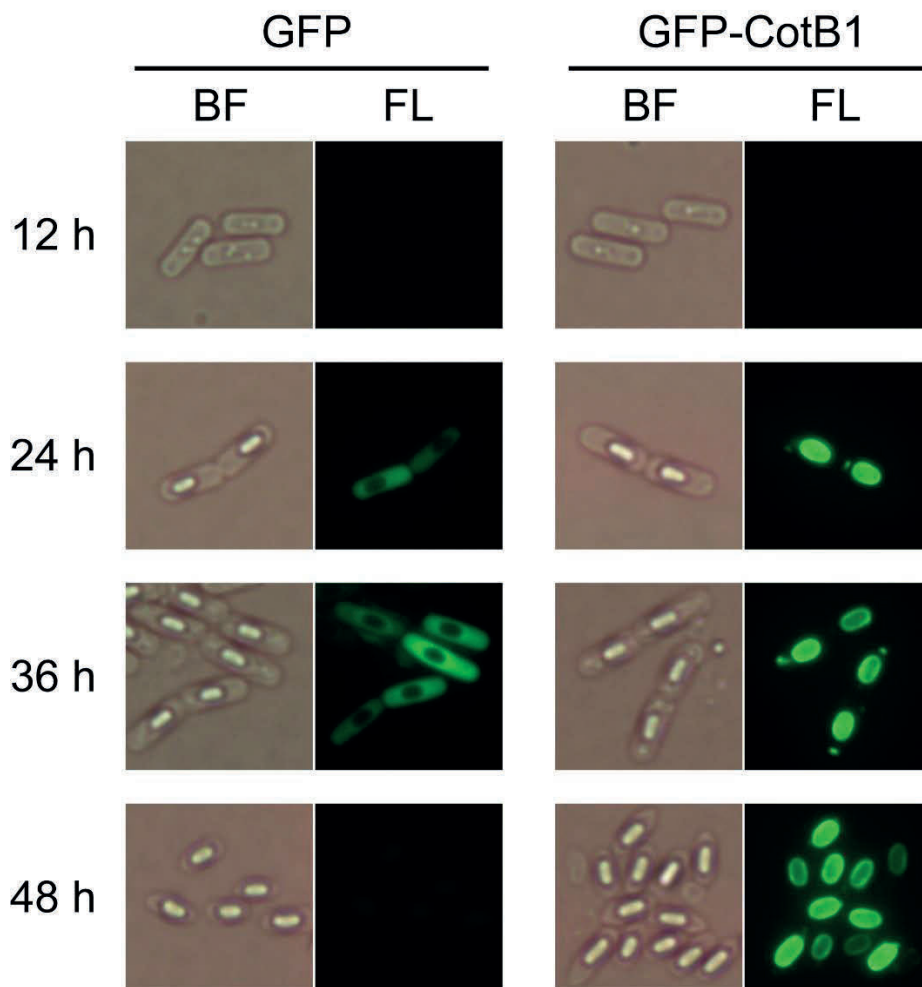


Fig. 2.8 Bright-field and fluorescence microscopic analysis of GFP-CotB1 during sporulation. The *B. cereus* wild-type strains carrying pHT-gfp-cotB1 (GFP-CotB1) or pHT-gfp (GFP) were grown in mR2A medium supplemented with 100 $\mu\text{g ml}^{-1}$ silicate. Samples were taken at the indicated times after inoculation and observed by bright-field (BF) and fluorescence (FL) microscopy. Reprinted with permission from “The C-Terminal Zwitterionic Sequence of CotB1 Is Essential for Biosilicification of the *Bacillus cereus* Spore Coat”, Kei Motomura, Takeshi Ikeda, Satoshi Matsuyama, Mohamed A. A. Abdelhamid, Tatsuya Tanaka, Takenori Ishida, Ryuichi Hirota, and Akio Kuroda. *Journal of Bacteriology*, 198: 276-282 (2016), copyright © American Society for Microbiology.

2-3-5 CotB1 may be the founding member of a subset of prokaryotic proteins that stimulate biosilicification

As described above, the C-terminal zwitterionic sequence of CotB1 is similar to diatom silica-forming peptides, silaffins and silacidins (Fig. 2.1), and is essential for biosilicification in vivo (Fig. 2.6B). By contrast, no proteins homologous to sponge silicatein α , which is involved in biosilicification in siliceous sponges (50, 51), are found in the *B. cereus* genome. These facts suggest that *B. cereus* and diatoms share similar molecular mechanisms for silica formation, although the very limited overlapping lengths between CotB1 and silaffins/silacidins prevent further investigation into the evolutionary relationships among them. Scheffel et al. proposed that preassembled protein-based templates are general components of the cellular machinery for silica morphogenesis in diatoms (8). The author's findings clearly indicate that this is also the case for bacteria, because *B. cereus* CotB1 is also a component of an insoluble supramolecular aggregate (the spore coat) that serves as a template for silica formation. The author believes this is the first report of an intracellular protein that stimulates biosilicification in prokaryotes.

The CotB1 homologs that contain the C-terminal zwitterionic sequence are common to biosilicifying *B. cereus* relatives (e.g., GenBank accession number AIF54819.1 of *B. anthracis*, ADH05148.1 of *B. thuringiensis*), but not to non-

biosilicifying *Bacillus* species (such as *B. subtilis*) or other organisms, indicating that CotB1 plays an important role in prokaryotic biosilicification. These facts are consistent with the previous finding that all of the biosilicifying bacteria, which were isolated from paddy field soil, belong to or are closely related to the *B. cereus* group (3). The author's findings indicate that CotB1 plays an important role in prokaryotic biosilicification. However, the presence of a CotB1 homolog is not sufficient for biosilicification. For example, biosilicification was not observed in the spores of *B. mycooides* (also a member of the *B. cereus* group) (3), although this bacterium has a CotB1 homolog with a zwitterionic sequence (GenBank accession number EEM01263.1). These findings clearly indicate the involvement of additional factor(s) in the biosilicification of *Bacillus* spores. Such factor(s) probably include the presence of silicate transporters, because spore biosilicification is likely to require active transport of silicate into the mother cells. Since biosilicification occurs before the release of the spores (3), silicate needs to be taken up via transporters on the mother cell surface. The slight decrease in silicate concentration in the culture supernatant in the $\Delta cotB1B2$ mutant (Fig. 2.4A) could be attributable to silicate uptake into the mother cells by the silicate transporters. Since the mutant cells cannot efficiently polymerize silicate, most of it is later released during mother cell lysis. In diatoms, silica deposition is tightly coupled to silicate transport, which is mediated by

specific transporters (52, 53). Influx and efflux silicate transporters have been also identified in higher plants (54, 55). However, counterparts of the eukaryotic silicate transporters have not been identified in prokaryotes. Elucidation of the mechanism of silicate transport in *B. cereus* may help explain the differences in biosilicification among *Bacillus* species, and could also provide new insights into the distribution of biosilicification in prokaryotes.

Chapter 3

Affinity purification of recombinant proteins using a novel silica-binding peptide as a fusion tag

3.1 Introduction

In Chapter 2, the author has investigated the role of the *Bacillus cereus* spore coat protein, CotB1, in prokaryotic biosilicification. Here, further studies have been conducted to demonstrate the applications of this protein and its C-terminal fragment as affinity tags for recombinant protein purification. Affinity tags are highly efficient tools for protein purification. A variety of proteins, domains, and peptides have been used as affinity tags to facilitate the purification of proteins of interest from crude extracts (22, 23, 56, 57). Previously, Kuroda and co-workers reported a novel affinity purification method using a silica-binding tag designated “Si-tag” (17, 18), with inexpensive commercial silica (SiO₂) particles serving as the specific adsorbent (19, 20). However, the large size of the Si-tag (273 amino acids [aa]) and high concentration of eluent (e.g., 2 M MgCl₂) required to release Si-tagged fusion proteins may negatively affect the intrinsic properties and function of the fusion partner. Therefore, the author has developed silica-based affinity method utilizing shorter silica-binding tags and milder elution conditions.

Recently, Hirota et al. reported that silica is deposited on the coat of *Bacillus cereus* spores as a layer of nanometer-sized particles (3). The spore coat is a proteinaceous layer composed of more than 50 proteins (27). As mentioned in Chapter 2, gene disruption

analysis revealed that the spore coat protein CotB1 (171 aa) mediates the accumulation of silica. Here the author found that the C-terminal 14-aa region (corresponding to residues 158-171 of CotB1) is rich in positively charged and serine residues (5 arginine and 3 serine residues). Such features are similar to those of the well-characterized silica-precipitating peptides (silaffins) isolated from diatoms (58), suggesting that CotB1, particularly its C-terminal 14-aa region (designated CotB1p), interacts with silica surfaces.

In this chapter, the author demonstrates that CotB1 binds strongly to silica surfaces. CotB1p also binds to silica surfaces, with affinity comparable to that of CotB1, suggesting that the C-terminal 14-aa region of CotB1 mediates silica binding. To develop a recombinant protein purification method using CotB1/CotB1p as silica-binding tags, small ubiquitin-like modifier (SUMO) technology was employed (59-61) to facilitate release of the target protein from the solid phase (62). The combination of silica-binding CotB1/CotB1p and SUMO protease-mediated site-specific cleavage at the C-terminus of the fused SUMO sequence enables purification of tagless target proteins with high purity and yield.

3.2 Material and Methods

3.2.1 Materials

Silica particles (α -quartz) with a diameter of approximately 0.8 μm were purchased from Soekawa Chemical Co., Ltd. (Tokyo, Japan) and used without any pretreatment. SUMO protease (with an N-terminal His-tag) was purchased from LifeSensors, Inc. (Malvern, PA, USA). All chemicals used in this study were of analytical grade.

3.2.2 Construction of expression plasmids for green fluorescent protein GFP-CotB1 and GFP-CotB1p fusions

The DNA fragment encoding CotB1 was amplified by polymerase chain reaction (PCR) from *B. cereus* ATCC 14579 genomic DNA using the primers CotB1-F and CotB1-R (a list of the primers used in the study is shown in Table 3.1). The resulting PCR fragment was digested with *Hind*III and *Xho*I and then inserted into the *Hind*III-*Xho*I sites of pET-47b (Novagen/Merck KGaA, Darmstadt, Germany). The resulting plasmid was designated pET-CotB1. Subsequently, a GFP-encoding DNA fragment was amplified by PCR from pGFPuv (Clontech Laboratories, Inc., Mountain View, CA, USA) using the primers GFP-F and GFP-R. The resulting PCR fragment was digested with *Sac*II and *Eco*RI and then cloned into the *Sac*II-*Eco*RI sites of pET-CotB1. The resulting plasmid

Table 3.1 Primers used in this study

Name	DNA sequence (5' to 3') ^a	Restriction site
CotB1-F	GCCGCAA <u>AAGCTT</u> GTGAGTTTATTTTCATTGTGAT	<i>HindIII</i>
CotB1-R	CCCCTC <u>TCGAGT</u> TATCTTCCTCTACTTGATTGTCT	<i>XhoI</i>
GFP-F	TAATAAC <u>CGCGG</u> ATATGAGTAAAGGAGAAGAACTT	<i>SacII</i>
GFP-R	AGTATAG <u>AATTC</u> GTTTGTAGAGCTCATCCATG	<i>EcoRI</i>
CotB1p-F	TCAGGTCGTGCTCGTGCACAA	
CotB1p-R	CGCCAAGGCCTGTACAGAATT	
GFP-		
CotB1-F	TAACTCGAGGCTTAATTAACCTAGGCT	
GFP-		
CotB1-R	CGCCAAGGCCTGTACAGAATT	
mCherry-F	AAGGTCTC <u>AAGG</u> TATGGTGAGCAAGGGCGAGGA	<i>BsaI</i>
mCherry-R	AAAGGTCTCTCTAGACTACTTGTACAGCTCGTCCA	<i>BsaI</i>
mChe-		
SUMO-F	GGCAGTATGTCCGACTCAGAAGTC	
mChe-		
SUMO-R	ACCGCCCATATGTATATCTCCTTCTTAAAG	

^a Restriction sites are underlined.

was designated pET-GFP-CotB1.

Inverse PCR using the primers CotB1p-F and CotB1p-R with pET- GFP-CotB1 serving as the template and self-ligation of the resulting amplified DNA was employed to construct pET-GFP-CotB1p. Another round of inverse PCR was performed using the primers GFP-CotB1-F and GFP-CotB1-R, and the resulting amplified DNA was self-ligated to construct pET-GFP.

3.2.3 Expression and purification of GFP-CotB1 and GFP-CotB1p

The expression plasmids pET-GFP-CotB1, pET-GFP-CotB1p, and pET-GFP were introduced into *Escherichia coli* Rosetta(DE3)pLysS (Novagen/Merck KGaA). The transformants were grown at 37°C in 2× YT medium (30) supplemented with 50 µg/mL of kanamycin and 30 µg/mL of chloramphenicol. When the culture reached an optical density at 600 nm of 0.5, 0.2 mM isopropyl-β-D-thiogalactopyranoside was added to the medium to induce expression of the recombinant proteins. After an additional 8 h of cultivation at 28°C (for pET-GFP-CotB1) or 4 h at 37°C (for pET-GFP-CotB1p and pET-GFP), the cells were harvested by centrifugation and the resulting pellets were resuspended in 25 mM Tris-HCl buffer (pH 8.0) containing 20% (v/v) glycerol. The cells were then disrupted using lysozyme and sonication followed by centrifugation to remove

cell debris. The supernatants containing soluble recombinant proteins with an N-terminal His-tag were loaded onto a HisTrap FF column (GE Healthcare UK Ltd, Buckinghamshire, UK) equilibrated with 25 mM Tris-HCl buffer (pH 8.0) containing 20% (v/v) glycerol. Proteins were eluted with a linear gradient from 0 to 0.5 M imidazole in the same buffer. Fractions containing the recombinant proteins were collected and then applied to a POROS HQ anion exchange column (Applied Biosystems/Life Technologies Corporation, Carlsbad, CA, USA) equilibrated with the same buffer. Proteins were eluted with a linear gradient from 0 to 1 M NaCl in the same buffer. Fractions containing the recombinant proteins were collected and dialyzed at 4°C against 25 mM sodium phosphate buffer (pH 8.0).

3.2.4 Determination of the dissociation constant (K_d) values for GFP-CotB1 and GFP-CotB1p

Purified GFP-CotB1 and GFP-CotB1p were diluted to various concentrations (10-100 nM) in 1 mL of 25 mM sodium phosphate buffer (pH 8.0). The diluted protein solutions were then mixed with 10 μ L of 10 mg/mL silica-particle suspension (corresponding to 0.1 mg dry weight of silica particles). After incubation for 15 min, the silica particles were removed by centrifugation at $5,000 \times g$ for 2 min. The amount of

each fusion protein bound to the silica particles was determined by subtracting the fluorescence intensity associated with the GFP remaining in the supernatant from the initial fluorescence intensity. The resulting data were fitted to the Langmuir isotherm to determine the K_d value.

3.2.5 Construction of expression plasmids for CotB1-SUMO-mCherry (CotB1-SC) and CotB1p-SUMO-mCherry (CotB1p-SC) fusions

In order to construct fusion proteins consisting of CotB1 (or CotB1p), SUMO, and a protein of interest, the author first constructed plasmids carrying the gene encoding either the CotB1-SUMO or CotB1p-SUMO fusion followed by two *BsaI* sites for cloning the protein of interest (63). The amino acid sequence of either CotB1 or CotB1p was fused with that of SUMO (*Saccharomyces cerevisiae* Smt3p; accession number NP_010798), in that order, with an intervening GGGs linker. The nucleotide sequences of the CotB1-SUMO and CotB1p-SUMO fusion genes were designed in order to optimize codon usage for translation in *E. coli*. The *BsaI* cloning sites and adjacent sequences, which were described by Panavas et al. (2009), were added downstream of the fusion gene so that the protein of interest could be fused directionally to the C-terminus of SUMO without any additional sequence. Because SUMO protease selectively cleaves the polypeptide chain

at the Gly-Gly motif located at the C-terminal end of the SUMO sequence in the resulting fusion protein, the desired protein with an authentic N-terminus would be released when the gene of interest is appropriately cloned downstream of the SUMO gene (60). In addition, an *NdeI* site was added at the ATG start codon of the fusion gene and a *BamHI* site was added downstream of the *BsaI* sites. The two designed DNA fragments (nucleotide sequences are shown in Figs. 3.1 and 3.2) were synthesized by BEX Co., Ltd. (Tokyo, Japan) and cloned into the *NdeI-BamHI* sites of pET-24b (Novagen/Merck KGaA). The resulting plasmids were designated pET-CotB1-SUMO (carrying the CotB1-SUMO fusion gene) and pET-CotB1p-SUMO (carrying the CotB1p-SUMO fusion gene). The gene encoding the fluorescent protein mCherry (64) was amplified by PCR from pmCherry (Clontech Laboratories, Inc.) using the primers mCherry-F and mCherry-R (Table 3.1). The amplified fragment was digested with *BsaI* and cloned into the *BsaI*-digested pET-CotB1-SUMO and pET-CotB1p-SUMO plasmids to construct pET-CotB1-SC and pET-CotB1p-SC, respectively.

Inverse PCR using the primers mChe-SUMO-F and mChe-SUMO-R with pET-CotB1-SC serving as the template and self-ligation of the resulting amplified DNA was employed to construct pET-SUMO-mCherry.

3.2.6 Expression of CotB1-SC and CotB1p-SC

The expression plasmids pET-CotB1-SC, pET-CotB1p-SC, and pET-SUMO-mCherry were introduced into *E. coli* Rosetta(DE3)pLysS, and the transformants were grown in 2× YT medium as described above. When the culture reached an optical density at 600 nm of 0.5, 0.2 mM isopropyl-β-D-thiogalactopyranoside was added to the medium to induce protein expression. After an additional 8 h of cultivation at 28°C (for pET-CotB1-SC) or 4 h at 37°C (for pET-CotB1p-SC and pET-SUMO-mCherry), the cells were harvested by centrifugation and the pellets were stored at –80°C until use.

3.2.7 Optimization of silica-binding conditions

The CotB1-SC and CotB1p-SC fusion proteins were expressed in *E. coli* Rosetta(DE3)pLysS harboring either pET-CotB1-SC or pET-CotB1p-SC, respectively, as described above. Cell pellets harvested from 1-mL cultures (typically 10 mg wet weight of cells) were suspended in 0.5 mL of 25 mM Tris-HCl buffer at various pHs (pH 7.0-9.0) or 25 mM sodium phosphate buffer (pH 6.0-8.0) and disrupted by sonication. After centrifugation at 20,000 × g for 30 min, the supernatants (cleared cell lysates) containing the recombinant proteins were mixed with 0.5 mL of silica-particle suspension in the same buffer (final silica concentration of 25 mg dry weight/mL) for 15 min at room temperature.

Silica particles with bound protein were collected by centrifugation at $5,000 \times g$ for 2 min and then washed three times with 1 mL of the same suspension buffer. After the supernatant was carefully removed, proteins still bound to the particles were released by boiling in Laemmli sample buffer (65) for 5 min and analyzed by sodium dodecyl sulfate-polyacrylamide gel electrophoresis (SDS-PAGE; 15%). Gels were stained with Coomassie brilliant blue (CBB) R-250 and the target protein was quantified by densitometric analysis using ImageJ software, version 1.41 (66).

Similar experiments were conducted in 25 mM Tris-HCl buffer (pH 8.0) with varying concentrations of silica (0-30 mg dry weight/mL) and nonionic detergent (0-1.5% [v/v] Tween 20 or Triton X-100) for varying periods of incubation time (1-30 min).

3.2.8 Affinity purification of mCherry using CotB1/CotB1p as a silica-binding tag

Cell pellets harvested from 10-mL cultures were resuspended in 2 mL of 25 mM Tris-HCl buffer (pH 8.0) and disrupted by sonication. After centrifugation at $20,000 \times g$ for 30 min, the cleared cell lysates were mixed with 250 mg dry weight of silica particles by gentle rotation for 15 min at room temperature. After centrifugation at $5,000 \times g$ for 2 min, the particles were washed three times with 25 mM Tris-HCl buffer (pH 8.0) containing 150 mM NaCl and then resuspended in 2 mL of the same buffer. SUMO

protease (80 units) was then added to the suspension. After a 3-h incubation at room temperature, the suspension was centrifuged at $5,000 \times g$ for 2 min. The resulting supernatants containing the cleaved mCherry protein were collected and analyzed by SDS-PAGE. The protein concentration was determined using the Bradford method (67) with bovine serum albumin as the standard.

3.2.9 Nucleotide sequence data

The nucleotide sequences of the CotB1-SUMO and CotB1p-SUMO fusions are available in the DDBJ/EMBL/GenBank databases under the accession numbers AB904509 and AB904510, respectively.

3.3 Results and Discussion

3.3.1 Binding of GFP-CotB1 and GFP-CotB1p to silica particles

To test whether CotB1 and its C-terminal 14-aa peptide CotB1p bind to silica surfaces, the respective GFP fusion proteins were constructed (Fig. 3.3). Cleared lysates of recombinant *E. coli* cells expressing GFP-CotB1, GFP-CotB1p, or GFP as a control were mixed with silica particles for 15 min at room temperature. Silica particles with bound protein were collected by centrifugation and washed three times with 25 mM Tris-HCl buffer (pH 8.0) containing 0.5% (v/v) Tween 20. Proteins remaining bound to the particles were released by boiling in Laemmli sample buffer (65) and then analyzed by SDS-PAGE. Densitometric analysis of the CBB-stained gel showed that 65% of the GFP-CotB1 and 60% of the GFP-CotB1p fusion proteins bound to the silica particles, whereas GFP alone did not bind to silica particles under the experimental conditions used (data not shown). These results clearly indicate that both CotB1 and CotB1p function as silica-binding fusion tags.

The author then evaluated the silica-binding affinity of GFP-CotB1 and GFP-CotB1p. Adsorption data for the purified proteins mixed with silica particles were fitted to the Langmuir isotherm (Fig. 3.4). The silica-binding K_d values for GFP-CotB1 and GFP-CotB1p were 2.09 and 1.24 nM, respectively. The maximum amount of GFP-CotB1

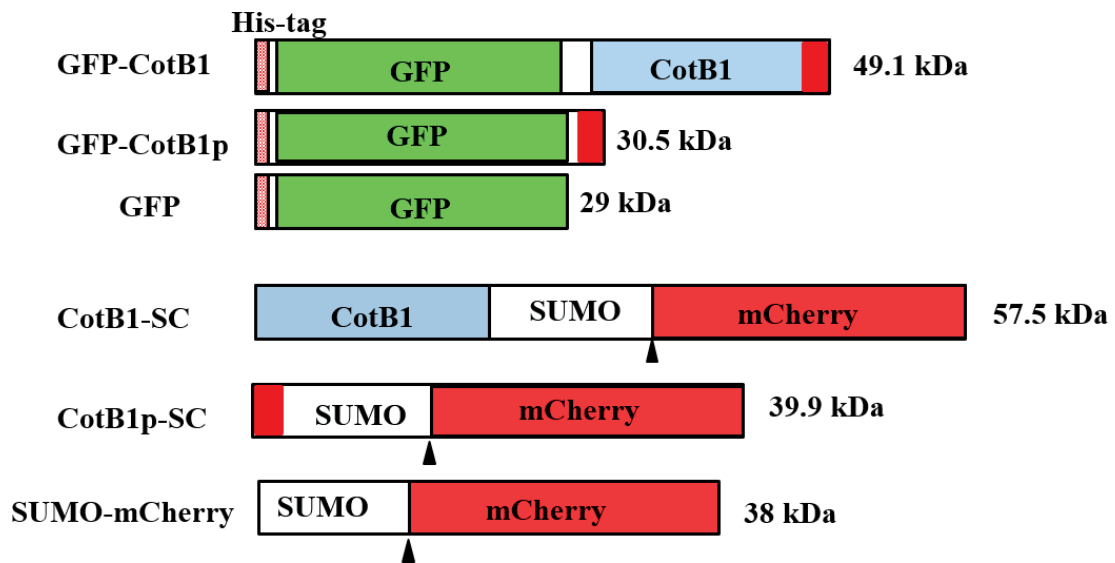


Fig. 3.3 Schematic representation of the structures of the CotB1/CotB1p fusion proteins constructed in this study. Arrowheads indicate SUMO protease cleavage sites. Reprinted with permission from “Affinity purification of recombinant proteins using a novel silica-binding peptide as a fusion tag”, Mohamed A. A. Abdelhamid, Kei Motomura, Takeshi Ikeda, Takenori Ishida, Ryuichi Hirota, and Akio Kuroda. *Applied Microbiology and Biotechnology*, 98:5677-5684 (2014), copyright © Springer.

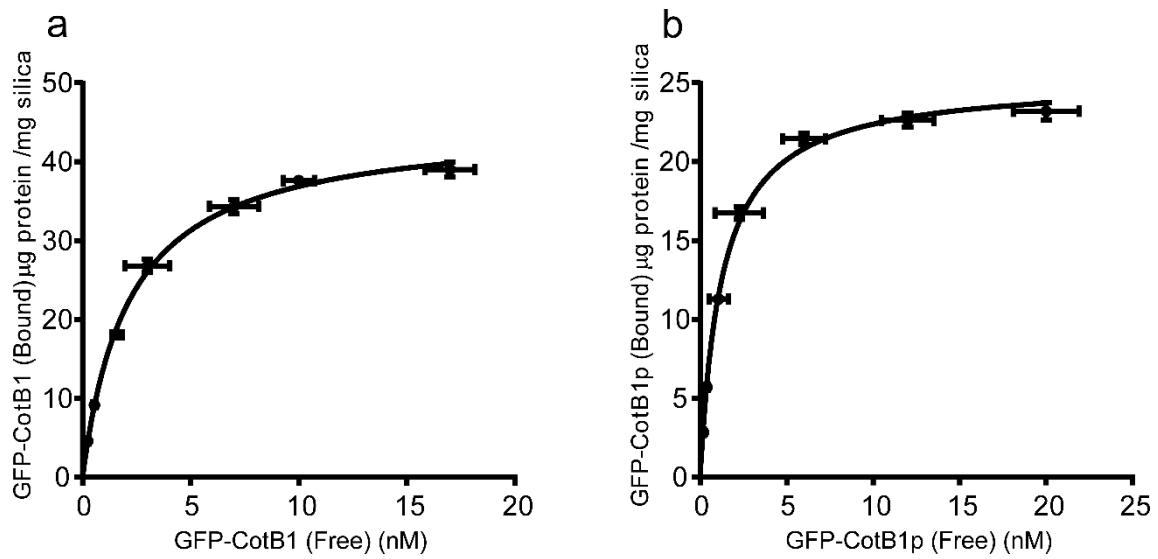


Fig. 3.4 Binding of GFP-CotB1 (a) and GFP-CotB1p (b) to silica particles. Data were fitted to the Langmuir isotherm (solid line) to determine the K_d value. Reprinted with permission from “Affinity purification of recombinant proteins using a novel silica-binding peptide as a fusion tag”, Mohamed A. A. Abdelhamid, Kei Motomura, Takeshi Ikeda, Takenori Ishida, Ryuichi Hirota, and Akio Kuroda. *Applied Microbiology and Biotechnology*, 98:5677-5684 (2014), copyright © Springer.

and GFP-CotB1p bound was 44.6 and 25.1 $\mu\text{g}/\text{mg}$ dry weight of silica particles (corresponding to 0.91 and 0.82 nmol/mg of silica), respectively.

3.3.2 Optimization of silica-binding conditions

In the strategy the author adopted for development of a silica-based affinity purification method using CotB1/CotB1p, silica particles were used as an adsorbent for the CotB1/CotB1p fusion proteins. To release the target protein from the adsorbed fusion proteins using this approach, a protease recognition site was introduced between the N-terminal CotB1/CotB1p tag and the C-terminal target protein. Addition of the appropriate protease would then result in cleavage of the silica-bound fusion protein and release of the tagless target protein into the liquid phase, with the tag region remaining bound to the solid phase. In the following experiments, the author used CotB1/CotB1p, SUMO, and mCherry fusion proteins (designated CotB1-SC and CotB1p-SC; Fig. 3.3) as models to evaluate the affinity purification method. The fluorescent protein mCherry was selected as the model target protein, and SUMO, the C-terminal end of which is selectively cleaved by SUMO protease, was introduced as the protease recognition site.

To maximize the yield of the developed affinity purification method, the optimal silica-binding conditions for CotB1/CotB1p fusion proteins were determined using

cleared lysates of recombinant *E. coli* cells expressing CotB1-SC or CotB1p-SC. Lysates of cell pellets harvested from 1-mL cultures (typically 10 mg wet weight of cells) were mixed with silica particles in a total volume of 1 mL, and the amount of protein bound to the silica particles was determined by SDS-PAGE as described in the Materials and Methods section.

The author first determined the optimal pH for silica binding, examining the pH range 6.0-9.0. Both the CotB1 and CotB1p fusion proteins bound to silica over a wide pH range, with slightly different optimal pH values (Fig. 3.5a). In contrast, SUMO-mCherry (without CotB1 nor CotB1p) did not bind to silica particles at any pH examined (data not shown), confirming that CotB1 (particularly the C-terminal CotB1p region) mediates silica binding. Because over 90% of both CotB1-SC and CotB1p-SC bound to silica at pH 8.0, the following experiments were performed in 25 mM Tris-HCl buffer at pH 8.0.

Next, the optimal silica concentration was determined. The amount of the bound protein increased proportionally to the amount of silica particles added, reaching a plateau of >90% binding of the fusion proteins with addition of >25 mg dry weight of silica particles in the 1-mL cleared lysate solution typically containing 10 mg wet weight of cells (Fig. 3.5b). At a silica concentration of 25 mg dry weight/mL, approximately 85% of both fusion proteins adsorbed to the silica particles during the first minute of the

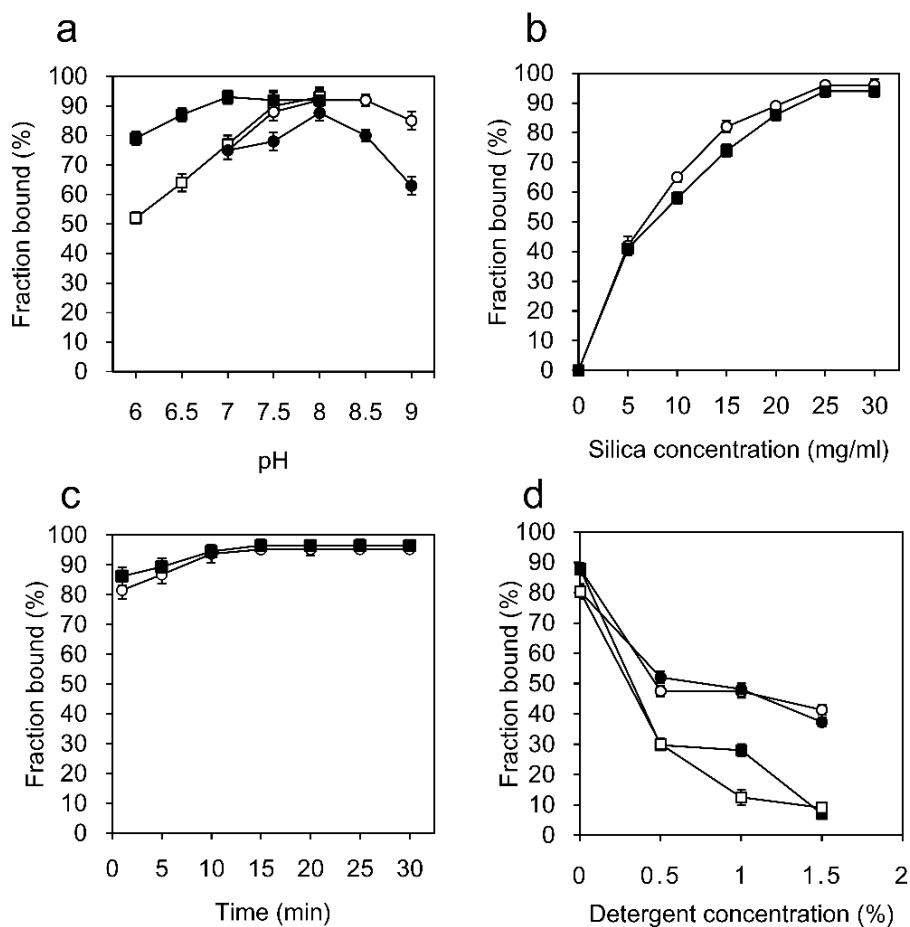


Fig. 3.5 Effect of buffer conditions and incubation time on silica binding of CotB1-SC and CotB1p-SC. (a) Effect of pH. Open circles and squares, CotB1-SC in 25 mM Tris-HCl buffer and CotB1-SC in 25 mM phosphate buffer, respectively. Closed circles and squares, CotB1p-SC in 25 mM Tris-HCl buffer and CotB1p-SC in 25 mM phosphate buffer, respectively. (b) Effect of silica concentration. Circles, CotB1-SC; squares, CotB1p-SC. (c) Effect of incubation time. Circles, CotB1-SC; squares, CotB1p-SC. (d) Effect of nonionic detergents. Open circles and squares, CotB1-SC with Tween 20 and Triton X-100, respectively. Closed circles and squares, CotB1p-SC with Tween 20 and Triton X-100, respectively. Reprinted with permission from “Affinity purification of recombinant proteins using a novel silica-binding peptide as a fusion tag”, Mohamed A. A. Abdelhamid, Kei Motomura, Takeshi Ikeda, Takenori Ishida, Ryuichi Hirota, and Akio Kuroda. *Applied Microbiology and Biotechnology*, 98:5677-5684 (2014), copyright © Springer.

incubation, and the amount of protein adsorbed reached a plateau within 15 min (Fig. 3.5c).

Finally, the author investigated the effect of adding detergent to the binding buffer because nonionic detergents (e.g., Tween 20 and Triton X-100) have been used in other studies to reduce nonspecific binding of host proteins to silica surfaces (68, 69). Although the author also found that addition of Tween 20 or Triton X-100 did reduce the degree of nonspecific binding of host proteins to the silica particles (data not shown), these detergents also reduced the binding of CotB1-SC and CotB1p-SC (Fig. 3.5d). Therefore, no detergents were added to the binding buffer in subsequent experiments.

3.3.3 Affinity purification of mCherry using CotB1/CotB1p as silica-binding tag

Using the optimized conditions described above, CotB1-SC (57.5 kDa) and CotB1p-SC (39.9 kDa) were isolated from cleared cell lysates by immobilization on silica particles and analyzed by SDS-PAGE (Fig. 3.6, lanes 2 and 6, open arrowheads). Some host proteins also adsorbed onto and remained adsorbed to the silica particles even after washing. To recover the tagless mCherry protein from the bound fusion proteins, SUMO protease was added to the suspension of CotB1-SC- or CotB1p-SC-bound silica particles. SDS-PAGE analysis revealed that most of each of the recombinant proteins was cleaved

after 3 h of incubation and that the CotB1-SUMO and CotB1p-SUMO fragments (30.8 and 13.2 kDa, respectively) remained bound to the silica particles (Fig. 3-6, lanes 3 and 7, closed arrowheads). The mCherry fragment (26.7 kDa) was released into the supernatant (Fig. 3-6, lanes 4 and 8). Because the author used much less SUMO protease compared with the recombinant proteins (less than 0.1% [w/w]), the SUMO protease band (~26 kDa) was not visible on SDS-PAGE (Fig. 3-6, lanes 4 and 8). The discrepancies between the calculated molecular masses and pattern of band migration on the gel could be ascribed to aberrant migration of the SUMO band (61) as well as the mCherry band (the mCherry parental protein mRFP1 [25.4 kDa] migrates as a >30 kDa band on SDS-PAGE [70]). Densitometric analysis of the CBB-stained protein bands showed that the purity of the released tagless mCherry was approximately 95%.

Typical results for the affinity purification of mCherry using the CotB1-SC and CotB1p-SC fusion proteins are summarized in Tables 3.2 and 3.3, respectively. The mCherry recovery rate was approximately 85%, with yields of 0.60 ± 0.06 and 1.13 ± 0.13 mg (mean \pm standard deviation from three independent experiments) per 10-mL culture for CotB1-SC and CotB1p-SC, respectively. The 2-fold higher yield obtained with CotB1p-SC compared to CotB1-SC was due to higher expression of CotB1p-SC in *E. coli* (Tables 3.2 and 3.3).

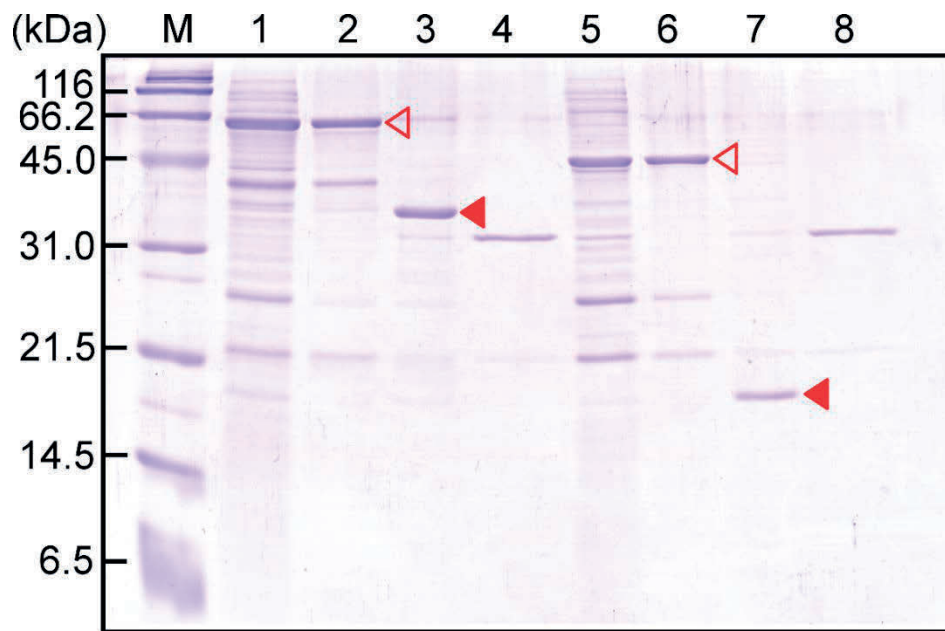


Fig. 3.6 SDS-PAGE analysis (15%) of the affinity purification of mCherry using silica particles as an adsorbent. CotB1 (lanes 1-4) or CotB1p (lanes 5-8) was used as a silica-binding tag. Lanes 1 and 5, cell lysate; lanes 2 and 6, silica-bound fraction; lanes 3 and 7, silica-bound fraction after SUMO protease treatment; lanes 4 and 8, proteins released from solid phase after SUMO protease treatment; lane M, molecular mass markers. For lanes 2, 3, 6, and 7, proteins bound to silica particles were released by boiling in Laemmli sample buffer (65). Proteins were stained with CBB R-250. Open arrowheads indicate the expressed CotB1-SC and CotB1p-SC fusion proteins. Closed arrowheads indicate the CotB1-SUMO and CotB1p-SUMO fragments after SUMO protease treatment. Reprinted with permission from “Affinity purification of recombinant proteins using a novel silica-binding peptide as a fusion tag”, Mohamed A. A. Abdelhamid, Kei Motomura, Takeshi Ikeda, Takenori Ishida, Ryuichi Hirota, and Akio Kuroda. *Applied Microbiology and Biotechnology*, 98:5677-5684 (2014), copyright © Springer.

Table 3.2 Purification of mCherry from *E. coli* using CotB1 as a silica-binding tag^a

Step	Total protein (mg)	Fusion protein (mg) ^b	Target protein (mg)	Purity (%) ^b	Purification (-fold)	Yield (%)
Cell lysate	9.28	1.42	(0.66) ^c	15	1.0	100 ^{b,c}
Silica-binding fraction	4.50	1.35	(0.63) ^c	30	2.0	95 ^{b,c}
SUMO protease elution	0.60	N.D.	0.56 ^b	93	6.2	84 ^b

^a Starting material was approximately 0.1 g wet weight of cells.

^b Determined by densitometric analysis of SDS-PAGE protein bands.

^c Calculated by multiplying the amount of fusion protein by the ratio of the molecular mass of mCherry (26.7 kDa) to the molecular mass of the fusion protein (57.5 kDa).

N.D., not detected.

Table 3.3 Purification of mCherry from *E. coli* using CotB1p as a silica-binding tag^a

Step	Total protein (mg)	Fusion protein (mg) ^b	Target protein (mg)	Purity (%) ^b	Purification (-fold)	Yield (%)
Cell lysate	8.54	1.90	(1.27) ^c	22	1.0	100 ^{b,c}
Silica-binding fraction	5.56	1.68	(1.13) ^c	30	1.4	89 ^{b,c}
SUMO protease elution	1.13	N.D.	1.09	95	4.3	85 ^b

^a Starting material was approximately 0.1 g wet weight of cells.

^b Determined by densitometric analysis of SDS-PAGE protein bands.

^c Calculated by multiplying the amount of fusion protein by the ratio of the molecular mass of mCherry (26.7 kDa) to the molecular mass of the fusion protein (39.9 kDa).

N.D., not detected.

3.3.4 Discussion

In this study, the author found that the *B. cereus* spore coat protein CotB1 and its C-terminal 14-aa peptide CotB1p bind to silica surfaces. The author demonstrated that both proteins function as silica-binding tags when fused to other proteins at either the N- or C-terminus. The resulting fusion proteins can be easily immobilized on silica surfaces by mixing the proteins in solution with silica materials.

The author's results strongly suggest that the 14-aa CotB1p region of CotB1 plays a crucial role in binding to silica because both CotB1p and full-length CotB1 showed comparable affinity for silica (Fig. 3.4). The amino acid sequence of CotB1p (SGRARAQRQSSRGR) is rich in positively charged arginine residues. CotB1p therefore has a high net positive charge, with a theoretical isoelectric point of 12.6. In contrast, the surface of silica is negatively charged under either neutral or basic conditions (71), suggesting that electrostatic attraction is a major driving force behind the binding of CotB1p (and also CotB1) to silica. This is also supported by the fact that the binding of CotB1p was inhibited at high ionic strength; in the presence of 1.0 M NaCl, only 15% of CotB1p-SC bound to the silica particles (data not shown). Although the CotB1/CotB1p fusion proteins constructed in this study have a net negative charge, with theoretical isoelectric points of 5.3-6.8, these proteins bound to silica surfaces via CotB1/CotB1p.

These results suggest that the positive charges in the CotB1p region of the fusion protein are capable of interacting with the negatively charged silica surface even though the net charge of the overall protein molecule is negative.

Although both CotB1 and CotB1p bind to silica, the author believes that the latter is a more promising silica-binding tag because of its small size. The CotB1p fusion protein was expressed more efficiently in *E. coli* than was the CotB1 fusion protein (Tables 3.2 and 3.3). In addition, the CotB1 fusion proteins (i.e., GFP-CotB1 and CotB1-SC) tended to form insoluble inclusion bodies in *E. coli* when expressed at 37°C, whereas both the CotB1p fusions (i.e., GFP-CotB1p and CotB1p-SC) and tagless proteins (i.e., GFP and SUMO-mCherry) were expressed in the soluble form in *E. coli* at 37°C (data not shown). These differences could be attributed to the larger molecular mass of CotB1, as increasing molecular mass tends to negatively affect the expression of fusion proteins.

To use the CotB1/CotB1p tags for silica-based affinity purification of target proteins, SUMO technology was employed to cleave the target protein from the silica-bound fusion protein. Using mCherry as a model target protein, the author demonstrated that this novel affinity purification method is highly efficient. The purity and yield obtained using this method are as high as the values reported by Lichty et al. (2005) for conventional affinity tags. One of the advantages of the developed method is that it

enables the removal of the affinity tag and recovery of a tagless target protein with an authentic N-terminus. Fused affinity tags that remain after purification may affect the intrinsic activity of the target protein and/or interfere with downstream analyses, such as determination of protein structure. The presence of a tag on a target protein is particularly unsuitable for therapeutic applications. Therefore, many approaches (most of which involve protease cleavage at the junction) have been developed to remove affinity tags from recombinant proteins (56, 72). However, the endoproteases that are commonly employed in these approaches have several disadvantages, for example, nonspecific cleavage of the target protein at locations other than the designed site and/or retention of nonnative amino acid(s) in the sequence of the protein of interest (56, 72, 73). In contrast to commonly used endoproteases, which recognize short, linear sequences (generally 4-8 aa), SUMO protease specifically recognizes the tertiary structure of SUMO and cleaves the polypeptide chain at the C-terminal end of the SUMO sequence, enabling the release of peptides or proteins with any desired N-terminal residue except proline (60). Therefore, the developed affinity purification method can be used to recover a wide variety of tagless proteins at high purity. Another advantage of the developed method is that protein elution does not require the addition of any harsh chemicals that could adversely affect protein activity.

Although the amount of SUMO protease used in this study for the release of the target protein was much less than the amount of the recombinant proteins used (see the Results section), further purification of the eluted, cleaved target protein necessitates removal of the SUMO protease from the solution. Because most commercially available SUMO proteases contain a His-tag, they can be easily removed by immobilized metal ion affinity chromatography (63). Albeit beyond the scope of this study, construction of CotB1/CotB1p-fused SUMO proteases might also be useful because these proteins would be retained on silica surfaces along with the CotB1/CotB1p-SUMO fragments after cleavage of the fusion protein.

Because of its small size and high affinity for silica, the CotB1p tag should be a powerful tool not only for the affinity purification application reported in this chapter but also for enzyme immobilization on silica supports and for developing silicon-based biomaterials, as has been reported for other silica-binding peptides and proteins (56, 68, 74-78). The author is currently developing silicon-based biomaterials using this promising tag as an interface.

Chapter 4

Application of volcanic ash particles for protein affinity purification with a minimized silica-binding tag

4.1 Introduction

Several attempts have recently been made to use silica-binding proteins/peptides as affinity tags, because inexpensive, unmodified silica (SiO₂) particles can be used as both the resin and ligand (for the tag) (19, 20, 79). Examples of such elutable, silica-binding tags include bacterial ribosomal protein L2 (also known as Si-tag) (17, 18) and a Car9 peptide (79). The Si-tag shows high affinity for silica and is suitable for stable immobilization of Si-tagged fusion proteins on silica materials. However, with regard to affinity purification, a high affinity may be disadvantageous because it requires rather harsh conditions (e.g., high concentration of divalent cations such as 2 M MgCl₂) for the elution of Si-tagged fusion proteins from silica surfaces (19, 20). Moreover, the large size of the Si-tag (273 amino acids) may negatively affect the intrinsic properties and function of the fusion protein. In contrast, the Car9 tag is a much shorter silica-binding tag (12 amino acids) and can be eluted under milder conditions (e.g., 1 M L-lysine) (79). However, it is still larger than the commonly used affinity tags such as His-tag and FLAG tag (80), which are 6–10 and 8 amino acids, respectively. These drawbacks motivated the author to develop an improved silica-based affinity purification method using a shorter silica-binding tag and milder elution conditions.

Previously, it was reported that silica is deposited on the coat of *Bacillus cereus*

spores and functions as a protective coating under acidic conditions (3). Furthermore, gene disruption analysis previously revealed that the spore coat protein, CotB1 (171 amino acids), mediates silica biomineralization. The polycationic C-terminal sequence of CotB1 (14 amino acids corresponding to residues 158–171), designated CotB1p, could be used as a short silica-binding tag (as mentioned in Chapter 2). Here, the author further shortened the length of this peptide to only seven amino acids while retaining the affinity for silica. Subsequently, a silica-based affinity purification method has been developed using the resultant short silica-binding peptide as an affinity tag, in which the protein of interest is eluted from silica under very mild conditions with 0.3–0.5 M L-arginine. Finally, the author demonstrated that naturally occurring silica-containing volcanic ash (designated *Shirasu*), instead of synthetic, pure silica particles, can be used as an affinity support in the developed method.

4.2 Materials and Methods

4.2.1 Materials

Silica particles (α -quartz), $\sim 0.8 \mu\text{m}$ in diameter, were purchased from Soekawa Chemical Co., Ltd (Tokyo, Japan) and used without any pretreatment. The Shirasu particles used in this study were provided by the Kagoshima Prefectural Institute of Industrial Technology. The Shirasu was harvested from a quarry in Kushira city, Kagoshima, Japan, and was screened through 5 mm and 38 μm mesh sieves and the resultant fine particles were used in this study.

4.2.2 Construction of expression plasmids

To construct expression plasmids for green fluorescent protein (GFP) fusions with truncated sequences of CotB1p, inverse PCR was employed using pET-GFP-CotB1p (constructed in Chapter 3) as the template with the following primer pairs: CB1M-F1/CB1M-R1, CB1M-F2/CB1M-R2, and CB1M-F3/ CB1M-R3 (all primers are listed in Table 4.1). The PCR products were self-ligated to construct pET-GFP-SB8, pET-GFP-SB10, and pET-GFP-SB7, respectively. Subsequently, plasmid pET-GFP-SB7 was used as a template for an additional round of inverse PCR with primer pairs of CB1M-

Table 4.1 Primers used in this study

Name	DNA sequence (5'→3')
CB1M-F1 ^a	TCTTTGTGCACGAGCGCGACCTGA
CB1M-R1 ^a	TAACCTCGAGGCTTAATTAACCTAGGCT
CB1M-F2 ^a	CGTGCACAAAGACAATCAAGTAGA
CB1M-R2 ^a	CGCCAAGGCCTGTACAGAATT
CB1M-F3 ^a	AGACAATCAAGTAGAGGAAGATAA
CB1M-R3 ^a	CGCCAAGGCCTGTACAGAATT
CB1M-F4 ^a	CAATCAAGTAGAGGAAGATAACTCGAG
CB1M-R4 ^a	CGCCAAGGCCTGTACAGAATT
CB1M-F5 ^a	TAACCTCGAGGCTTAATTAACCTAGGCT
CB1M-R5 ^a	TCCTCTACTTGATTGTCTCGCCAAGG
SB7M-F1 ^a	GCACAATCAAGTAGAGGAAGATAA
SB7M-F2 ^a	AGAGCATCAAGTAGAGGAAGATAA
SB7M-F3 ^a	AGACAAGCAAGTAGAGGAAGATAA
SB7M-F4 ^a	AGACAATCAGCTAGAGGAAGATAA
SB7M-F5 ^a	AGACAATCAAGTGCAGGAAGATAA
SB7M-F6 ^a	AGACAATCAAGTAGAGCAAGATAA
SB7M-F7 ^a	AGACAATCAAGTAGAGGAGCATAA
SB7M-R ^a	CGCCAAGGCCTGTACAGAATT
R7-S	AGCTTCGTCGTCGCCGTCGTCGTCGCTAAC
R7-AS	CTAGGTTAGCGACGACGACGGCGACGACGA
SB7-SC-F ^a	CGTCAGTCAAGCCGTGGTCGTG
SB7-SC-R ^a	CATATGTATATCTCCTTCTTAAAGTTAAAC
SB7-mC-F ^a	ATGGTGAGCAAGGGCGAGGAG
SB7-mC-R ^a	ACGACCACGGCTTGACTGACG

^a These primers were phosphorylated at the 5' end.

F4/CB1M-R4 and CB1M-F5/CB1M-R5 to generate two additional plasmids pET-GFP-SB7v1 and pET-GFP-SB7v2, respectively.

To construct seven alanine-scanning mutants of the SB7 peptide (see Results), inverse PCR was employed using pET-GFP-SB7 as a template; SB7M-R and one of SB7M-F (1–7) were used as primers and the PCR products were self-ligated.

Expression plasmids for the hepta-arginine-tagged GFP were constructed as follows: A DNA fragment encoding the nine arginine residues was prepared by annealing synthetic oligonucleotides R7-S and R7-AS. The resultant double-stranded DNA carried a 5'-AGCT overhang at the upstream end and a 5'-CTAG overhang at the downstream end, identical to the cohesive ends of *HindIII*- and *AvrII*-digested fragments, respectively. The DNA fragment was ligated with *HindIII*- and *AvrII*-digested pET-GFP-CotB1 (constructed in Chapter 3) to construct pET-GFP-R7.

To construct expression plasmids for mCherry with an N-terminal SB7-tag (SB7-mCherry), a two-step inverse PCR was employed using pET-CotB1p-SC (constructed in Chapter 3) as the template with the primers SB7-SC-F and SB7-SC-R in the first-round PCR. The amplified DNA were self-ligated and then used as a template in the second-round PCR with the primers SB7-mC-F and SB7-mC-R. The resultant DNA self-ligated to form pET-SB7-mCherry.

4.2.3 Expression of recombinant proteins

The expression plasmids were transformed into *Escherichia coli* Rosetta2 (DE3). The transformants were grown at 37°C in 2× YT medium (30) supplemented with 50 µg/mL of kanamycin, 30 µg/mL of chloramphenicol and 1% (w/v) glucose. When the culture reached an optical density of 0.5 at 600 nm, 0.2 mM isopropyl-β-D-thiogalactopyranoside was added to the medium to induce expression of recombinant proteins. After an additional 3 h of cultivation at 37°C, the cells were harvested by centrifugation and the resulting pellets were stored at –80°C until use.

4.2.4 Silica-binding assay of recombinant proteins

Pellets of recombinant cells harvested from 1 mL cultures (typically 10 mg wet weight of the cells) were suspended in 0.5 mL of 25 mM Tris-HCl buffer (pH 8.0) containing 0.5% (v/v) Tween 20, and disrupted by sonication. After centrifugation at 20,000 × g for 30 min, each supernatant (cleared cell lysate) containing 0.5 mg of total protein was mixed with 0.5 mL of silica-particle suspension in the same buffer (final silica concentration of 40 mg dry weight/mL) for 5 min at room temperature. Silica particles with the bound protein were collected by centrifugation at 5,000 × g for 2 min and then washed thrice with 1 mL of the same buffer. After the supernatant was carefully removed,

proteins that still bound to the particles were released by boiling in sodium dodecyl sulfate (SDS) gel-loading buffer (30) for 5 min and analyzed by SDS-polyacrylamide gel electrophoresis (SDS-PAGE; 12.5%). Gels were stained with Coomassie brilliant blue R-250, and the target protein was quantified by densitometric analysis using the ImageJ software, version 1.41 (66).

4.2.5 Affinity purification of SB7-tagged proteins using silica or Shirasu particles as the adsorbent

Pellets of recombinant cells expressing GFP with a C-terminal SB7-tag (GFP-SB7) or SB7-mCherry harvested from 5–10 mL cultures (~0.05–0.1 g wet weight of cells) were suspended in 2 mL of 25 mM Tris-HCl buffer (pH 8.0) containing 0.5% (v/v) Tween 20 and disrupted by sonication. After centrifugation at $20,000 \times g$ for 30 min, cleared cell lysates were mixed with 0.4 g dry weight of silica particles or with 0.35 g dry weight of Shirasu particles by gentle rotation for 5 min at room temperature. After centrifugation at $5,000 \times g$ for 2 min, the particles were washed thrice with 2 mL of the same buffer. Proteins were eluted by resuspending the particles with 2 mL of 25 mM Tris-HCl buffer (pH 8.0) containing 0.5 or 0.3 M L-arginine for silica and Shirasu particles, respectively. The suspension was centrifuged at $5,000 \times g$ for 2 min. The resultant supernatant

containing the eluted proteins was collected. The elution step was repeated (total volume of eluted fractions was 4 mL).

For comparison, GFP-SB7, which also contains an N-terminal His-tag, was purified from the same amount of cells by His-tag affinity purification using Ni-NTA agarose (Qiagen GmbH, Germany). Purification was performed per the batch purification protocol provided by the manufacturer.

4.2.6 Protein assay

The protein concentration was determined with the Bio-Rad Protein Assay reagent (Bio-Rad, Hercules, CA) with bovine serum albumin as the standard.

4.3 Results and Discussion

4.3.1 Minimization of the silica-binding CotB1p tag

To minimize the size [length] of the 14-amino-acid silica-binding CotB1p-tag (SGRARAQRQSSRGR), the following three truncated mutants of CotB1p were fused to the C-terminus of GFP: T1 (SGRARAQR, corresponding to residues 1–8 of the CotB1p peptide), T2 (RAQRQSSRGR, corresponding to residues 5–14 of the CotB1p peptide), and T3 (RQSSRGR, corresponding to residues 8–14 of the CotB1p peptide). The affinity of these peptides for silica in 25 mM Tris-HCl buffer (pH 8.0) containing 0.5% (v/v) Tween 20 was compared to that of the original CotB1p; the surfactant Tween 20 was added to the buffer to prevent weak, non-specific interactions with the surface of silica particles. Densitometric analysis of the protein bands obtained on SDS-PAGE gels showed that more than 80% of GFP-CotB1p bound to silica particles, whereas GFP alone hardly bound to silica under the conditions used (Fig. 4.1). Although the truncated mutant T1 showed relatively weak binding (about 70% of the protein bound to silica particles), affinities of T2 and T3 were comparable to that of original CotB1p (Fig. 4.1). Because further truncation of the smallest peptide T3 (i.e., removal of the first or seventh arginine residue of the RQSSRGR sequence) caused significant reduction in affinity for silica (Fig. 4.1, T3-v1 and T3-v2), the author chose T3 (hereafter renamed as SB7 tag) as the optimal peptide for further investigation, as its short length did not compromise its high affinity.

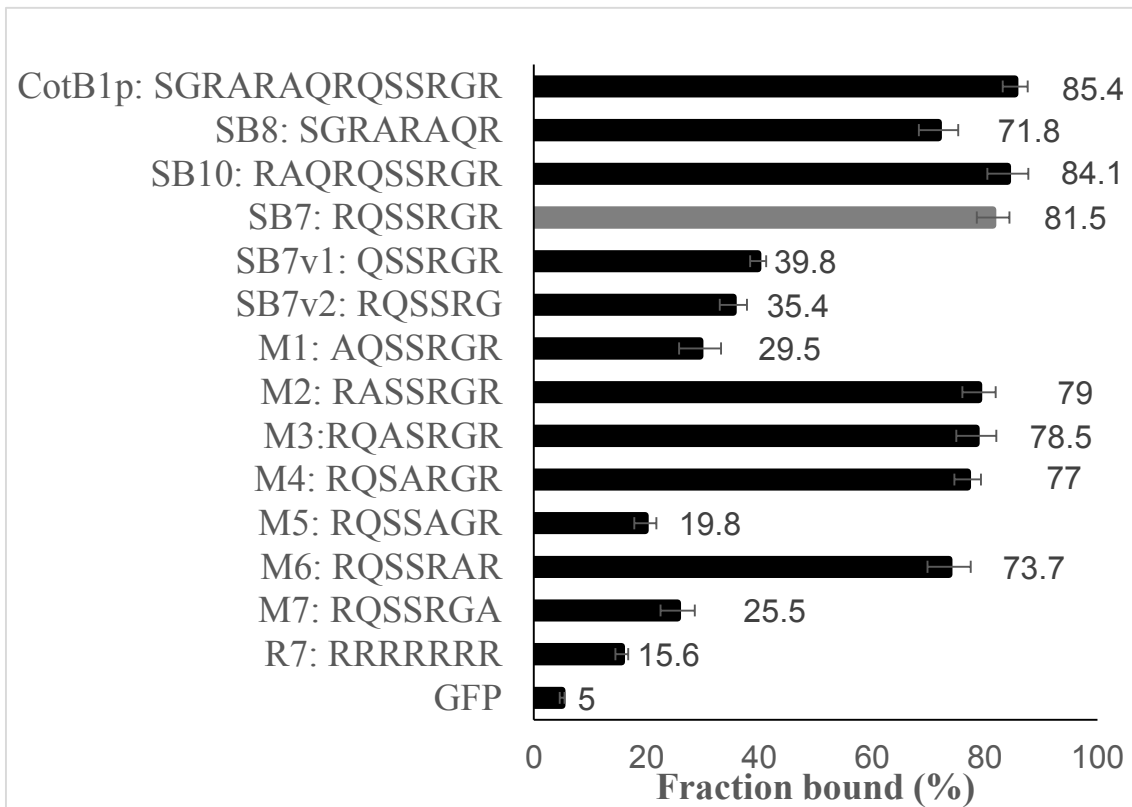


Fig. 4.1 Minimization of the silica-binding CotB1p tag and identification of amino acids important for silica binding. These data represent the percentage of a tagged GFP that bound to silica particles in 25 mM Tris-HCl (pH 8.0) containing 0.5% Tween 20. Data of hepta-arginine -tagged GFP are provided for comparison. Values are means \pm standard deviations of triplicate measurements.

4.3.2 Alanine scanning mutagenesis of the SB7 peptide

To gain a better understanding of the binding mechanism of SB7, alanine scanning mutagenesis was performed for all seven residues of SB7 in GFP-SB7 (Fig. 4.1). As expected, the author found that the three arginine residues are essential for strong binding to silica; when one of the arginine residues was replaced with alanine, the fraction bound to silica drastically reduced from 81% to 30% or less (Fig. 4.1; M1, M5, and M7). Alanine replacement of one of the other residues (glutamine, two serine, and glycine residues) did not significantly affect binding to silica, suggesting the relatively lesser contribution of these residues (Fig. 4.1; M2–4 and M6). Unexpectedly, when all seven residues were replaced with arginine, the resultant hepta-arginine peptide (i.e. RRRRRRR sequence) showed much weaker binding to silica than did the original SB7 despite the fact that the former has a higher net positive charge than the latter (Fig. 4.1; hepta-arginine).

4.3.3 L-Arginine as an efficient eluent for the silica-bound SB7 tag

The established use of L-lysine solution for efficient release of a silica-bound tag rich in positively charged lysine residues in a competitive manner and the fact that arginine residues in the SB7 tag play important roles in silica binding prompted the author

to use L-arginine as a competitive eluent to release SB7-tagged proteins from the surface of silica particles. As expected, by using 0.5 M arginine solution (pH 8.0) as an eluent, the author succeeded in recovering more than 90% of bound GFP-SB7 from silica particles in a functional form (see below).

The feasibility of affinity purification of SB7-tagged proteins was validated. SDS-PAGE analysis of bound and unbound proteins (Fig. 4.2) showed that GFP-SB7 was the major protein that bound to silica particles under these conditions (Fig. 4.2, lane 3); very little amount of the fusion protein remained in the unbound fraction (Fig. 4.2, lane 2), indicating that most of the expressed GFP-SB7 bound to silica particles. To recover the GFP-SB7, the previously described elution step was performed and the bound GFP-SB7 was released into the supernatant (Fig. 4.2, lane 5). This elution step was repeated to maximize purification yield. After the two elution steps, a small amount of GFP-SB7 remained bound to the silica particles (Fig. 4.2, lane 4), indicating that L-arginine serves as an efficient eluent for the SB7-tag. Moreover, the eluted fraction showed the ratio of absorbance at 280 nm to that at 260 nm of >1.6 , indicating little, if any, contamination with nucleic acids (81). Table 4.2 shows typical results from the purification. The purity and recovery of the protein were evaluated to be $91\% \pm 3\%$ and $78 \pm 3\%$ (mean \pm standard deviation from three independent experiments), respectively.

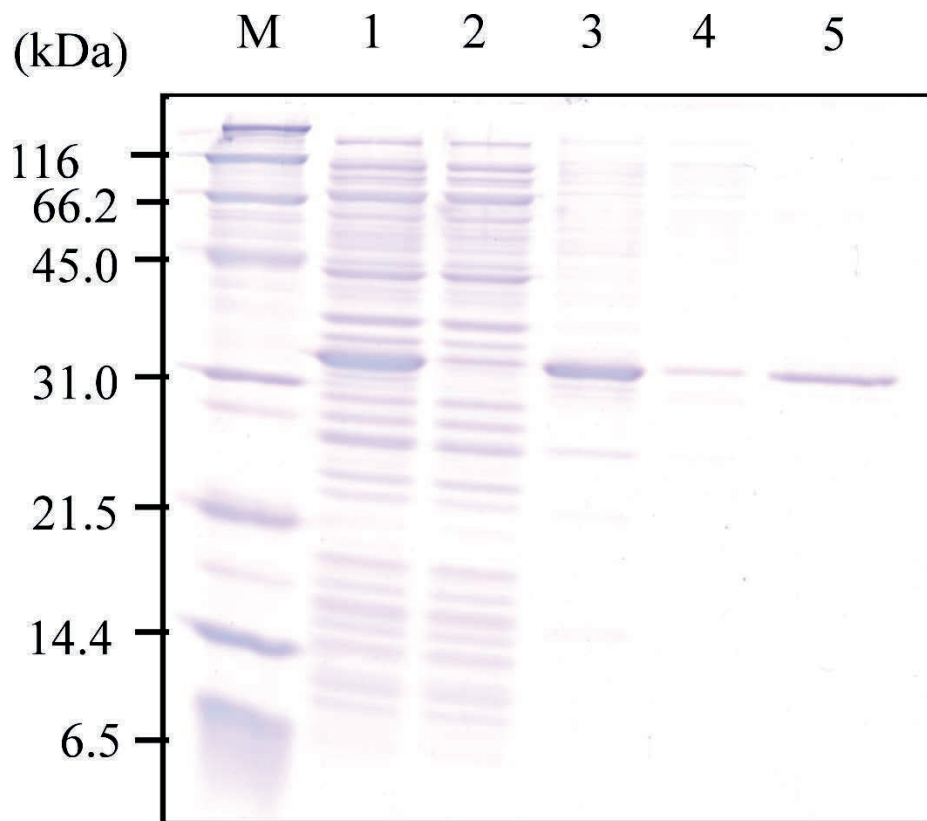


Fig. 4.2 SDS-PAGE analysis of the affinity purification fractions of GFP-SB7 using silica particles and L-arginine as the adsorbent and eluent, respectively. The arrowhead indicates the position of GFP-SB7. Lane 1, cleared cell lysate; lane 2, silica-unbound fraction; lane 3, silica-bound fraction; lane 4, silica-bound fraction after L-arginine elution; lane 5, L-arginine-eluted fraction; lane M, molecular mass markers. For lanes 3 and 4, proteins bound to silica particles were released by boiling in SDS gel-loading sample buffer (30).

4.3.4 Affinity purification of SB7-tagged proteins by using natural silica-containing particles as the adsorbent

To minimize the cost for affinity purification, the author next tested the feasibility of using natural silica-containing volcanic ash particles (Shirasu), instead of synthetic, pure silica particles, as the adsorbent for affinity purification of SB7-tagged proteins. Purification of GFP-SB7 was conducted as described above except that Shirasu particles were used instead of silica particles and the L-arginine concentration in the elution buffer was reduced from 0.5 M to 0.3 M. Table 4.2 and Fig. 4.3 (lanes 1-5) compare typical purification results obtained with silica or Shirasu particles as the adsorbent. Despite the lower L-arginine concentration, GFP-SB7 was efficiently released from Shirasu particles (Fig. 4.3, lane 5), leaving virtually no residual GFP-SB7 bound to the particles (Fig. 4.3, lane 4). The yield and purity were comparable to those obtained using silica particles with 0.5 M L-arginine (Fig. 4.3, lanes 2 and 3). By contrast, only 60% of the bound GFP-SB7 was released from silica particles with 0.3 M L-arginine (data not shown). Efficient release of GFP-SB7 from Shirasu particles with lower L-arginine concentration indicates a lower affinity of SB7 for Shirasu than for pure silica. Such differences can be ascribed to the lower silica content and, possibly, to the presence of alumina in Shirasu. In contrast to negatively charged silica surfaces, alumina surfaces are

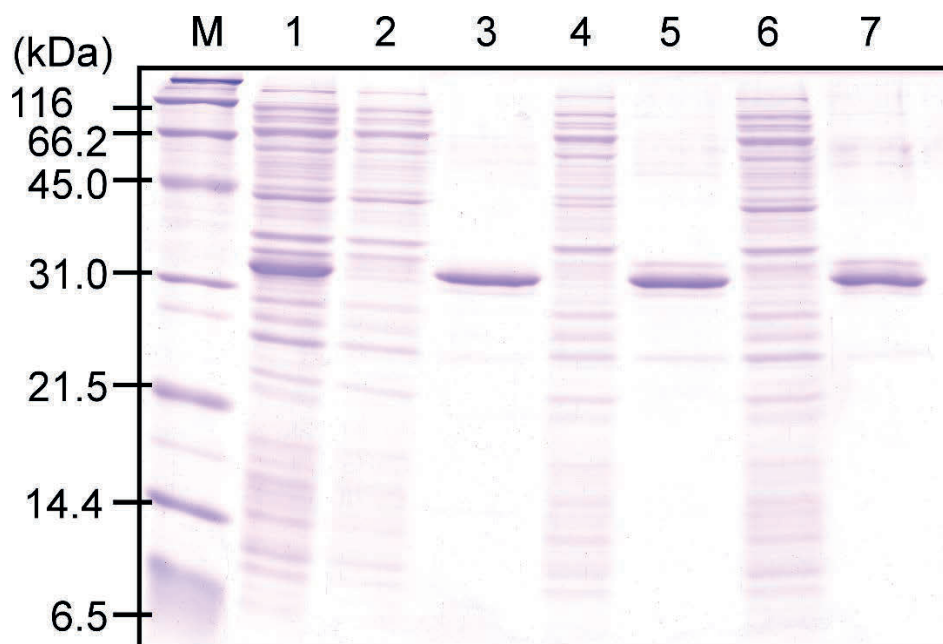


Fig. 4.3 Comparative analysis of SB7-tag and His-tag purification by SDS-PAGE. GFP-SB7 was purified from the recombinant *E. coli* by SB7-tag purification using silica (lanes 2 and 3) or Shirasu particles (lanes 4 and 5) as an adsorbent, or by His-tag purification using Ni-NTA resin (lanes 6 and 7). The arrowhead indicates the position of GFP-SB7. Lane 1, cleared cell lysate; lanes 2, 4, and 6, unbound fractions for silica, Shirasu, and Ni-NTA, respectively; lanes 3, 5 and 7, eluted fraction from silica, Shirasu, and Ni-NTA, respectively; lane M, molecular mass markers.

electrically neutral or even slightly positively charged in aqueous solutions at pH 8 (82). Therefore, the presence of alumina might moderately attenuate the interaction between the SB7-tag and silica surface in Shirasu, thus reducing the L-arginine concentration required for eluting the tag.

For comparison of purification efficiency to the widely used His-tag affinity purification, cleared cell lysate containing GFP-SB7, which has an N-terminal His-tag, was also subjected to immobilized metal-ion affinity chromatography using Ni-NTA resin according to the manufacturer's recommendation; GFP-SB7 was adsorbed onto the Ni-NTA resin and then released by addition of 0.5 M imidazole. Table 4.3 shows the typical results of His-tag affinity purification, and lanes 6 and 7 in Fig. 4.3 show the SDS-PAGE analysis of the unbound and released proteins, respectively. The comparison of SB7-tag and His-tag purifications indicate that SB7-tag purification results in similar purity and higher yield than that achieved with His-tag purification (Fig. 4.3, and compare Tables 4.2 and 4.3).

Table 4.2 SB7-tag purification of GFP-SB7 from *E. coli* using silica or Shirasu particles as an adsorbent^a

Step	Total protein (mg)	Amount of GFP-SB7 (mg) ^b	Purity (%) ^b	Purification (-fold)	Yield (%) ^b
Cell lysate	4.83	0.69	14	1	100
Eluted fraction from silica	0.59	0.54	91	6.4	78
Eluted fraction from Shirasu	0.71	0.63	88	6.2	91

^a One of three aliquots of the cell lysate was subjected to affinity purification using silica particles as the adsorbent, and another was subjected to purification using Shirasu particles as the adsorbent; the remaining one was subjected to His-tag purification (see Table 4.3). The starting material was approximately 0.1 g (wet weight) each of cells.

^b Determined by densitometric analysis of the protein bands on SDS-polyacrylamide gel.

Table 4.3 His-tag purification of GFP-SB7 from *Escherichia coli*^a

Step	Total protein (mg)	Amount of GFP-SB7 (mg) ^b	Purity (%) ^b	Purification (-fold)	Yield (%) ^b
Cell lysate	4.83	0.69	14	1	100
Eluted fraction	0.59	0.52	89	6.2	76

^a The starting material was approximately 0.1 g wet weight of cells.

^b Determined by densitometric analysis of the protein bands on a SDS-polyacrylamide gel.

To test the versatility of the developed purification method, another protein mCherry with an N-terminal SB7-tag (SB7-mCherry) was used (Table 4.4 and Fig. 4.4). This protein also bound efficiently to Shirasu particles (Fig. 4.4, lane 2) and was released from the particles and obtained with high purity and yield when eluted with 0.3 M L-arginine solution (Fig. 4.4, lane 3). These results further support the efficiency of the developed method and demonstrate that the SB7 peptide can function as an affinity tag when fused to other proteins at either the N- or C-terminus.

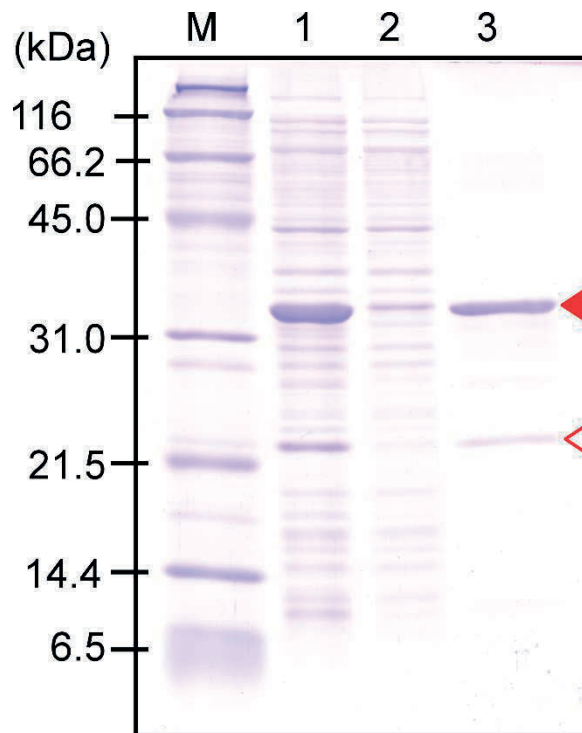


Fig. 4.4 SDS-PAGE analysis of the affinity purification fractions of SB7-mCherry with Shirasu particles as an adsorbent. Closed arrowhead indicates the position of SB7-mCherry. The band indicated by the open arrowhead is an mCherry fragment derived from partial hydrolysis of the chromophore acylimine bond during protein boiling (83). Lane 1, clear cell lysate; lane 2, silica-unbound fraction; lane 3, L-arginine-eluted fraction; lane M, molecular mass markers.

Table 4.4 SB7-tag purification of SB7-mCherry from *E. coli* using Shirasu particles as an adsorbent^a

Step	Total protein (mg)	Amount of SB7-mCherry (mg) ^b	Purity (%) ^b	Purification (-fold)	Yield (%) ^b
Cell lysate	2.15	0.59	27	1	100
Eluted fraction	0.575	0.51	89	3.3	88

^a The starting material was approximately 50 mg wet weight of cells.

^b Determined by densitometric analysis of the protein bands on a SDS-polyacrylamide gel.

4.3.5 Discussion

Shorter affinity tags are preferable to longer ones as they are less likely to affect the intrinsic properties and functions of the fusion partner. Hence, in this study, the seven-amino-acid silica-binding SB7-tag was successfully constructed by minimizing the length of the previously reported CotB1p-tag. Its length is comparable to that of the commonly used His-tag (6–10 amino acids). High abundance of positively charged arginine residues in the SB7 tag (and original CotB1p) suggested that these residues play important roles in binding to silica. Electrostatic attraction between positively charged amino acid residues and the negatively charged silica surface has been reported to be a major driving force of silica-binding proteins/peptides (19, 20, 68, 79, 84, 85). Alanine scanning mutagenesis of the SB7-tag and comparison with the hepta-arginine tag (Fig. 4.1) strongly suggested that not only positively charged arginine residues but also uncharged non-arginine residues in the SB7 sequence play important roles in the binding to negatively charged silica surfaces, most probably as spacers between the positively charged arginine residues. Low affinity of the hepta-arginine sequence for silica could be ascribed to structural confinement of the peptides derived from intramolecular repulsion between positively charged arginine side chains; although polyarginine peptides adopt an extended, random coil-like conformation, their conformational flexibility is somewhat restricted by

the presence of the intramolecular repulsion (86, 87). This might result in unsuitable configurations of the positive charges for silica binding. Consistent with this observation, other researchers have reported the importance of peptide conformational flexibility in binding to solid surfaces (88).

Using the SB7-tag as an affinity tag, a novel affinity purification method has been developed, in which silica or Shirasu particles serve as the adsorbent for SB7-tagged proteins, with L-arginine as the eluent. The major advantages of the author's method are the small size of the tag (only seven amino acids in length), cost-effectiveness of the adsorbents, and mild elution with L-arginine, the last two of which are further discussed below.

Silica has been widely used as a chromatographic support because of its superior mechanical strength and chemical stability. By contrast to conventional affinity purification methods, which require a ligand to be immobilized on a support, the author utilized unmodified bare silica itself as both a support and ligand for an SB7-tag. Because of the low cost of silica particles, this method is much less expensive than conventional affinity purification methods. On the basis of the actual purification results (Tables 4.2 and 4.3) and retail prices of the materials used, the author calculated the resin costs for 1 mg GFP purification to be about \$0.9 for SB7 tag and \$5 for His-tag. Elution costs for

these tags were negligible (<\$0.1) because the eluents, L-arginine and imidazole, respectively, are inexpensive. Although silica is also used as an adsorbent for nucleic acids, silica interacts with them only in the presence of chaotropic salts (e.g., NaI, NaClO₄, and guanidinium thiocyanate) (89-91). Because nucleic acids did not bind to silica surfaces under the conditions used, the author did not apply any steps for nucleic acid removal prior to the purification, making the approach less time-consuming. Furthermore, the use of the natural silica-containing particles (i.e., Shirasu) as the adsorbent could further reduce the purification cost. Shirasu is mainly composed of silica (71%–73%) and aluminum oxide (alumina; Al₂O₃) (13–15%) (92) and is widely distributed in large quantities among the southern Kyushu region of Japan (93). Size-separated shirasu particles are used in various applications, depending on their size, as construction materials, thermal insulation materials, cosmetics, etc. The availability of the particles of well-defined size are suitable as an affinity support. The use of the low-cost natural particles as an affinity support enables further reduction in purification cost. Because of their chemical stability, silica and Shirasu can endure harsh cleaning procedures and can be recovered and reused without loss of binding capacities, resulting in further cost saving.

The addition of L-arginine to a protein solution has been reported to stabilize the protein against aggregation (94, 95). The author's method utilizes only L-arginine as an

eluent and does not require any other additives that could adversely affect protein structure and/or function. Therefore, the author believes that the developed method would be suitable to purify relatively unstable, aggregation-prone proteins while preserving their intrinsic activity. In addition, L-arginine has also been reported to suppress weak protein-surface interactions (96). This property might play a role in efficient elution in the purification process by reducing re-binding of released SB7-tagged proteins.

Taken together, the small size of the SB7 tag, in combination with the protein-stabilizing effect of L-arginine, would help minimize alteration of the intrinsic properties of target proteins during purification. The SB7 tag allows natural silica-containing materials to be used as an affinity support, resulting in a considerable reduction in purification costs. This approach paves the way for the use of naturally occurring materials as adsorbents for simple, low-cost affinity purification.

Chapter 5
General conclusion

Silicon (Si), the second most abundant element in the Earth's crust, is an important mineral for living organisms. In eukaryotes ranging from microorganisms to higher plants, silicon is taken up as silicic acid, then condensed as biogenic silica through natural process, named biosilicification. In the work described in this thesis, the author identified the first prokaryotic protein involved in biosilicification. Moreover, this protein has been utilized for engineering silica-binding tags for protein immobilization and purification.

In chapter 2, the protein causing the formation of silica layer in and around *Bacillus cereus* spore coat has been determined. Several peptides and proteins, including diatom silaffin and silacidin peptides, are involved in eukaryotic silica biomineralization (biosilicification). Homologous sequence search revealed a silacidin-like sequence in the C-terminal region of CotB1, a spore coat protein of *B. cereus*. The negatively charged silacidin-like sequence is followed by a positively charged arginine-rich sequence of 14 amino acids, which is remarkably similar to the silaffins. These sequences impart a zwitterionic character to the C-terminus of CotB1. Interestingly, the *cotB1* gene appears to form a bicistronic operon with its paralog, *cotB2*, the product of which, however, lacks the C-terminal zwitterionic sequence. A $\Delta cotB1B2$ mutant strain grew as fast and formed spores at the same rate as wild-type bacteria, but did not show biosilicification.

Complementation analysis showed that CotB1, but neither CotB2 nor C-terminally truncated mutants of CotB1, could restore the biosilicification activity in the $\Delta cotB1B2$ mutant, suggesting that the C-terminal zwitterionic sequence of CotB1 is essential for the process. The author found that the kinetics of CotB1 expression, as well as its localization, correlated well with the time course of biosilicification and the location of the deposited silica. This is the first report of a protein directly involved in prokaryotic biosilicification.

Building upon this research, novel silica-binding tags have been engineered for protein purification and immobilization (Chapter 3). The author demonstrated that *B. cereus* CotB1 (171 amino acids [aa]) and its C-terminal 14-aa region (corresponding to residues 158-171, designated CotB1p) show strong affinity for silica particles, with dissociation constants at pH 8.0 of 2.09 and 1.24 nM, respectively. Using CotB1 and CotB1p as silica-binding tags, a silica-based affinity purification method has been developed in which silica particles are used as an adsorbent for CotB1/CotB1p fusion proteins. Small ubiquitin-like modifier (SUMO) technology was employed to release the target proteins from the adsorbed fusion proteins. SUMO-protease mediated site-specific cleavage at the C-terminus of the fused SUMO sequence released the tagless target proteins into the liquid phase while leaving the tag region still bound to the solid phase. Using the fluorescent protein mCherry as a model, this purification method achieved 85 %

recovery, with a purity of 95% and yields of 0.60 ± 0.06 and 1.13 ± 0.13 mg per 10-mL bacterial culture for the CotB1-SUMO-mCherry and CotB1p-SUMO-mCherry fusions, respectively. CotB1p demonstrated high affinity for silica and is a promising fusion tag for both affinity purification and enzyme immobilization on silica supports.

Furthermore, the author developed a method utilizing an even shorter silica-binding tag and mild elution conditions for silica-based affinity purification (Chapter 4). The C-terminal 7-aa region of CotB1p peptide (designated SB7-tag), a short silica-binding peptide, has been used as an affinity tag with L-arginine as an eluent. The combination of the protein-stabilizing effect of L-arginine and small size of the tag would help minimize alteration of the intrinsic properties of target proteins. The author also demonstrated that “shirasu”, volcanic ash broadly deposited in Southern Kyushu, can be used as an affinity support in the developed method, thus enabling purification of recombinant proteins at much lower cost compared to the commercially available silica particles. This affinity method enables purification of recombinant proteins at low cost with the purity and yield comparable with the commonly used His-tag purification method.

In conclusion, this research includes the first identification and characterization of prokaryotic protein involved in biosilicification, and the application of this protein (as

well as the peptides derived from CotB1) to protein purification and immobilization. However, further study is needed for the complete understanding of the molecular mechanism of biosilicification. In particular, identification of the genes and proteins that control the transport of silicon in its soluble form (silicic acid) into the bacterial cell is important for fully understanding of biosilicification.

References

1. **Lowenstam HA, Weiner S.** 1989. On biomineralization. Oxford University Press, New York.
2. **Patwardhan S.** 2011. Biomimetic and bioinspired silica: Recent developments and applications. *Chem. Commun* **47**: 7567-7582.
3. **Hirota R, Hata Y, Ikeda T, Ishida T, Kuroda A.** 2010. The silicon layer supports acid resistance of *Bacillus cereus* spores. *J Bacteriol* **192**:111-116.
4. **Doi K, Fujino Y, Inagaki F, Kawatsu R, Tahara M, Ohshima T, Okaue Y, Yokoyama T, Iwai S, Ogata S.** 2009. Stimulation of Expression of a Silica-Induced Protein (Sip) in *Thermus thermophilus* by Supersaturated Silicic Acid. *Appl. Environ Microbiol* **75**: 2406-2413.
5. **Epstein E.** 1999. Silicon. *Annu Rev Plant Physiol Plant Mol Biol* **50**:641-664.
6. **Round FE, Crawford RM, Mann DG.** 1990. The diatoms: biology and morphology of the genera. Cambridge University Press, Cambridge.
7. **Kroger N, Deutzmann R, Sumper M.** 1999. Polycationic peptides from diatom biosilica that direct silica nanosphere formation. *Science* **286**:1129-1132.

8. **Scheffel A, Poulsen N, Shian S, Kroger N.** 2011. Nanopatterned protein microrings from a diatom that direct silica morphogenesis. *Proc Natl Acad Sci USA* **108**:3175-3180.
9. **Wenzl S, Hett R, Richthammer P, Sumper M.** 2008. Silacidins: highly acidic phosphopeptides from diatom shells assist in silica precipitation in vitro. *Angew Chem Int Ed* **47**:1729-1732.
10. **Kroger N, Lorenz S, Brunner E, Sumper M.** 2002. Self-assembly of highly phosphorylated silaffins and their function in biosilica morphogenesis. *Science* **298**:584-586.
11. **Otzen D.** 2012. The role of proteins in biosilicification. *Scientifica* **2012**:ID 867562.
12. **Sumper M, Kroger N.** 2004. Silica formation in diatoms: the function of long-chain polyamines and silaffins. *J Mater Chem* **14**:2059-2065.
13. **Richthammer P, Bormel M, Brunner E, van Pee KH.** 2011. Biomineralization in diatoms: the role of silacidins. *ChemBioChem* **12**:1362-1366.
14. **Johnstone K, Ellar DJ, Appleton TC.** 1980. Location of metal ions in *Bacillus megaterium* spores by high-resolution electron probe X-ray microanalysis. *FEMS Microbiol Lett* **7**:97-101.

15. **Stewart M, Somlyo AP, Somlyo AV, Shuman H, Lindsay JA, Murrell WG.** 1980. Distribution of calcium and other elements in cryosectioned *Bacillus cereus* T spores, determined by high-resolution scanning electron probe X-ray microanalysis. *J Bacteriol* **143**:481-491.
16. **Lechner CC, Becker CFW.** 2015. Silaffins in silica biomineralization and biomimetic silica precipitation. *Marine Drugs* **13**: 5297-5333.
17. **Ikeda T, Kuroda A.** 2011. Why does the silica-binding protein "Si-tag" bind strongly to silica surfaces? Implications of conformational adaptation of the intrinsically disordered polypeptide to solid surfaces. *Colloids Surf B: Biointerfaces* **86**:359-363.
18. **Taniguchi K, Nomura K, Hata Y, Nishimura T, Asami Y, Kuroda A.** 2007. The Si-tag for immobilizing proteins on a silica surface. *Biotechnol Bioeng* **96**:1023-1029.
19. **Ikeda T, Motomura K, Agou Y, Ishida T, Hirota R, Kuroda A.** 2011. The silica-binding Si-tag functions as an affinity tag even under denaturing conditions. *Protein Expr Purif* **77**:173-177.
20. **Ikeda T, Ninomiya K, Hirota R, Kuroda A.** 2010. Single-step affinity purification of recombinant proteins using the silica-binding Si-tag as a fusion partner. *Protein Expr Purif* **71**:91-95.

21. **Lichty JJ, Malecki JL, Agnew HD, Michelson-Horowitz DJ, Tan S.** 2005. Comparison of affinity tags for protein purification. *Protein Expr Purif* **41**:98-105.
22. **Malhotra A.** 2009. Tagging for protein expression. *Methods Enzymol* **463**:239-258.
23. **Waugh DS.** 2005. Making the most of affinity tags. *Trends Biotechnol* **23**:316-320.
24. **Nicholson WL, Munakata N, Horneck G, Melosh HJ, Setlow P.** 2000. Resistance of *Bacillus* endospores to extreme terrestrial and extraterrestrial environments. *Microbiol Mol Biol Rev* **64**:548-572.
25. **Driks A.** 1999. *Bacillus subtilis* spore coat. *Microbiol Mol Biol Rev* **63**:1-20.
26. **Henriques AO, Moran CP, Jr.** 2000. Structure and assembly of the bacterial endospore coat. *Methods* **20**:95-110.
27. **Henriques AO, Moran CP, Jr.** 2007. Structure, assembly, and function of the spore surface layers. *Annu Rev Microbiol* **61**:555-588.
28. **Kroger N, Deutzmann R, Sumper M.** 2001. Silica-precipitating peptides from diatoms: the chemical structure of silaffin-1A from *Cylindrotheca fusiformis*. *J Biol Chem* **276**:26066-26070.
29. **Ivanova N, Sorokin A, Anderson I, Galleron N, Candelon B, Kapatral V, Bhattacharyya A, Reznik G, Mikhailova N, Lapidus A, Chu L, Mazur M, Goltzman E, Larsen N, D'Souza M, Walunas T, Grechkin Y, Pusch G, Haselkorn**

- R, Fonstein M, Ehrlich SD, Overbeek R, Kyrpides N.** 2003. Genome sequence of *Bacillus cereus* and comparative analysis with *Bacillus anthracis*. *Nature* **423**:87-91.
30. **Green MR, Sambrook J.** 2012. *Molecular cloning: a laboratory manual*, 4th ed. Cold Spring Harbor Laboratory Press, Cold Spring Harbor, New York.
31. **Reasoner DJ, Geldreich EE.** 1985. A new medium for the enumeration and subculture of bacteria from potable water. *Appl Environ Microbiol* **49**:1-7.
32. **Harwood CR, Cutting SM.** 1990. *Molecular biological methods for Bacillus*. John Wiley & Sons, Chichester, United Kingdom.
33. **Arnaud M, Chastanet A, Debarbouille M.** 2004. New vector for efficient allelic replacement in naturally nontransformable, low-GC-content, gram-positive bacteria. *Appl Environ Microbiol* **70**:6887-6891.
34. **Steinmetz M, Richter R.** 1994. Easy cloning of mini-Tn10 insertions from the *Bacillus subtilis* chromosome. *J Bacteriol* **176**:1761-1763.
35. **Turgeon N, Laflamme C, Ho J, Duchaine C.** 2006. Elaboration of an electroporation protocol for *Bacillus cereus* ATCC 14579. *J Microbiol Methods* **67**:543-548.

36. **Murphy E.** 1985. Nucleotide sequence of a spectinomycin adenyltransferase AAD(9) determinant from *Staphylococcus aureus* and its relationship to AAD(3") (9). Mol Gen Genet **200**:33-39.
37. **Isticato R, Esposito G, Zilhao R, Nolasco S, Cangiano G, De Felice M, Henriques AO, Ricca E.** 2004. Assembly of multiple CotC forms into the *Bacillus subtilis* spore coat. J Bacteriol **186**:1129-1135.
38. **Updyke TV, Engelhorn SC.** 2000. System for pH-neutral stable electrophoresis gel. United States patent 6,162,338.
39. **Arantes O, Lereclus D.** 1991. Construction of cloning vectors for *Bacillus thuringiensis*. Gene **108**:115-119.
40. **Eichenberger P, Fujita M, Jensen ST, Conlon EM, Rudner DZ, Wang ST, Ferguson C, Haga K, Sato T, Liu JS, Losick R.** 2004. The program of gene transcription for a single differentiating cell type during sporulation in *Bacillus subtilis*. PLoS Biol **2**:1664-1683.
41. **Aronson A, Goodman B, Smith Z.** 2014. The regulated synthesis of a *Bacillus anthracis* spore coat protein that affects spore surface properties. J Appl Microbiol **116**:1241-1249.

42. **Todd SJ, Moir AJG, Johnson MJ, Moir A.** 2003. Genes of *Bacillus cereus* and *Bacillus anthracis* encoding proteins of the exosporium. *J Bacteriol* **185**:3373-3378.
43. **Abhyankar W, Hossain AH, Djajasaputra A, Permpoonpattana P, Ter Beek A, Dekker HL, Cutting SM, Brul S, de Koning LJ, de Koster CG.** 2013. In pursuit of protein targets: proteomic characterization of bacterial spore outer layers. *J Proteome Res* **12**:4507-4521.
44. **Cutting S, Zheng LB, Losick R.** 1991. Gene encoding two alkali-soluble components of the spore coat from *Bacillus subtilis*. *J Bacteriol* **173**:2915-2919.
45. **Donovan W, Zheng L, Sandman K, Losick R.** 1987. Genes encoding spore coat polypeptides from *Bacillus subtilis*. *J Mol Biol* **196**:1-10.
46. **Zilhao R, Serrano M, Isticato R, Ricca E, Moran CP, Jr., Henriques AO.** 2004. Interactions among CotB, CotG, and CotH during assembly of the *Bacillus subtilis* spore coat. *J Bacteriol* **186**:1110-1119.
47. **Kim H, Hahn M, Grabowski P, McPherson DC, Otte MM, Wang R, Ferguson CC, Eichenberger P, Driks A.** 2006. The *Bacillus subtilis* spore coat protein interaction network. *Mol Microbiol* **59**:487-502.
48. **Mallozzi M, Bozue J, Giorno R, Moody KS, Slack A, Cote C, Qiu DL, Wang R, McKenney P, Lai EM, Maddock JR, Friedlander A, Welkos S, Eichenberger P,**

- Driks A.** 2008. Characterization of a *Bacillus anthracis* spore coat-surface protein that influences coat-surface morphology. *FEMS Microbiol Lett* **289**:110-117.
49. **Thompson BM, Hsieh HY, Spreng KA, Stewart GC.** 2011. The co-dependence of BxpB/ExsFA and BclA for proper incorporation into the exosporium of *Bacillus anthracis*. *Mol Microbiol* **79**:799-813.
50. **Cha JN, Shimizu K, Zhou Y, Christiansen SC, Chmelka BF, Stucky GD, Morse DE.** 1999. Silicatein filaments and subunits from a marine sponge direct the polymerization of silica and silicones *in vitro*. *Proc Natl Acad Sci U S A* **96**:361-365.
51. **Shimizu K, Cha J, Stucky GD, Morse DE.** 1998. Silicatein \square : cathepsin L-like protein in sponge biosilica. *Proc Natl Acad Sci U S A* **95**:6234-6238.
52. **Martin-Jezequel V, Hildebrand M, Brzezinski MA.** 2000. Silicon metabolism in diatoms: Implications for growth. *J Phycol* **36**:821-840.
53. **Thamatrakoln K, Hildebrand M.** 2008. Silicon uptake in diatoms revisited: a model for saturable and nonsaturable uptake kinetics and the role of silicon transporters. *Plant Physiol* **146**:1397-1407.
54. **Ma JF, Tamai K, Yamaji N, Mitani N, Konishi S, Katsuhara M, Ishiguro M, Murata Y, Yano M.** 2006. A silicon transporter in rice. *Nature* **440**:688-691.

55. **Ma JF, Yamaji N, Mitani N, Tamai K, Konishi S, Fujiwara T, Katsuhara M, Yano M.** 2007. An efflux transporter of silicon in rice. *Nature* **448**:209-212.
56. **Arnau J, Lauritzen C, Petersen GE, Pedersen J.** 2006. Current strategies for the use of affinity tags and tag removal for the purification of recombinant proteins. *Protein Expr Purif* **48**:1-13.
57. **Terpe K.** 2003. Overview of tag protein fusions: From molecular and biochemical fundamentals to commercial systems. *Appl Microbiol Biotechnol* **60**:523-533.
58. **Pamirsky IE, Golokhvast KS.** 2013. Silaffins of diatoms: From applied biotechnology to biomedicine. *Mar Drugs* **11**:3155-3167
59. **Butt TR, Edavettal SC, Hall JP, Mattern MR.** 2005. SUMO fusion technology for difficult-to-express proteins. *Protein Expr Purif* **43**:1-9.
60. **Malakhov MP, Mattern MR, Malakhova OA, Drinker M, Weeks SD, Butt TR.** 2004. SUMO fusions and SUMO-specific protease for efficient expression and purification of proteins. *J Struct Funct Genomics* **5**:75-86.
61. **Marblestone JG, Edavettal SC, Lim Y, Lim P, Zuo X, Butt TR.** 2006. Comparison of SUMO fusion technology with traditional gene fusion systems: Enhanced expression and solubility with SUMO. *Protein Sci* **15**:182-189.

62. **Lee C-D, Sun H-C, Hu S-M, Chiu C-F, Homhuan A, Liang S-M, Leng C-H, Wang T-F.** 2008. An improved SUMO fusion protein system for effective production of native proteins. *Protein Sci* **17**:1241-1248.
63. **Panavas T, Sanders C, Butt TR.** 2009. SUMO fusion technology for enhanced protein production in prokaryotic and eukaryotic expression systems. In: Ulrich HD (ed) *Methods in Molecular Biology: SUMO Protocols*, Humana Press, New York, pp 303-317
64. **Shaner NC, Campbell RE, Steinbach PA, Giepmans BNG, Palmer AE, Tsien RY.** 2004. Improved monomeric red, orange and yellow fluorescent proteins derived from *Discosoma* sp. red fluorescent protein. *Nat Biotechnol* **22**:1567-1572.
65. **Laemmli UK.** 1970. Cleavage of structural proteins during the assembly of the head of bacteriophage T4. *Nature* **227**:680-685.
66. **Schneider CA, Rasband WS, Eliceiri KW.** 2012. NIH Image to ImageJ: 25 years of image analysis. *Nat Methods* **9**:671-675.
67. **Bradford MM.** 1976. A rapid and sensitive method for quantitation of microgram quantities of protein utilizing principle of protein-dye binding. *Anal Biochem* **72**:248-254.

68. **Bolivar JM, Nidetzky B.** 2012. Positively charged mini-protein Z_{basic2} as a highly efficient silica binding module: Opportunities for enzyme immobilization on unmodified silica supports. *Langmuir* **28**:10040-10049.
69. **Castelletti L, Verzola B, Gelfi C, Stoyanov A, Righetti PG.** 2000. Quantitative studies on the adsorption of proteins to the bare silica wall in capillary electrophoresis III: Effects of adsorbed surfactants on quenching the interaction. *J Chromatogr A* **894**:281-289.
70. **Campbell RE, Tour O, Palmer AE, Steinbach PA, Baird GS, Zacharias DA, Tsien RY.** 2002. A monomeric red fluorescent protein. *Proc Natl Acad Sci USA* **99**:7877-7882.
71. **Iler RK.** 1979. *The Chemistry of Silica*. John Wiley & Sons, Inc., New York
72. **Waugh DS.** 2011. An overview of enzymatic reagents for the removal of affinity tags. *Protein Expr Purif* **80**:283-293.
73. **Jenny RJ, Mann KG, Lundblad RL.** 2003. A critical review of the methods for cleavage of fusion proteins with thrombin and factor Xa. *Protein Expr Purif* **31**:1-11.
74. **Choi O, Kim B-C, An J-H, Min K, Kim YH, Um Y, Oh M-K, Sang B-I.** 2011. A biosensor based on the self-entrapment of glucose oxidase within biomimetic silica nanoparticles induced by a fusion enzyme. *Enzyme Microb Technol* **49**:441-445.

75. **Fukuyama M, Nishida M, Abe Y, Amemiya Y, Ikeda T, Kuroda A, Yokoyama S.** 2011. Detection of antigen-antibody reaction using Si ring optical resonators functionalized with an immobilized antibody-binding protein. *Jpn J Appl Phys* **50**:04DL07.
76. **Fukuyama M, Yamatogi S, Ding H, Nishida M, Kawamoto C, Amemiya Y, Ikeda T, Noda T, Kawamoto S, Ono K, Kuroda A, Yokoyama S.** 2010. Selective detection of antigen-antibody reaction using Si ring optical resonators. *Jpn J Appl Phys* **49**:04DL09.
77. **Hnilova M, Khatayevich D, Carlson A, Oren EE, Gresswell C, Zheng S, Ohuchi F, Sarikaya M, Tamerler C.** 2012. Single-step fabrication of patterned gold film array by an engineered multi-functional peptide. *J Colloid Interface Sci* **365**:97-102.
78. **Yamatogi S, Amemiya Y, Ikeda T, Kuroda A, Yokoyama S.** 2009. Si ring optical resonators for integrated on-chip biosensing. *Jpn J Appl Phys* **48**:04C188.
79. **Coyle BL, Baneyx F.** 2014. A cleavable silica-binding affinity tag for rapid and inexpensive protein purification. *Biotechnol Bioeng* **111**:2019-2026.
80. **Pina AS, Lowe CR, Roque ACA.** 2014. Challenges and opportunities in the purification of recombinant tagged proteins. *Biotechnol Adv* **32**:366-381.

81. **Layne E.** 1957. Spectrophotometric and turbidimetric methods for measuring proteins. *Methods Enzymol* **3**:447-454.
82. **Kosmulski M.** 2009. Compilation of PZC and IEP of sparingly soluble metal oxides and hydroxides from literature. *Adv Colloid Interface Sci* **152**:14-25.
83. **Gross LA, Baird GS, Hoffman RC, Baldrige KK, Tsien RY.** 2000. The structure of the chromophore within DsRed, a red fluorescent protein from coral. *Proc Natl Acad Sci USA* **97**:11990-11995.
84. **Fukuta M, Zheng B, Uenuma M, Okamoto N, Uraoka Y, Yamashita I, Watanabe H.** 2014. Controlled charged amino acids of Ti-binding peptide for surfactant-free selective adsorption. *Colloids Surf B: Biointerfaces* **118**:25-30.
85. **Sunna A, Chi F, Bergquist PL.** 2013. A linker peptide with high affinity towards silica-containing materials. *New Biotechnol* **30**:485-492.
86. **Krimm S, Mark JE.** 1968. Conformations of polypeptides with ionized side chains of equal length. *Proc Natl Acad Sci USA* **60**:1122-&.
87. **Mao AH, Crick SL, Vitalis A, Chicoine CL, Pappu RV.** 2010. Net charge per residue modulates conformational ensembles of intrinsically disordered proteins. *Proc Natl Acad Sci USA* **107**:8183-8188.

88. **Corni S, Hnilova M, Tamerler C, Sarikaya M.** 2013. Conformational behavior of genetically-engineered dodecapeptides as a determinant of binding affinity for gold. *Journal of Physical Chemistry C* **117**:16990-17003.
89. **Boom R, Sol CJA, Salimans MMM, Jansen CL, Wertheim-van Dillen PME, van der Noordaa J.** 1990. Rapid and simple method for purification of nucleic acids. *J Clin Microbiol* **28**:495-503.
90. **Chen CW, Thomas CA.** 1980. Recovery of DNA segments from agarose gels. *Anal Biochem* **101**:339-341.
91. **Vogelstein B, Gillespie D.** 1979. Preparative and analytical purification of DNA from agarose. *Proc Natl Acad Sci USA* **76**:615-619.
92. **Shimada K, Fukushige Y.** 1975. Properties of volcanic glass in Shirasu. *Yogyo-Kyokai-Shi* **83**:565-570.
93. **Haruyama M.** 1973. Geological, physical, and mechanical properties of "Shirasu" and its engineering classification. *Soils Found* **13**:45-60.
94. **Arakawa T, Tsumoto K, Kita Y, Chang B, Ejima D.** 2007. Biotechnology applications of amino acids in protein purification and formulations. *Amino Acids* **33**:587-605.

95. **Tsumoto K, Umetsu M, Kumagai I, Ejima D, Philo JS, Arakawa T. 2004.** Role of arginine in protein refolding, solubilization, and purification. *Biotechnol Prog* **20**:1301-8.
96. **Ejima D, Yumioka R, Arakawa T, Tsumoto K. 2005.** Arginine as an effective additive in gel permeation chromatography. *J Chromatogr A* **1094**:49-55.

Acknowledgments

Praise be to Allah, his majesty for his uncountable blessings, and best prayers and peace be upon the Prophet Mohamed the most beloved Prophet of Allah, his relatives and noble companions.

I would like to express my sincere gratitude to my academic advisor Dr. Akio Kuroda, Professor of the Department of Molecular Biotechnology, Graduate School of Advanced Sciences of Matter, Hiroshima University, for his kind instruction, scientific guidance, and encouragement throughout this study.

I would like to express my deep appreciation to Dr. Takeshi Ikeda, Assistant Professor of the Department of Molecular Biotechnology, Graduate School of Advanced Sciences of Matter, Hiroshima University, for his instruction and continuous encouragement throughout this study, as well as his experimental guidance.

I would like to thank Dr. Kei Motomura, postdoctoral researcher of Kuroda Lab, for his experimental guidance, advice, suggestions that benefited me much in the completion and success of this study.

I would like to thank Dr. Junichi Kato and Dr. Tsunehiro Aki, Professors of the Department of Molecular Biotechnology, Graduate School of Advanced Sciences of Matter, Hiroshima University, for their precious advices and the review of this thesis.

I also thank Dr. Hisakage Funabashi, Tenure-track Lecturer of the Institute for Sustainable Sciences and Development, Dr. Ryuichi Hirota, and Dr. Takenori Ishida, Assistant Professors of the Department of Molecular Biotechnology, Graduate School of Advanced Sciences of Matter, Hiroshima University, for valuable discussions throughout this study.

Many thanks go to Mr. Tomoki Nishimura and Mr. Alexandrov Maxym, researchers of Kuroda Lab and Ms. Takako Sawahara, the secretary of Kuroda Lab, for their support.

I would like to thank my colleagues, graduate and undergraduate students of Kuroda Lab for their kind help and support.

I would like to thank my parents, my wife and my beloved sons, for their continuous encouragement and support.

Finally, I would like to thank my government, Egypt, in particular the Ministry of Higher Education and Scientific Research for honoring me and funding me to conduct this research in Japan. My thanks are also for my professors and colleagues of the Department of Botany and Microbiology, Faculty of Science, Minia University, Egypt, for their support.

Mohamed A. A. Abdelhamid

Articles

- 1) The C-terminal zwitterionic sequence of CotB1 is essential for biosilicification of the *Bacillus cereus* spore coat

Kei Motomura, Takeshi Ikeda, Satoshi Matsuyama, Mohamed A. A. Abdelhamid,

Tatsuya Tanaka, Takenori Ishida, Ryuichi Hirota, and Akio Kuroda.

Journal of Bacteriology, 198: 276-282 (2016).

- 2) Affinity purification of recombinant proteins using a novel silica-binding peptide as a fusion tag.

Mohamed A. A. Abdelhamid, Kei Motomura, Takeshi Ikeda, Takenori Ishida,

Ryuichi Hirota, and Akio Kuroda.

Applied Microbiology and Biotechnology, 98:5677-5684 (2014)

The C-Terminal Zwitterionic Sequence of CotB1 Is Essential for Biosilicification of the *Bacillus cereus* Spore Coat

Kei Motomura, Takeshi Ikeda, Satoshi Matsuyama, Mohamed A. A. Abdelhamid, Tatsuya Tanaka, Takenori Ishida, Ryuichi Hirota, Akio Kuroda

Department of Molecular Biotechnology, Graduate School of Advanced Sciences of Matter, Hiroshima University, Higashi-Hiroshima, Hiroshima, Japan

ABSTRACT

Silica is deposited in and around the spore coat layer of *Bacillus cereus*, and enhances the spore's acid resistance. Several peptides and proteins, including diatom silaffin and silacidin peptides, are involved in eukaryotic silica biomineralization (biosilicification). Homologous sequence search revealed a silacidin-like sequence in the C-terminal region of CotB1, a spore coat protein of *B. cereus*. The negatively charged silacidin-like sequence is followed by a positively charged arginine-rich sequence of 14 amino acids, which is remarkably similar to the silaffins. These sequences impart a zwitterionic character to the C terminus of CotB1. Interestingly, the *cotB1* gene appears to form a bicistronic operon with its paralog, *cotB2*, the product of which, however, lacks the C-terminal zwitterionic sequence. A Δ *cotB1B2* mutant strain grew as fast and formed spores at the same rate as wild-type bacteria but did not show biosilicification. Complementation analysis showed that CotB1, but neither CotB2 nor C-terminally truncated mutants of CotB1, could restore the biosilicification activity in the Δ *cotB1B2* mutant, suggesting that the C-terminal zwitterionic sequence of CotB1 is essential for the process. We found that the kinetics of CotB1 expression, as well as its localization, correlated well with the time course of biosilicification and the location of the deposited silica. To our knowledge, this is the first report of a protein directly involved in prokaryotic biosilicification.

IMPORTANCE

Biosilicification is the process by which organisms incorporate soluble silicate in the form of insoluble silica. Although the mechanisms underlying eukaryotic biosilicification have been intensively investigated, prokaryotic biosilicification was not studied until recently. We previously demonstrated that biosilicification occurs in *Bacillus cereus* and its close relatives, and that silica is deposited in and around a spore coat layer as a protective coating against acid. The present study reveals that a *B. cereus* spore coat protein, CotB1, which carried a C-terminal zwitterionic sequence, is essential for biosilicification. Our results provide the first insight into mechanisms required for biosilicification in prokaryotes.

Silicon (Si), the second most abundant element in the Earth's crust, is an important mineral for living organisms. It acts as the main component of structural skeletons of diatoms, radiolarians, and siliceous sponges (1). Si is also utilized by some plants (e.g., rice and cucumber) to protect against biotic and abiotic stresses (2). The presence of Si in bacterial spores was first noted several decades ago (3, 4). Until recently, however, there have been no reports on the precise localization of Si and its biological function in prokaryotes. In a recent study, we demonstrated that the *Bacillus cereus* group, a very homogenous cluster of six species, and its close relatives accumulate Si in and around their spore coat layer and that the Si-containing layer enhances acid resistance of the spores (5). In Si-accumulating organisms, Si is taken up from the environment as soluble silicate ($\text{Si}[\text{OH}]_4$), a biologically available form of Si in nature, which is then polymerized and accumulated as insoluble silica (SiO_2). Such silica biomineralization (biosilicification) in eukaryotes is under genetic control, which in turn implies the existence of specific gene products guiding biosilicification. However, no proteins or peptides involved in prokaryotic biosilicification have been identified thus far.

The best-known example of biosilicification occurs in diatoms, which are eukaryotic unicellular algae that possess cell walls consisting of amorphous silica with a species-specific micro- and nano-patterning (6). To date, several peptides and proteins involved in diatom biosilicification have been identified, including silaffins, silacidins, and silaffin-like cingulins (7–9). The silaffins are short

peptides that undergo extensive posttranslational modifications such as phosphorylation and polyamine conjugation. Due to a zwitterionic character imparted by negative charges of the phosphate groups and positive charges of the polyamines, silaffins easily self-assemble into supramolecular aggregates, which serve as the templates for silica formation (7, 10–12). The negatively charged silacidin peptides also form supramolecular aggregates with positively charged long-chain polyamines, and act as the templates for silica formation (8, 13). These observations indicate the importance of combining positive and negative charges in order to direct biosilicification.

Spores of *Bacillus* species are highly resilient dormant cell types

Received 19 June 2015 Accepted 15 October 2015

Accepted manuscript posted online 26 October 2015

Citation Motomura K, Ikeda T, Matsuyama S, Abdelhamid MAA, Tanaka T, Ishida T, Hirota R, Kuroda A. 2016. The C-terminal zwitterionic sequence of CotB1 is essential for biosilicification of the *Bacillus cereus* spore coat. *J Bacteriol* 198:276–282. doi:10.1128/JB.00447-15.

Editor: W. W. Metcalf

Address correspondence to Takeshi Ikeda, ikedatakeshi@hiroshima-u.ac.jp.

K. Motomura and T. Ikeda contributed equally to this article.

Supplemental material for this article may be found at <http://dx.doi.org/10.1128/JB.00447-15>.

Copyright © 2015, American Society for Microbiology. All Rights Reserved.

TABLE 1 Plasmids used in this study

Plasmid	Description ^a	Source or reference
pIC333	Source of an Sp ^r cassette	24
pMAD	Thermosensitive shuttle vector for allelic replacement; Amp ^r in <i>E. coli</i> , Em ^r in <i>B. cereus</i>	23
pMADΔ <i>cotB1B2</i>	pMAD carrying up- and downstream regions of <i>cotB1B2</i> with an inserted Sp ^r cassette	This study
pMADΔ <i>cotG</i>	pMAD carrying up- and downstream regions of <i>cotG</i> with an inserted Sp ^r cassette	This study
pHT304	Shuttle vector; Amp ^r in <i>E. coli</i> , Em ^r in <i>B. cereus</i>	29
pHT- <i>cotB1B2</i>	pHT304 carrying <i>cotB1</i> and <i>cotB2</i> with the promoter region of <i>cotB1B2</i>	This study
pHT- <i>cotB1</i>	pHT304 carrying <i>cotB1</i> with the promoter region of <i>cotB1B2</i>	This study
pHT- <i>cotB2</i>	pHT304 carrying <i>cotB2</i> with the promoter region of <i>cotB1B2</i>	This study
pHT- <i>cotB1</i> -141	pHT- <i>cotB1</i> lacking silacidin-like and arginine-rich sequences	This study
pHT- <i>cotB1</i> -157	pHT- <i>cotB1</i> lacking arginine-rich sequence	This study
pHT- <i>cotB1</i> -142/157	pHT- <i>cotB1</i> lacking silacidin-like sequence	This study
pGFPuv	Source of <i>gfp</i> gene	Clontech Laboratories
pHT- <i>gfp</i> - <i>cotB1</i>	pHT304 carrying <i>gfp</i> -fused <i>cotB1</i>	This study
pHT- <i>gfp</i>	pHT304 carrying <i>gfp</i>	This study

^a Amp^r, ampicillin resistance; Em^r, erythromycin resistance; Sp^r, spectinomycin resistance.

that can withstand extremes of temperature, radiation, and chemical assault (14). These spore properties are attributable to the physical and chemical composition of the structures that encase the spore (15, 16). The outermost portion of *Bacillus* spores consists of cortex, spore coat, and, in some species, exosporium. The spore coat, where silica is deposited in *B. cereus*, is composed of more than 50 proteins (17). Silica accumulation in and around the *B. cereus* spore coat strongly suggests that spore coat proteins play an important role in biosilicification. We report here that one of the spore coat proteins, CotB1, carries a negatively charged silacidin-like sequence on its C terminus, followed by a positively charged arginine-rich sequence. We demonstrate that the zwitterionic C terminus of CotB1 plays an essential role in prokaryotic biosilicification.

MATERIALS AND METHODS

In silico screening for silica-forming proteins. A database of *B. cereus* spore coat protein sequences (as reported by Henriques et al. [17]) was constructed with the sequences obtained from the NCBI website (<http://www.ncbi.nlm.nih.gov/>). Previously characterized silica-forming peptides (silaffin-1A₁, -1A₂, and -1B of *Cylindrotheca fusiformis* [7, 18] and silacidins A, B, and C of *Thalassiosira pseudonana* [9]) were used as query sequences. Searching for spore coat proteins with significant similarity to the silica-forming peptides was conducted using the BLAST program obtained from the NCBI FTP server (<ftp://ftp.ncbi.nih.gov/blast/>) with an E value of 10 as a threshold.

Bacterial strains and growth conditions. *B. cereus* strain NBRC 15305, which corresponds to strain ATCC 14579 (19), was obtained from the NITE Biological Resource Center (NBRC; Chiba, Japan) and used as the wild-type strain in the present study. The wild-type and mutant strains of *B. cereus* were routinely grown at 28°C in LB medium (20). Sporulation was induced at 28°C by nutrient exhaustion in mR2A medium (an R2A medium [21] supplemented with 0.6 mM CaCl₂, 0.03 mM MnCl₂, 0.05 mM ZnCl₂, and 0.05 mM FeSO₄). We note that the concentrations of CaCl₂ and MnCl₂ in the medium are three times higher than in our previous report (5) in order to induce efficient sporulation for *B. cereus*. Spore development was monitored by bright-field microscopy, and the timing of entry into sporulation was defined as the end of the exponential growth phase (22). *Escherichia coli* JM109 was used as a host for cloning and was grown at 37°C in 2× YT medium (20). When necessary, spectinomycin (250 μg ml⁻¹ for *B. cereus*), erythromycin (10 μg ml⁻¹ for *B. cereus*), and carbenicillin (50 μg ml⁻¹ for *E. coli*) were added to the medium.

Mutant construction. The *cotB1B2* deletion mutant was constructed by using the allelic replacement method described by Arnaud et al. (23).

DNA fragments (~1 kb each) corresponding to the up- and downstream regions of *cotB1B2* were amplified from the chromosomal DNA of *B. cereus* using the primer pairs *cotB1*-F1/*cotB1*-R1 and *cotB2*-F1/*cotB2*-R1 (nucleotide sequences are given in Table S1 in the supplemental material) and then treated with BglII and SalI, respectively. A spectinomycin resistance (Sp^r) cassette was amplified from pIC333 (24) with the primers *spc*-F1 and *spc*-R1 and was digested with BglII and SalI. These three fragments were ligated by T4 DNA ligase, and the resultant fragment was amplified by PCR with the primers *cotB1*-F1 and *cotB2*-R1. The PCR fragment was digested with MluI and inserted into the MluI site of the pMAD vector (23), which was obtained from the Pasteur Institute (Paris, France), yielding pMADΔ*cotB1B2* (Table 1). The plasmid was then introduced into the *B. cereus* wild-type strain by electroporation (25), and the transformants were selected at 30°C on LB agar plates with 250 μg ml⁻¹ spectinomycin and 50 μg ml⁻¹ X-Gal (5-bromo-4-chloro-3-indolyl-β-D-galactopyranoside). Integration and excision of pMADΔ*cotB1B2* were performed as described by Arnaud et al. (23) with slight modifications: the double-crossover deletion mutants were screened by blue/white screening on LB agar plates without spectinomycin, because they showed unexpectedly low spectinomycin resistance when the Sp^r cassette was inserted into the *cotB1B2* locus. The insufficient resistance can be ascribed to the incomplete promoter sequence of the Sp^r cassette (26) and the upstream *cotB1B2* promoter, which is not active in vegetative cells (see Results and Discussion). These weak promoters could not support sufficient expression of the Sp^r cassette, although the cassette works appropriately when inserted into the *tetB* locus of the wild-type strain (23). Disruption of *cotB1B2* was confirmed by PCR amplification with the primer pairs *cotB1*-F2/*spc*-R2 and *cotB2*-R2/*spc*-F2.

The *cotG* deletion mutant was constructed in a similar way by replacing the primers *cotB1*-F1, *cotB1*-R1, *cotB2*-F1, and *cotB2*-R1 with *cotG*-F1, *cotG*-R1, *cotG*-F2, and *cotG*-R2, respectively, to yield pMADΔ*cotG*. Disruption of *cotG* was confirmed by PCR amplification with the primer pairs *cotG*-F3/*spc*-R2 and *cotG*-R3/*spc*-F2.

Extraction of spore coat proteins. Spores were prepared by growing *B. cereus* strains in mR2A medium supplemented with 100 μg ml⁻¹ silicate at 28°C for 48 h and were harvested by centrifugation. The pellets were sonicated in buffer containing 25 mM Tris-HCl (pH 7.5), 1 mM EDTA, 15% glycerol, 0.1 M NaCl, and protease inhibitor cocktail (Nacalai Tesque, Kyoto, Japan) to disrupt residual mother cells, and then the spores were separated from the suspension by centrifugation as reported by Isticko et al. (27). Spore coat proteins were extracted from the spores with sodium dodecyl sulfate (SDS) gel-loading buffer (20) containing 50 mM Tris-HCl (pH 6.8), 100 mM dithiothreitol, 10% glycerol, 2% SDS, and 0.1% bromophenol blue at 100°C for 10 min. The extracts were immediately fractionated on 12.5% Bis-Tris SDS-PAGE gels with 3-(*N*-mor-

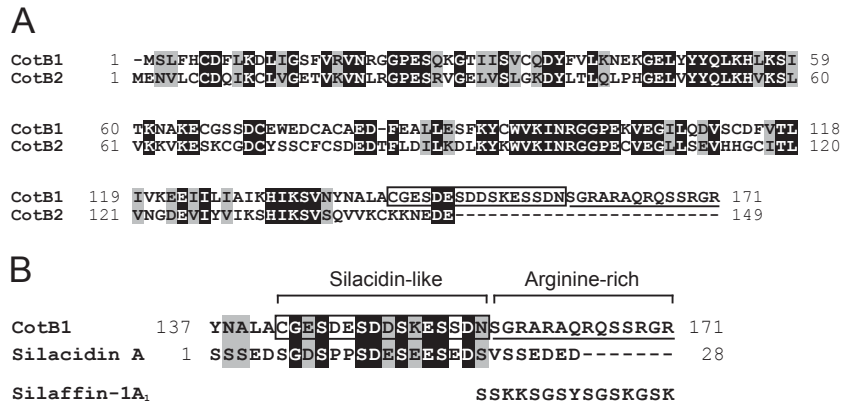


FIG 1 Pairwise alignment of *B. cereus* CotB1 and CotB2 and primary structure of *T. pseudonana* silicidin A. Alignments of CotB1 with CotB2 (A) and with silicidin A (B) were performed using the CLUSTAL W program at GenomeNet (<http://www.genome.jp/>) with default parameters. Black-shaded and gray-shaded amino acid residues indicate identity and similarity, respectively. The boxed sequence of CotB1 (CGESDESDDSKESSDN) was identified by a local BLAST search for sequences with significant similarity to silicidin A (SGDSPPSDESESESDS). The underlined sequence indicates the arginine-rich region of CotB1. The amino acid sequence of *C. fusiformis* silaffin-1A₁ is given for comparison.

pholino)propanesulfonic acid running buffer (28) and stained with Coomassie brilliant blue R-250.

Silicate uptake assay. *B. cereus* cells grown overnight with shaking at 28°C in R2A medium were inoculated (5%) into mR2A medium supplemented with 100 µg ml⁻¹ silicate. The cultures were incubated at 28°C with shaking. Samples taken from the cultures at 12-h intervals were centrifuged, and then the silicate concentrations in the supernatants were measured by using a silicate test kit (Merck, Darmstadt, Germany) according to the manufacturer’s instructions.

Acid resistance assay. Sporulation of *B. cereus* strains was induced in mR2A medium with or without 100 µg ml⁻¹ silicate as described above. After the cultures were kept standing at 4°C for 12 h, the spores were collected by centrifugation at 8,100 × g for 10 min and washed twice with cold sterile distilled water. The purified spores were suspended in distilled water to an optical density of 1.0 at 600 nm. Spores were centrifuged and resuspended in equal volumes of 0.2 N HCl. At the designated times, samples were diluted with cold water and spread on R2A agar plates. Spore viability was determined by counting the colonies after a 24-h incubation at 28°C.

Plasmid construction and transformation. For complementation tests, a DNA fragment containing the *cotB1B2* genes with their putative promoter and terminator regions was amplified by PCR from the chromosomal DNA of *B. cereus* using the primers cotB1-F3 and cotB2-R3 (see Table S1 in the supplemental material). The PCR fragment was digested with BamHI and EcoRI and then inserted into the same sites of plasmid pHT304 (29), yielding pHT-cotB1B2. The plasmids carrying either *cotB1* or *cotB2* gene were amplified by inverse PCR using pHT-cotB1B2 as a template with the primer pairs cotB1-F4/cotB1-R2 and cotB2-F2/cotB2-R4, respectively. The amplified DNA fragments were self-ligated to yield pHT-cotB1 and pHT-cotB2, respectively. To construct the plasmids carrying truncated mutants of *cotB1*, another round of inverse PCR was performed using pHT-cotB1 as a template with the primer pairs cotB1-F5/cotB1-R3, cotB1-F6/cotB1-R3, and cotB1-F6/cotB1-R4. The amplified DNA fragments were self-ligated to yield pHT-cotB1-141, pHT-cotB1-157, and pHT-cotB1-142/157, respectively. These plasmids were introduced into the Δ *cotB1B2* strain by electroporation as described above, and then the transformants were selected at 28°C on LB agar plates with 10 µg ml⁻¹ erythromycin. To construct a plasmid expressing green fluorescent protein (GFP)-fused CotB1 under the control of the promoter of *cotB1B2*, the vector backbone was amplified by inverse PCR using pHT-cotB1 as a template with the primers cotB2-F2 and cotB1-R5. A GFP-encoding DNA fragment was amplified by PCR from pGFPuv (Clontech Laboratories, Mountain View, CA) using the phosphorylated primers

gfp-F1 and gfp-R1. These PCR products were ligated by T4 DNA ligase, yielding pHT-gfp-cotB1. As a control, plasmid pHT-gfp, which expresses GFP under the control of the promoter of *cotB1B2*, was prepared by the same procedures using the primer pairs cotB2-F2/cotB1-R2 and gfp-F1/gfp-R2. These plasmids were introduced into the wild-type strain by electroporation as described above.

Microscopy. Sporulating cells and spores grown in mR2A medium supplemented with silicate were harvested at various time points and observed under a BX51 fluorescence microscope equipped with an UPlanApo ×100/1.35 objective lens and a U-MNIBA3 filter (Olympus, Tokyo, Japan). Images were captured using a DP72 cooled charge-coupled device camera (Olympus). For transmission electron microscopy (TEM), spores were prepared without silicate as described above. Ultrathin sections of the spores were prepared and stained as described previously (5) except that spores were initially fixed with 2.5% glutaraldehyde in 0.1 M cacodylate buffer (pH 7.2) containing 0.1% MgSO₄ for 4 h at 4°C, followed by postfixation with 1% OsO₄ in 0.2 M cacodylate buffer (pH 7.2) for 10 h at 4°C. The ultrathin sections were observed under a JEM-1400 transmission electron microscope (JEOL, Tokyo, Japan) operating at an accelerating voltage of 80 kV.

RESULTS AND DISCUSSION

Silicidin-like sequence in the C-terminal region of CotB1. To identify the proteins involved in the biosilicification of *B. cereus* spores, we performed a local BLAST search of spore coat proteins using sequences of previously characterized silica-forming peptides (diatom silaffins and silicidins) as queries. Among the 53 spore coat proteins that have been identified in *B. cereus* to date (17), a C-terminal region of CotB1 (GenBank accession number AAP07429.1) showed significant similarity to silicidin A (50% identity over 16 amino acids, E value 8.5) (Fig. 1, boxed). Silicidin A is a highly acidic peptide of 28 amino acids that is isolated from cell walls of the diatom *T. pseudonana* (9). Interestingly, a gene encoding a CotB1 paralog, namely, CotB2 (GenBank accession number AAP07430.1), is located in tandem downstream of the *cotB1* gene on the *B. cereus* genome (see Fig. S1 in the supplemental material). The *cotB1* and *cotB2* genes are separated by only 20 bp. The *cotB1* gene is preceded by a putative σ^K promoter (30), which is activated in the mother cell during the late stage of sporulation, whereas no canonical promoter sequence is found in the 500-bp sequence preceding the *cotB2* open reading frame. These

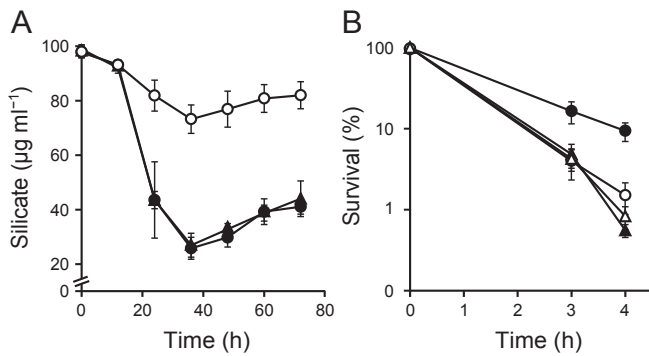


FIG 2 Silicate uptake and spore acid resistance of the *B. cereus* wild type and $\Delta cotB1B2$ and $\Delta cotG$ mutants. (A) Silicate concentrations in the culture supernatant of the wild-type (●), $\Delta cotB1B2$ (○), and $\Delta cotG$ (▲) strains were measured at the indicated times after inoculation into mR2A medium supplemented with $100 \mu\text{g ml}^{-1}$ silicate. Microscopic observation showed that engulfed forespores formed during the 12 to 24 h period and that mature spores were gradually released from the mother cells after 36 h. (B) Viability of wild-type (circles) and $\Delta cotB1B2$ (triangles) spores in 0.2 N HCl. Spores were produced in the presence (closed symbols) or absence (open symbols) of silicate. The data represent the means and standard deviations of the results of at least three independent experiments.

facts imply that the *cotB1* and *cotB2* genes are present in a single transcriptional unit. Although CotB1 and CotB2 are highly similar to each other (49% identity and 66% similarity over 131 amino acids), CotB1 is longer than CotB2 (171 versus 149 amino acids) and contains a characteristic C-terminal extension (Fig. 1). The extension overlaps the silacidin A-like sequence identified by the local BLAST search (residues 142 to 157) (Fig. 1, boxed), which is rich in serine, aspartate, and glutamate residues, as is the case for silacidin A. The downstream region (residues 158 to 171) (Fig. 1, underlined) is rich in serine and positively charged arginine residues. Such properties are common to diatom silaffins, although the majority of positively charged residues in silaffins are lysines (e.g., silaffin R5 [SSKKS⁺GSYSGSKGSKRRIL]) (7). The presence of the negatively charged silacidin-like sequence and positively charged arginine-rich sequence would impart a zwitterionic character to the C-terminal extension of CotB1.

CotB1 is involved in the biosilicification of *B. cereus* spores.

In order to investigate whether CotB1 and/or CotB2 is involved in the biosilicification, we constructed a $\Delta cotB1B2$ mutant strain. The mutant contains a chromosomal mutation that replaces the entire *cotB1* and *cotB2* genes with an *Sp^r* cassette. We also constructed another mutant strain, a $\Delta cotG$ mutant, as a negative control, in which the *Sp^r* cassette replaces the gene encoding another spore coat protein Coty (31) (formerly known as an exosporium protein ExsB [32]; however, recent studies showed that most of this protein is located in the spore coat [31, 33]). These mutant strains grew as fast and formed spores at the same rate as the wild type in mR2A medium with $100 \mu\text{g ml}^{-1}$ silicate (data not shown), suggesting that the *cotB1B2* and *cotG* disruption did not affect vegetative growth or spore formation. Biosilicification of the spores was evaluated by measuring the decrease in silicate concentration in the culture supernatant during incubation, because our previous study indicated that most of the silicate removed from the culture supernatant is deposited as silica in the spores (5). During the early stationary phase (24 to 36 h after inoculation), the silicate concentration in the culture supernatants of the wild type and $\Delta cotG$ mutant decreased by about $75 \mu\text{g ml}^{-1}$, while that

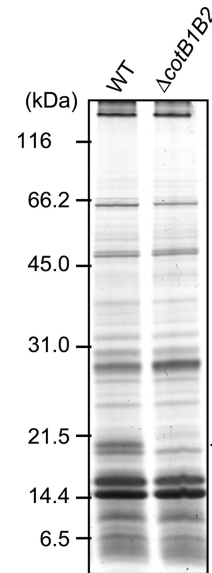


FIG 3 SDS-PAGE analysis (12.5%) of the spore coat proteins. Sporulation of the *B. cereus* wild type (WT) and $\Delta cotB1B2$ mutant was induced in mR2A medium supplemented with $100 \mu\text{g ml}^{-1}$ silicate for 48 h. The arrowhead indicates the position corresponding to the expected size of CotB1 (19.3 kDa).

in the $\Delta cotB1B2$ culture supernatant decreased by only about $25 \mu\text{g ml}^{-1}$ (Fig. 2A), indicating that one or both of the *cotB1B2* genes are involved in biosilicification.

We previously reported that the biosilicification of the spore coat increased spore viability under acidic conditions (5). To investigate whether *cotB1B2* disruption affects acid resistance, we purified spores from the wild-type and mutant strains, which were produced in mR2A medium with or without silicate, and treated them with 0.2 N HCl. Consistent with our previous results (5), the wild-type spores prepared in the presence of silicate showed higher survival rates than those prepared in the absence of silicate (Fig. 2B). This was also the case for the $\Delta cotG$ mutant (data not shown). In contrast, and as expected, the presence of silicate did not affect the survival rates of the $\Delta cotB1B2$ spores (Fig. 2B). The $\Delta cotB1B2$ spores prepared with or without silicate showed survival rates similar to those of the wild-type spores prepared without silicate (Fig. 2B). These data indicate that biosilicification-associated acid resistance was significantly reduced in the $\Delta cotB1B2$ spores.

In order to exclude the possibility that the decrease in the silicate uptake and acid resistance in the $\Delta cotB1B2$ mutant was caused by incomplete coat assembly, we examined wild-type and $\Delta cotB1B2$ spores following thin-section TEM and found no measurable differences in spore coat structure (see Fig. S2 in the supplemental material). Consistent with this, SDS-PAGE analysis of spore coat proteins from the $\Delta cotB1B2$ mutant showed specific loss of a protein with a molecular mass consistent with that of CotB1 (19.3 kDa) in the $\Delta cotB1B2$ spores (Fig. 3, arrowhead). The absence of CotB2 could not be unequivocally identified on the SDS gel because of the overlap with other highly expressed protein bands near the expected molecular mass of CotB2 (16.8 kDa). These results indicate that the disruption of *cotB1B2* genes did not measurably disrupt the overall spore coat assembly, as reported for several other spore coat proteins (34–36). Therefore, the de-

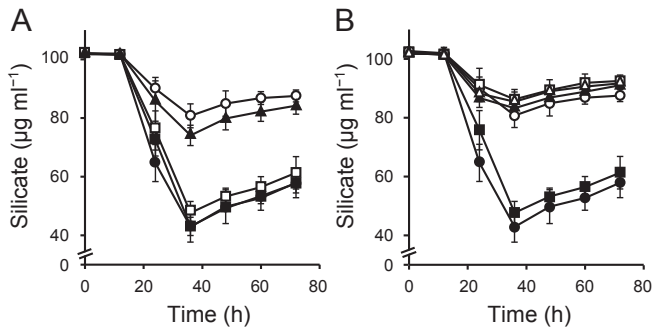


FIG 4 Complementation analysis of $\Delta cotB1B2$. (A) Silicate concentrations in the culture supernatant of the *B. cereus* wild-type strain carrying pHT304 (●), $\Delta cotB1B2$ carrying pHT304 (○), pHT-cotB1B2 (■), pHT-cotB1 (□), or pHT-cotB2 (▲) were measured at the indicated times after inoculation into mR2A medium supplemented with 100 $\mu\text{g ml}^{-1}$ silicate. (B) The same experiment was performed for the wild-type strain carrying pHT304 (●), $\Delta cotB1B2$ carrying pHT304 (○), pHT-cotB1 (■), pHT-cotB1-141 (□), pHT-cotB1-157 (▲), or pHT-cotB1-142/157 (△). The data represent the means and standard deviations of the results of at least three independent experiments.

crease in acid resistance in the $\Delta cotB1B2$ mutant is not due to incomplete coat assembly.

To perform gene complementation analysis, we constructed plasmids carrying *cotB1*, *cotB2*, or both of these genes with the native promoter region of *cotB1B2*, designated pHT-cotB1, pHT-cotB2, and pHT-cotB1B2, respectively. Wild-type levels of biosilicification were restored by the introduction of either pHT-cotB1 or pHT-cotB1B2 into the $\Delta cotB1B2$ mutant, whereas this was not the case for pHT-cotB2 (Fig. 4A). The reduction in acid resistance caused by *cotB1B2* disruption was also restored by the introduction of pHT-cotB1 and pHT-cotB1B2 but not pHT-cotB2 (data not shown). These results clearly indicate that only CotB1 is involved in the biosilicification.

A C-terminal zwitterionic sequence is essential for biosilicification. As noted above, CotB1 (but not CotB2) has a C-terminal extension consisting of a negatively charged silacidin-like region (residues 142 to 157) and a positively charged arginine-rich region (residues 158 to 171) (Fig. 1). To investigate whether the zwitterionic extension is essential for biosilicification, we constructed three plasmids encoding C-terminally truncated mutants of CotB1: pHT-cotB1-141 encodes CotB1 lacking residues 142 to 171, pHT-cotB1-157 encodes CotB1 lacking residues 158 to 171, and pHT-cotB1-142/157 encodes CotB1 lacking the residues between 142 and 157. Introduction of any of these mutant plasmids into the $\Delta cotB1B2$ did not restore the biosilicification (Fig. 4B), although comparable amounts of the C-terminally truncated CotB1 proteins were expressed and integrated in the spores (see Fig. S3 in the supplemental material). These results strongly suggest that both the silacidin-like and arginine-rich sequences, which would impart a zwitterionic character to the C terminus of CotB1, are essential for biosilicification.

Expression and localization of CotB1. To further examine the relationship between CotB1 and biosilicification, we monitored the time course of expression and subcellular localization of CotB1 during sporulation. First, we constructed a plasmid containing the *cotB1B2* promoter region followed by a chimeric gene, *gfp-cotB1*, that encodes CotB1 with an N-terminal GFP (pHT-gfp-cotB1), and then we introduced it into the $\Delta cotB1B2$ mutant. However, the levels of biosilicification were not completely re-

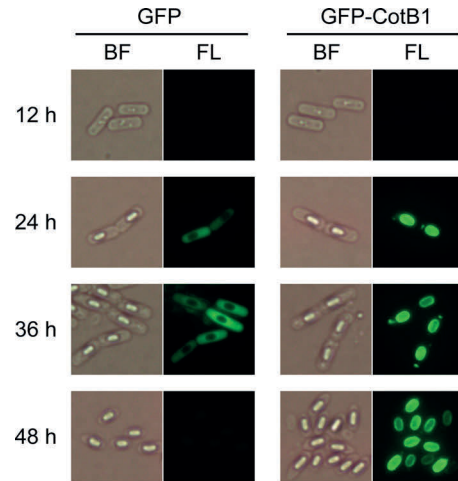


FIG 5 Bright-field and fluorescence microscopic analysis of GFP-CotB1 during sporulation. The *B. cereus* wild-type strains carrying pHT-gfp-cotB1 (GFP-CotB1) or pHT-gfp (GFP) were grown in mR2A medium supplemented with 100 $\mu\text{g ml}^{-1}$ silicate. Samples were taken at the indicated times after inoculation and observed by bright-field (BF) and fluorescence (FL) microscopy.

stored in the transformant (data not shown), implying that the presence of the fused GFP attenuates CotB1 function. Therefore, we introduced pHT-gfp-cotB1 into the wild-type strain, producing a merodiploid strain that contains *gfp-cotB1* fusion on the plasmid in addition to the native *cotB1* chromosomal locus. The transformant grew and sporulated normally in mR2A medium, and its levels of biosilicification were the same as those of the wild-type strain (data not shown). In the merodiploid strain, no fluorescence signals were detected under fluorescence microscopy at 12 h after inoculation, which is approximately 2 h after entry into sporulation (Fig. 5). At 24 h after inoculation, when the silicate uptake started and the engulfed forespores could be observed by bright-field microscopy, green fluorescence was distributed around the entire forespores (Fig. 5). This expression time course agrees well with the presence of a putative σ^K promoter (30) upstream of the *cotB1* gene, which is activated in the mother cell during the late stage of sporulation (see Fig. S1 in the supplemental material). Subsequently, GFP fluorescence was consistently associated with the developing spores, and finally formed a complete ring around the mature spores. This fluorescence localization pattern is essentially the same as those of previously reported GFP-fused spore proteins located in the exosporium and/or spore coat (37–39), where silica is deposited in *B. cereus* (5). In contrast, in the wild-type strain carrying pHT-gfp that contains only the *gfp* gene instead of *gfp-cotB1*, GFP fluorescence was dispersed throughout the mother cell cytoplasm and did not localize on the spore. Taken together, the timing of CotB1 expression and its localization agree well with the time course of biosilicification and the location of the deposited silica, supporting the direct involvement of this protein in silica formation.

CotB1 may be the founding member of a subset of prokaryotic proteins that stimulate biosilicification. As described above, the C-terminal zwitterionic sequence of CotB1 is similar to diatom silica-forming peptides, silaffins and silacidins (Fig. 1), and is essential for biosilicification *in vivo* (Fig. 4B). In contrast, no proteins homologous to sponge silicatein α , which is involved in biosilicification in siliceous sponges (40, 41), are found in the *B. cereus* genome.

These facts suggest that *B. cereus* and diatoms share similar molecular mechanisms for silica formation, although the very limited overlapping lengths between CotB1 and silaffins/silacidins prevent further investigation into the evolutionary relationships among them. Scheffel et al. proposed that preassembled protein-based templates are general components of the cellular machinery for silica morphogenesis in diatoms (8). Our findings clearly indicate that this is also the case for bacteria, because *B. cereus* CotB1 is also a component of an insoluble supramolecular aggregate (the spore coat) that serves as a template for silica formation. To the best of our knowledge, this is the first report of an intracellular protein that stimulates biosilicification in prokaryotes.

The CotB1 homologs that contain the C-terminal zwitterionic sequence are common to biosilicifying *B. cereus* relatives (e.g., GenBank accession numbers AIF54819.1 [*B. anthracis*] and ADH05148.1 [*B. thuringiensis*]) but not to nonbiosilicifying *Bacillus* species (such as *B. subtilis*) or other organisms. These facts are consistent with our previous finding that all of the biosilicifying bacteria, which we isolated from paddy field soil, belong to or are closely related to the *B. cereus* group (5). Our findings indicate that CotB1 plays an important role in prokaryotic biosilicification. However, the presence of a CotB1 homolog is not sufficient for biosilicification. For example, biosilicification was not observed in the spores of *B. mycoides* (also a member of the *B. cereus* group) (5), although this bacterium has a CotB1 homolog with a zwitterionic sequence (GenBank accession number EEM01263.1). These findings clearly indicate the involvement of an additional factor(s) in the biosilicification of *Bacillus* spores. Such a factor(s) probably includes the presence of silicate transporters, because spore biosilicification is likely to require active transport of silicate into the mother cells. Since biosilicification occurs before the release of the spores (5), silicate needs to be taken up via transporters on the mother cell surface. The slight decrease in silicate concentration in the culture supernatant in the $\Delta cotB1B2$ mutant (Fig. 2A) could be attributable to silicate uptake into the mother cells by the silicate transporters. Since the mutant cells cannot efficiently polymerize silicate, most of it is later released during mother cell lysis. In diatoms, silica deposition is tightly coupled to silicate transport, which is mediated by specific transporters (42, 43). Influx and efflux silicate transporters have been also identified in higher plants (44, 45). However, counterparts of the eukaryotic silicate transporters have not been identified in prokaryotes. Elucidation of the mechanism of silicate transport in *B. cereus* may help explain the differences in biosilicification among *Bacillus* species and could also provide new insights into the distribution of biosilicification in prokaryotes.

ACKNOWLEDGMENTS

We thank Didier Lereclus for the gift of the pHT304 plasmid. We also thank Kanae Koike for technical assistance in TEM analysis.

FUNDING INFORMATION

New Energy and Industrial Technology Development Organization (NEDO) of Japan provided funding to Takeshi Ikeda under grant number 09C46130a. Japan Society for the Promotion of Science (JSPS) provided funding to Takeshi Ikeda under grant number 25660061. Institute for Fermentation, Osaka (IFO) provided funding to Takeshi Ikeda.

REFERENCES

- Lowenstam HA, Weiner S. 1989. On biomineralization. Oxford University Press, New York, NY.
- Epstein E. 1999. Silicon. *Annu Rev Plant Physiol Plant Mol Biol* 50:641–664. <http://dx.doi.org/10.1146/annurev.arplant.50.1.641>.
- Jonhstone K, Ellar DJ, Appleton TC. 1980. Location of metal ions in *Bacillus megaterium* spores by high-resolution electron probe X-ray microanalysis. *FEMS Microbiol Lett* 7:97–101. <http://dx.doi.org/10.1111/j.1574-6941.1980.tb01584.x>.
- Stewart M, Somlyo AP, Somlyo AV, Shuman H, Lindsay JA, Murrell WG. 1980. Distribution of calcium and other elements in cryosectioned *Bacillus cereus* T spores, determined by high-resolution scanning electron probe X-ray microanalysis. *J Bacteriol* 143:481–491.
- Hirota R, Hata Y, Ikeda T, Ishida T, Kuroda A. 2010. The silicon layer supports acid resistance of *Bacillus cereus* spores. *J Bacteriol* 192:111–116. <http://dx.doi.org/10.1128/JB.00954-09>.
- Round FE, Crawford RM, Mann DG. 1990. The diatoms: biology and morphology of the genera. Cambridge University Press, Cambridge, United Kingdom.
- Kröger N, Deutzmann R, Sumper M. 1999. Polycationic peptides from diatom biosilica that direct silica nanosphere formation. *Science* 286:1129–1132. <http://dx.doi.org/10.1126/science.286.5442.1129>.
- Scheffel A, Poulsen N, Shian S, Kröger N. 2011. Nanopatterned protein microrings from a diatom that direct silica morphogenesis. *Proc Natl Acad Sci U S A* 108:3175–3180. <http://dx.doi.org/10.1073/pnas.1012842108>.
- Wenzl S, Hett R, Richthammer P, Sumper M. 2008. Silacidins: highly acidic phosphopeptides from diatom shells assist in silica precipitation in vitro. *Angew Chem Int Ed Engl* 47:1729–1732. <http://dx.doi.org/10.1002/anie.200704994>.
- Kröger N, Lorenz S, Brunner E, Sumper M. 2002. Self-assembly of highly phosphorylated silaffins and their function in biosilica morphogenesis. *Science* 298:584–586. <http://dx.doi.org/10.1126/science.1076221>.
- Otzen D. 2012. The role of proteins in biosilicification. *Scientifica* 2012:867562. <http://dx.doi.org/10.6064/2012/867562>.
- Sumper M, Kröger N. 2004. Silica formation in diatoms: the function of long-chain polyamines and silaffins. *J Mater Chem* 14:2059–2065. <http://dx.doi.org/10.1039/b401028k>.
- Richthammer P, Börmel M, Brunner E, van Pée KH. 2011. Biominalization in diatoms: the role of silacidins. *ChemBioChem* 12:1362–1366. <http://dx.doi.org/10.1002/cbic.201000775>.
- Nicholson WL, Munakata N, Horneck G, Melosh HJ, Setlow P. 2000. Resistance of *Bacillus* endospores to extreme terrestrial and extraterrestrial environments. *Microbiol Mol Biol Rev* 64:548–572. <http://dx.doi.org/10.1128/MMBR.64.3.548-572.2000>.
- Driks A. 1999. *Bacillus subtilis* spore coat. *Microbiol Mol Biol Rev* 63:1–20.
- Henriques AO, Moran CP, Jr. 2000. Structure and assembly of the bacterial endospore coat. *Methods* 20:95–110. <http://dx.doi.org/10.1006/meth.1999.0909>.
- Henriques AO, Moran CP, Jr. 2007. Structure, assembly, and function of the spore surface layers. *Annu Rev Microbiol* 61:555–588. <http://dx.doi.org/10.1146/annurev.micro.61.080706.093224>.
- Kröger N, Deutzmann R, Sumper M. 2001. Silica-precipitating peptides from diatoms: the chemical structure of silaffin-1A from *Cylindrotheca fusiformis*. *J Biol Chem* 276:26066–26070. <http://dx.doi.org/10.1074/jbc.M102093200>.
- Ivanova N, Sorokin A, Anderson I, Galleron N, Candelon B, Kapatral V, Bhattacharyya A, Reznik G, Mikhailova N, Lapidus A, Chu L, Mazur M, Goltsman E, Larsen N, D'Souza M, Walunas T, Grechkin Y, Pusch G, Haselkorn R, Fonstein M, Ehrlich SD, Overbeek R, Kyrpides N. 2003. Genome sequence of *Bacillus cereus* and comparative analysis with *Bacillus anthracis*. *Nature* 423:87–91. <http://dx.doi.org/10.1038/nature01582>.
- Green MR, Sambrook J. 2012. Molecular cloning: a laboratory manual, 4th ed. Cold Spring Harbor Laboratory Press, Cold Spring Harbor, NY.
- Reasoner DJ, Geldreich EE. 1985. A new medium for the enumeration and subculture of bacteria from potable water. *Appl Environ Microbiol* 49:1–7.
- Harwood CR, Cutting SM. 1990. Molecular biological methods for *Bacillus*. John Wiley & Sons, Chichester, United Kingdom.
- Arnaud M, Chastanet A, Débarbouillé M. 2004. New vector for efficient allelic replacement in naturally nontransformable, low-GC-content, gram-positive bacteria. *Appl Environ Microbiol* 70:6887–6891. <http://dx.doi.org/10.1128/AEM.70.11.6887-6891.2004>.
- Steinmetz M, Richter R. 1994. Easy cloning of mini-Tn10 insertions from the *Bacillus subtilis* chromosome. *J Bacteriol* 176:1761–1763.
- Turgeon N, Laflamme C, Ho J, Duchaine C. 2006. Elaboration of an

- electroporation protocol for *Bacillus cereus* ATCC 14579. *J Microbiol Methods* 67:543–548. <http://dx.doi.org/10.1016/j.mimet.2006.05.005>.
26. Murphy E. 1985. Nucleotide sequence of a spectinomycin adenylyltransferase AAD(9) determinant from *Staphylococcus aureus* and its relationship to AAD(3⁺)(9). *Mol Gen Genet* 200:33–39. <http://dx.doi.org/10.1007/BF00383309>.
 27. Isticato R, Esposito G, Zilhão R, Nolasco S, Cangiano G, De Felice M, Henriques AO, Ricca E. 2004. Assembly of multiple CotC forms into the *Bacillus subtilis* spore coat. *J Bacteriol* 186:1129–1135. <http://dx.doi.org/10.1128/JB.186.4.1129-1135.2004>.
 28. Updyke TV, Engelhorn SC. 2000. System for pH-neutral stable electrophoresis gel. US patent 6,162,338.
 29. Arantes O, Lereclus D. 1991. Construction of cloning vectors for *Bacillus thuringiensis*. *Gene* 108:115–119. [http://dx.doi.org/10.1016/0378-1119\(91\)90495-W](http://dx.doi.org/10.1016/0378-1119(91)90495-W).
 30. Eichenberger P, Fujita M, Jensen ST, Conlon EM, Rudner DZ, Wang ST, Ferguson C, Haga K, Sato T, Liu JS, Losick R. 2004. The program of gene transcription for a single differentiating cell type during sporulation in *Bacillus subtilis*. *PLoS Biol* 2:e328. <http://dx.doi.org/10.1371/journal.pbio.0020328>.
 31. Aronson A, Goodman B, Smith Z. 2014. The regulated synthesis of a *Bacillus anthracis* spore coat protein that affects spore surface properties. *J Appl Microbiol* 116:1241–1249. <http://dx.doi.org/10.1111/jam.12452>.
 32. Todd SJ, Moir AJG, Johnson MJ, Moir A. 2003. Genes of *Bacillus cereus* and *Bacillus anthracis* encoding proteins of the exosporium. *J Bacteriol* 185:3373–3378. <http://dx.doi.org/10.1128/JB.185.11.3373-3378.2003>.
 33. Abhyankar W, Hossain AH, Djajasaputra A, Permpoonpattana P, Ter Beek A, Dekker HL, Cutting SM, Brul S, de Koning LJ, de Koster CG. 2013. In pursuit of protein targets: proteomic characterization of bacterial spore outer layers. *J Proteome Res* 12:4507–4521. <http://dx.doi.org/10.1021/pr4005629>.
 34. Cutting S, Zheng L, Losick R. 1991. Gene encoding two alkali-soluble components of the spore coat from *Bacillus subtilis*. *J Bacteriol* 173:2915–2919.
 35. Donovan W, Zheng L, Sandman K, Losick R. 1987. Genes encoding spore coat polypeptides from *Bacillus subtilis*. *J Mol Biol* 196:1–10. [http://dx.doi.org/10.1016/0022-2836\(87\)90506-7](http://dx.doi.org/10.1016/0022-2836(87)90506-7).
 36. Zilhão R, Serrano M, Isticato R, Ricca E, Moran CP, Jr, Henriques AO. 2004. Interactions among CotB, CotG, and CotH during assembly of the *Bacillus subtilis* spore coat. *J Bacteriol* 186:1110–1119. <http://dx.doi.org/10.1128/JB.186.4.1110-1119.2004>.
 37. Kim H, Hahn M, Grabowski P, McPherson DC, Otte MM, Wang R, Ferguson CC, Eichenberger P, Driks A. 2006. The *Bacillus subtilis* spore coat protein interaction network. *Mol Microbiol* 59:487–502. <http://dx.doi.org/10.1111/j.1365-2958.2005.04968.x>.
 38. Mallozzi M, Bozue J, Giorno R, Moody KS, Slack A, Cote C, Qiu D, Wang R, McKenney P, Lai EM, Maddock JR, Friedlander A, Welkos S, Eichenberger P, Driks A. 2008. Characterization of a *Bacillus anthracis* spore coat-surface protein that influences coat-surface morphology. *FEMS Microbiol Lett* 289:110–117. <http://dx.doi.org/10.1111/j.1574-6968.2008.01380.x>.
 39. Thompson BM, Hsieh HY, Spreng KA, Stewart GC. 2011. The co-dependence of BxpB/ExsFA and BclA for proper incorporation into the exosporium of *Bacillus anthracis*. *Mol Microbiol* 79:799–813. <http://dx.doi.org/10.1111/j.1365-2958.2010.07488.x>.
 40. Cha JN, Shimizu K, Zhou Y, Christiansen SC, Chmelka BF, Stucky GD, Morse DE. 1999. Silicatein filaments and subunits from a marine sponge direct the polymerization of silica and silicones *in vitro*. *Proc Natl Acad Sci U S A* 96:361–365. <http://dx.doi.org/10.1073/pnas.96.2.361>.
 41. Shimizu K, Cha J, Stucky GD, Morse DE. 1998. Silicatein α : cathepsin L-like protein in sponge biosilica. *Proc Natl Acad Sci U S A* 95:6234–6238. <http://dx.doi.org/10.1073/pnas.95.11.6234>.
 42. Martin-Jézéquel V, Hildebrand M, Brzezinski MA. 2000. Silicon metabolism in diatoms: implications for growth. *J Phycol* 36:821–840. <http://dx.doi.org/10.1046/j.1529-8817.2000.00019.x>.
 43. Thamatrakoln K, Hildebrand M. 2008. Silicon uptake in diatoms revisited: a model for saturable and nonsaturable uptake kinetics and the role of silicon transporters. *Plant Physiol* 146:1397–1407. <http://dx.doi.org/10.1104/pp.107.107094>.
 44. Ma JF, Tamai K, Yamaji N, Mitani N, Konishi S, Katsuhara M, Ishiguro M, Murata Y, Yano M. 2006. A silicon transporter in rice. *Nature* 440:688–691. <http://dx.doi.org/10.1038/nature04590>.
 45. Ma JF, Yamaji N, Mitani N, Tamai K, Konishi S, Fujiwara T, Katsuhara M, Yano M. 2007. An efflux transporter of silicon in rice. *Nature* 448:209–212. <http://dx.doi.org/10.1038/nature05964>.

Table S1. DNA primers used in this study

Primer	Sequence (5' to 3') ^a
Mutant construction	
spc-F1	GGAGATCTGTATAATAAAGAATAATTATTAATC
spc-R1	ATTGGTCGACTAAATTAAGTAATAAAGCGTTCTC
cotB1-F1	ACGGACGCGTTTTGTAAAGATGACCTTG
cotB1-R1	AAAGATCTGAGAAAACCCCTTCCATTAA
cotB2-F1	AGATGTCGACTGTTTAATAAATAAGAGGGGCATT
cotB2-R1	TATAACGCGTTAGCTCGTACACAATGTTTATAAG
cotG-F1	ATCTACGCGTTAACGTATTATACCCTTGAATGCG
cotG-R1	CGAGATCTAGAAATCCTCCTTATCATGTATTAAG
cotG-F2	TAACGTCGACTTTTTATACCACCCAAAAAAGGC
cotG-R2	AATTACGCGTAATGGCCCAATCACATTAGTTG
Mutant screening	
spc-F2	GTGATGATAAGTGGGAAGGACTAT
spc-R2	TTGCTCATGATTTACCTCGTTG
cotB1-F2	AAATGGCATATTTAGTATAGAAGCAATATACTGTT
cotB2-R2	TAATTGATAACGAATTCGGAAACTGCTC
cotG-F3	TCGGCCTCATAAACGAAACTGTGAA
cotG-R3	TAAGCGAATGAGTTCTGCACCAGAA
Plasmid construction	
cotB1-F3	GCGAGAGGATCCAAAGACGAAGATTAAACTA
cotB2-R3	TCAGGTGAATTCATATCCTCCTTCCTACGAA
cotB1-F4	TTATCTCCTCTACTTGATTGTC
cotB1-R2	TGTTTAATAAATAAGAGGGGCAT
cotB2-F2	GAGAAAACCCCTTCCATTAATTT
cotB2-R4	TTGGAGAATGTATTATGCTGTGA
cotB1-F5	TGCTAAAGCATTATAGTTAACACTTTTAA
cotB1-R3	TAATGTTTAATAAATAAGAGGGGC
cotB1-F6	ATTATCGCTACTTTCCTTACTATCG
cotB1-R4	TCAGGTCGTGCTCGTGCAAA
cotB1-R5	AGTTTATTTTCATTGTGATTTTTTGAAAGAC
gfp-F1 ^b	ATGAGTAAAGGAGAAGAAGACTTTTCAC
gfp-R1 ^b	TTTGTAGAGCTCATCCATGCCATG
gfp-R2 ^b	TTATTTGTAGAGCTCATCCATGCCA

^a Underlined sequences indicate restriction sites.

^b These primers were phosphorylated at the 5' end.

1 GTAGTCTACCATGTTAAAAGCATATTTTTTTCTAGCTAGGACAAACATAGAGAACGTAAC 60

61 CTGTACAGATACATATACTATCAGTGCAAAAGCTTATAAATTAATGGAAGGGGTTTTTCTC 120

cotB1

121 **GTG**AGTTTATTTTCATTGTGATTTTTTGAAGACTTAATTGGATCTTTTGTGAGAGTAAAC 180
M S L F H C D F L K D L I G S F V R V N

181 AGGGGTGGTCCAGAATCTCAAAAAGGAACAATAATATCAGTATGTCAGGACTACTTCGTA 240
R G G P E S Q K G T I I S V C Q D Y F V

241 TTGAAGAATGAAAAAGGTGAGCTTTTACTATCAACTTAAACATCTAAAAAGTATTACA 300
L K N E K G E L Y Y Y Q L K H L K S I T

301 AAAAATGCGAAAGAATGTGGATCAAGTGATTGTGAGTGGGAAGATTGCGCCTGTGCAGAA 360
K N A K E C G S S D C E W E D C A C A E

361 GATTTTGAAGCACTACTTGAAAGTTTTCAAAATATTGCTGGGTGAAAATTAATCGCGGCGGT 420
D F E A L L E S F K Y C W V K I N R G G

421 CCAGAGAAAGTGAAGGCATTTTGCAAGATGTTTCTTGTGACTTCGTAACATTAATCGTA 480
P E K V E G I L Q D V S C D F V T L I V

481 AAAGAAGAAATTATATTAATTGCAATAAAGCATATTTAAAAGTGTTAACTATAATGCTTTA 540
K E E I I L I A I K H I K S V N Y N A L

541 GCATGCGGAGAGAGTGATGAGAGCGACGATAGTAAGGAAAGTAGCGATAATTCAGGTCGT 600
A C G E S D E S D D S K E S S D N S G R

601 GCTCGTGCACAAAGACAATCAAGTAGAGGAAGATAATAAGAAAGGGGGATACGAAA**TTGG** 660
A R A Q R Q S S R G R * M E

cotB2

661 AGAATGTATTATGCTGTGACCAAATTAATGTTTGTGAGACTGTAAAAGTAAACC 720
N V L C C D Q I K C L V G E T V K V N L

721 TTCGTGGACCAGAAAGTCGAGTTGGTGTGAGCTCGTATCGTTAGGAAAAGATTATCTAACGT 780
R G P E S R V G E L V S L G K D Y L T L

781 TACAGTTACCTCATGGTGAATTAGTATATTATCAGTTGAAACATGTGAAGAGTCTAGTGA 840
Q L P H G E L V Y Y Q L K H V K S L V K

841 AGAAAGTGAAGAAAGTAAATGTGGCGATTGCTATAGTTTCATGTTTCTGCTCTGATGAGG 900
K V K E S K C G D C Y S S C F C S D E D

901 ATACTTTTTTAGATATATTTAAAAGACTTGAAGTATAAGTGGGTAAAAATTAATCGTGGCG 960
T F L D I L K D L K Y K W V K I N R G G

961 GTCCAGAGTGTGTGGAAGGTTTATTAAGTGAGGTACACCATGGCTGTATTACACTAGTAA 1020
P E C V E G L L S E V H H G C I T L V N

1021 ACGGTGATGAAGTTATTTATGTAATTAAGTCTCATATTAAGAGTGTGAGTCAAGTAGTTA 1080
G D E V I Y V I K S H I K S V S Q V V K

1081 AATGTAAAAAGAATGAAGATGAATAATGTTTAATAAATAAGAGGGGCATTATGAGGGAAA 1140
C K K N E D E *

Fig. S1. Nucleotide sequence of *cotB1B2* genes with its promoter region (retrieved from GenBank accession number AE016877.1; region 368,717–369,856). Consensus sequence of a putative σ^K -specific promoter is underlined, and the initiation codons of *cotB1* and *cotB2* are written in boldface type. The elements in the consensus sequence AC and CATA---TA correspond to the –35 and –10 regions of the promoter, respectively (1).

1. Eichenberger P, Fujita M, Jensen ST, Conlon EM, Rudner DZ, Wang ST, Ferguson C, Haga K, Sato T, Liu JS, Losick R. 2004. The program of gene transcription for a single differentiating cell type during sporulation in *Bacillus subtilis*. PLoS Biol 2:1664–1683.

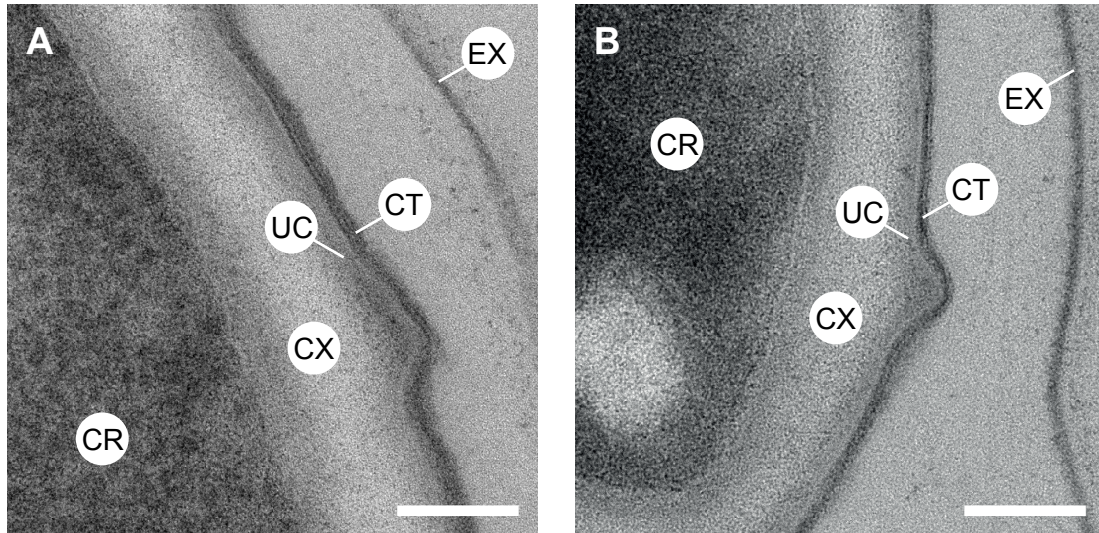


Fig. S2. Spore coat structures of the *B. cereus* wild type and $\Delta cotB1B2$ mutant. TEM images of ultrathin-sections of the wild-type spores (A) and $\Delta cotB1B2$ spores (B). Dark-staining spore coat (CT) and underlying undercoat (UC) are visible in both images. Scale bar, 100 nm. CR, core; CX, cortex; EX, exosporium.

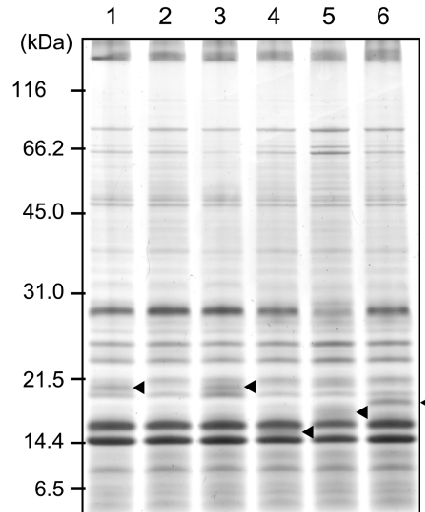


Fig. S3. SDS-PAGE analysis (12.5%) of the spore coat proteins of the *B. cereus* $\Delta cotB1B2$ mutant harboring plasmids encoding C-terminally truncated CotB1 proteins. Sporulation was induced in mR2A medium supplemented with $100 \mu\text{g ml}^{-1}$ silicate for 48 h. Lane 1, wild-type strain carrying pHT304; lanes 2–6, $\Delta cotB1B2$ carrying pHT304 (lane 2), pHT-cotB1 (lane 3), pHT-cotB1-141 (lane 4), pHT-cotB1-157 (lane 5), or pHT-cotB1-142/157 (lane 6). The arrowheads indicate the position of the expressed proteins.

Affinity purification of recombinant proteins using a novel silica-binding peptide as a fusion tag

Mohamed A. A. Abdelhamid · Kei Motomura ·
Takeshi Ikeda · Takenori Ishida · Ryuichi Hirota ·
Akio Kuroda

Received: 27 January 2014 / Revised: 2 April 2014 / Accepted: 4 April 2014 / Published online: 23 April 2014
© Springer-Verlag Berlin Heidelberg 2014

Abstract We recently reported that silica is deposited on the coat of *Bacillus cereus* spores as a layer of nanometer-sized particles (Hirota et al. 2010 J Bacteriol 192: 111-116). Gene disruption analysis revealed that the spore coat protein CotB1 mediates the accumulation of silica (our unpublished results). Here, we report that *B. cereus* CotB1 (171 amino acids [aa]) and its C-terminal 14-aa region (corresponding to residues 158-171, designated CotB1p) show strong affinity for silica particles, with dissociation constants at pH 8.0 of 2.09 and 1.24 nM, respectively. Using CotB1 and CotB1p as silica-binding tags, we developed a silica-based affinity purification method in which silica particles are used as an adsorbent for CotB1/CotB1p fusion proteins. Small ubiquitin-like modifier (SUMO) technology was employed to release the target proteins from the adsorbed fusion proteins. SUMO-protease-mediated site-specific cleavage at the C-terminus of the fused SUMO sequence released the tagless target proteins into the liquid phase while leaving the tag region still bound to the solid phase. Using the fluorescent protein mCherry as a model, our purification method achieved 85 % recovery, with a purity of 95 % and yields of 0.60 ± 0.06 and 1.13 ± 0.13 mg per 10-mL bacterial culture for the CotB1-SUMO-mCherry and CotB1p-SUMO-mCherry fusions, respectively. CotB1p, a short 14-aa peptide, which demonstrates high affinity for

silica, could be a promising fusion tag for both affinity purification and enzyme immobilization on silica supports.

Keywords Affinity purification · Fusion tag · Silica-binding peptide · Small ubiquitin-like modifier · *Bacillus cereus* · CotB1

Introduction

Affinity tags are highly efficient tools for protein purification. A variety of proteins, domains, and peptides have been used as affinity tags to facilitate the purification of proteins of interest from crude extracts (Arnau et al. 2006; Malhotra 2009; Terpe 2003; Waugh 2005). We previously reported a novel affinity purification method using a silica-binding tag designated “Si-tag” (Ikeda and Kuroda 2011; Taniguchi et al. 2007), with inexpensive commercial silica (SiO₂) particles serving as the specific adsorbent (Ikeda et al. 2010, 2011). The purity and yield achieved with this method are comparable to conventional affinity purification methods (Lichty et al. 2005) but at lower cost (Ikeda et al. 2010). Si-tag affinity purification can be used even under denaturing conditions (i.e., 8 M urea), enabling purification of inclusion body proteins (Ikeda et al. 2011). However, the large size of the Si-tag (273 amino acids [aa]) and high concentration of divalent cations (e.g., 2 M MgCl₂) required to elute Si-tagged fusion proteins may negatively affect the intrinsic properties and function of the fusion partner. Another potential disadvantage of the large protein affinity tag is that it wastes more metabolic energy during overproduction than small tags do (Malhotra 2009; Waugh 2005). These drawbacks motivated us to develop a method utilizing shorter silica-binding tags and milder elution conditions for silica-based affinity purification.

We recently reported that silica is deposited on the coat of *Bacillus cereus* spores as a layer of nanometer-sized particles

Mohamed A. A. Abdelhamid and Kei Motomura contributed equally to this work.

Electronic supplementary material The online version of this article (doi:10.1007/s00253-014-5754-z) contains supplementary material, which is available to authorized users.

M. A. A. Abdelhamid · K. Motomura · T. Ikeda (✉) · T. Ishida · R. Hirota · A. Kuroda

Department of Molecular Biotechnology, Graduate School of Advanced Sciences of Matter, Hiroshima University, 1-3-1 Kagamiyama, Higashi-Hiroshima, Hiroshima 739-8530, Japan
e-mail: ikedatakeshi@hiroshima-u.ac.jp

(Hirota et al. 2010). The spore coat is a proteinaceous shell composed of more than 50 proteins (Henriques and Moran 2007). Gene disruption analysis revealed that the spore coat protein CotB1 (171 aa) mediates the accumulation of silica (Motomura et al. in preparation). We also found that the C-terminal 14-aa region (corresponding to residues 158–171) is rich in positively charged and serine residues (five arginine and three serine residues). Such features are similar to those of the well-characterized silica-precipitating peptides (silaffins) isolated from diatoms (Pamirsky and Golokhvast 2013), suggesting that CotB1, particularly its C-terminal 14-aa region (designated CotB1p), interacts with silica surfaces (Motomura et al. in preparation).

In this report, we demonstrate that CotB1 binds strongly to silica surfaces. CotB1p also binds to silica surfaces, with affinity comparable to that of CotB1, suggesting that the C-terminal 14-aa region of CotB1 mediates silica binding. To develop a recombinant protein purification method using CotB1/CotB1p as silica-binding tags, we employed small ubiquitin-like modifier (SUMO) technology (Butt et al. 2005; Malakhov et al. 2004; Marblestone et al. 2006) to facilitate release of the target protein from the solid phase (Lee et al. 2008). The combination of silica-binding CotB1/CotB1p and SUMO-protease-mediated site-specific cleavage at the C-terminus of the fused SUMO sequence enables purification of tagless target proteins with high purity and yield.

Materials and methods

Materials

Silica particles (α -quartz) with a diameter of approximately 0.8 μm were purchased from Soekawa Chemical Co., Ltd. (Tokyo, Japan) and used without any pretreatment. SUMO protease (with an N-terminal His-tag) was purchased from LifeSensors, Inc. (Malvern, PA, USA). All chemicals used in this study were of analytical grade.

Construction of expression plasmids for GFP-CotB1 and GFP-CotB1p fusions

The DNA fragment encoding CotB1 was amplified by polymerase chain reaction (PCR) from *B. cereus* ATCC 14579 genomic DNA using the primers CotB1-F and CotB1-R (a list of the primers used in the study is shown in Table 1). The resulting PCR fragment was digested with *Hind*III and *Xho*I and then inserted into the *Hind*III-*Xho*I sites of pET-47b (Novagen/Merck KGaA, Darmstadt, Germany). The resulting plasmid was designated pET-CotB1. Subsequently, a green fluorescent protein (GFP)-encoding DNA fragment was amplified by PCR from pGFPuv (Clontech Laboratories, Inc., Mountain View, CA, USA) using the primers GFP-F and

Table 1 Primers used in this study

Name	DNA sequence (5' to 3') ^a	Restriction site
CotB1-F	GCCGCAAAGCTTGTGAGT TTATTCATTGTGAT	<i>Hind</i> III
CotB1-R	CCCCTCTCGAGTTATCTTC CTCTACTTGATTGTCT	<i>Xho</i> I
GFP-F	TAATAACCGCGGATATGA GTAAAGGAGAAGAAGCTT	<i>Sac</i> II
GFP-R	AGTATAGAATTCCGTTTGTA GAGCTCATCCATG	<i>Eco</i> RI
CotB1p-F	TCAGGTCGTGCTCGTGCACAA	
CotB1p-R	CGCCAAGGCCTGTACAGAATT	
GFP-CotB1-F	TAACTCGAGGCTTAATTAAC CTAGGCT	
GFP-CotB1-R	CGCCAAGGCCTGTACA GAATT	
mCherry-F	AAGGTCTCAAGGTATGGTGA GCAAGGGCGAGGA	<i>Bsa</i> I
mCherry-R	AAAGGTCTCTCTAGACTACTT GTACAGCTCGTCCA	<i>Bsa</i> I
mChe-SUMO-F	GGCAGTATGTCGGACT CAGAAATC	
mChe-SUMO-R	ACCGCCCATATGTATATCTC CTTCTTAAAG	

^a Restriction sites are underlined

GFP-R. The resulting PCR fragment was digested with *Sac*II and *Eco*RI and then cloned into the *Sac*II-*Eco*RI sites of pET-CotB1. The resulting plasmid was designated pET-GFP-CotB1.

Inverse PCR using the primers CotB1p-F and CotB1p-R with pET-GFP-CotB1 serving as the template and self-ligation of the resulting amplified DNA were employed to construct pET-GFP-CotB1p. Another round of inverse PCR was performed using the primers GFP-CotB1-F and GFP-CotB1-R, and the resulting amplified DNA was self-ligated to construct pET-GFP.

Expression and purification of GFP-CotB1 and GFP-CotB1p

The expression plasmids pET-GFP-CotB1, pET-GFP-CotB1p, and pET-GFP were introduced into *Escherichia coli* Rosetta(DE3)pLysS (Novagen/Merck KGaA). The transformants were grown at 37 °C in 2 \times YT medium (Green and Sambrook 2012) supplemented with 50 $\mu\text{g}/\text{mL}$ of kanamycin and 30 $\mu\text{g}/\text{mL}$ of chloramphenicol. When the culture reached an optical density at 600 nm of 0.5, 0.2 mM isopropyl- β -D-thiogalactopyranoside was added to the medium to induce expression of the recombinant proteins. After an additional 8 h of cultivation at 28 °C (for pET-GFP-CotB1) or 4 h at 37 °C (for pET-GFP-CotB1p and pET-GFP), the cells were harvested by centrifugation, and the resulting pellets were resuspended in 25 mM Tris-HCl buffer (pH 8.0) containing 20 % (v/v) glycerol. The

cells were then disrupted using lysozyme and sonication, followed by centrifugation to remove cell debris. The supernatants containing soluble recombinant proteins with an N-terminal His-tag were loaded onto a HisTrap FF column (GE Healthcare UK Ltd, Buckinghamshire, UK) equilibrated with 25 mM Tris-HCl buffer (pH 8.0) containing 20 % (v/v) glycerol. Proteins were eluted with a linear gradient from 0 to 0.5 M imidazole in the same buffer. Fractions containing the recombinant proteins were collected and then applied to a POROS HQ anion exchange column (Applied Biosystems/Life Technologies Corporation, Carlsbad, CA, USA) equilibrated with the same buffer. Proteins were eluted with a linear gradient from 0 to 1 M NaCl in the same buffer. Fractions containing the recombinant proteins were collected and dialyzed at 4 °C against 25 mM sodium phosphate buffer (pH 8.0).

Determination of the dissociation constants (K_d) values for GFP-CotB1 and GFP-CotB1p

Purified GFP-CotB1 and GFP-CotB1p were diluted to various concentrations (10–100 nM) in 1 mL of 25 mM sodium phosphate buffer (pH 8.0). The diluted protein solutions were then mixed with 10 μ L of 10 mg/mL silica particle suspension (corresponding to 0.1 mg dry weight of silica particles). After incubation for 15 min, the silica particles were removed by centrifugation at $5,000\times g$ for 2 min. The amount of each fusion protein bound to the silica particles was determined by subtracting the fluorescence intensity associated with the GFP remaining in the supernatant from the initial fluorescence intensity. The resulting data were fitted to the Langmuir isotherm to determine the K_d value.

Construction of expression plasmids for CotB1-SUMO-mCherry (CotB1-SC) and CotB1p-SUMO-mCherry (CotB1p-SC) fusions

In order to construct fusion proteins consisting of CotB1 (or CotB1p), SUMO, and a protein of interest, we first constructed plasmids carrying the gene encoding either the CotB1-SUMO or CotB1p-SUMO fusion followed by two *Bsa*I sites for cloning the protein of interest (Panavas et al. 2009). The amino acid sequence of either CotB1 or CotB1p was fused with that of SUMO (*Saccharomyces cerevisiae* Smt3p; accession number NP_010798), in that order, with an intervening GGS linker. The nucleotide sequences of the CotB1-SUMO and CotB1p-SUMO fusion genes were designed in order to optimize codon usage for translation in *E. coli*. The *Bsa*I cloning sites and adjacent sequences, which were described by Panavas et al. (2009), were added downstream of the fusion gene so that the protein of interest could be fused directionally to the C-terminus of SUMO without any additional sequence. Because SUMO protease selectively cleaves the polypeptide

chain at the Gly-Gly motif located at the C-terminal end of the SUMO sequence in the resulting fusion protein, the desired protein with an authentic N-terminus would be released when the gene of interest is appropriately cloned downstream of the SUMO gene (Malakhov et al. 2004). In addition, an *Nde*I site was added at the ATG start codon of the fusion gene, and a *Bam*HI site was added downstream of the *Bsa*I sites. The two designed DNA fragments (nucleotide sequences are shown in Figs. S1 and S2, which are available as electronic supplementary material) were synthesized by BEX Co., Ltd. (Tokyo, Japan) and cloned into the *Nde*I-*Bam*HI sites of pET-24b (Novagen/Merck KGaA). The resulting plasmids were designated pET-CotB1-SUMO (carrying the CotB1-SUMO fusion gene) and pET-CotB1p-SUMO (carrying the CotB1p-SUMO fusion gene).

The gene encoding the fluorescent protein mCherry (Shaner et al. 2004) was amplified by PCR from pmCherry (Clontech Laboratories, Inc.) using the primers mCherry-F and mCherry-R (Table 1). The amplified fragment was digested with *Bsa*I and cloned into the *Bsa*I-digested pET-CotB1-SUMO and pET-CotB1p-SUMO plasmids to construct pET-CotB1-SC and pET-CotB1p-SC, respectively.

Inverse PCR using the primers mChe-SUMO-F and mChe-SUMO-R with pET-CotB1-SC serving as the template and self-ligation of the resulting amplified DNA were employed to construct pET-SUMO-mCherry.

Expression of CotB1-SC and CotB1p-SC

The expression plasmids pET-CotB1-SC, pET-CotB1p-SC, and pET-SUMO-mCherry were introduced into *E. coli* Rosetta(DE3)pLysS, and the transformants were grown in $2\times$ YT medium as described above. When the culture reached an optical density at 600 nm of 0.5, 0.2 mM isopropyl- β -D-thiogalactopyranoside was added to the medium to induce protein expression. After an additional 8 h of cultivation at 28 °C (for pET-CotB1-SC) or 4 h at 37 °C (for pET-CotB1p-SC and pET-SUMO-mCherry), the cells were harvested by centrifugation, and the pellets were stored at -80 °C until use.

Optimization of silica-binding conditions

The CotB1-SC and CotB1p-SC fusion proteins were expressed in *E. coli* Rosetta(DE3)pLysS harboring either pET-CotB1-SC or pET-CotB1p-SC, respectively, as described above. Cell pellets harvested from 1-mL cultures (typically 10 mg wet weight of cells) were suspended in 0.5 mL of 25 mM Tris-HCl buffer at various pHs (pH 7.0–9.0) or 25 mM sodium phosphate buffer (pH 6.0–8.0) and disrupted by sonication. After centrifugation at $20,000\times g$ for 30 min, the supernatants (cleared cell lysates) containing the recombinant proteins were mixed with 0.5 mL of silica-particle suspension in the same buffer (final silica concentration of 25 mg

dry weight/mL) for 15 min at room temperature. Silica particles with bound protein were collected by centrifugation at $5,000\times g$ for 2 min and then washed three times with 1 mL of the same suspension buffer. After the supernatant was carefully removed, proteins still bound to the particles were released by boiling in Laemmli sample buffer (Laemmli 1970) for 5 min and analyzed by sodium dodecyl sulfate-polyacrylamide gel electrophoresis (SDS-PAGE; 15 %). Gels were stained with Coomassie brilliant blue (CBB) R-250, and the target protein was quantified by densitometric analysis using ImageJ software, version 1.41 (Schneider et al. 2012).

Similar experiments were conducted in 25 mM Tris-HCl buffer (pH 8.0) with varying concentrations of silica (0–30 mg dry weight/mL) and nonionic detergent (0–1.5 % [v/v] Tween 20 or Triton X-100) for varying periods of incubation time (1–30 min).

Affinity purification of mCherry using CotB1/CotB1p as a silica-binding tag

Cell pellets harvested from 10-mL cultures were resuspended in 2 mL of 25 mM Tris-HCl buffer (pH 8.0) and disrupted by sonication. After centrifugation at $20,000\times g$ for 30 min, the cleared cell lysates were mixed with 250 mg dry weight of silica particles by gentle rotation for 15 min at room temperature. After centrifugation at $5,000\times g$ for 2 min, the particles were washed three times with 25 mM Tris-HCl buffer (pH 8.0) containing 150 mM NaCl and then resuspended in 2 mL of the same buffer. SUMO protease (80 units) was then added to the suspension. After 3-h incubation at room temperature, the suspension was centrifuged at $5,000\times g$ for 2 min. The resulting supernatants containing the cleaved mCherry protein were collected and analyzed by SDS-PAGE. The protein concentration was determined using the Bradford method (Bradford 1976) with bovine serum albumin as the standard.

Nucleotide sequence data

The nucleotide sequences of the CotB1-SUMO and CotB1p-SUMO fusions are available in the DDBJ/EMBL/GenBank databases under the accession numbers AB904509 and AB904510, respectively.

Results

Binding of GFP-CotB1 and GFP-CotB1p to silica particles

To test whether CotB1 and its C-terminal 14-aa peptide CotB1p bind to silica surfaces, we constructed the respective GFP fusion proteins (Fig. 1). Cleared lysates of recombinant

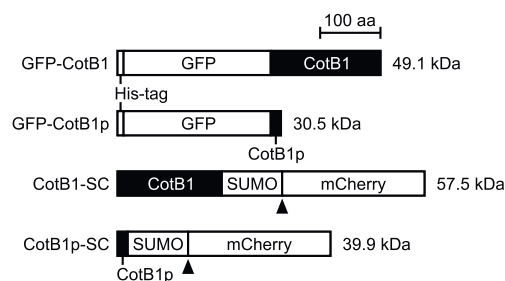


Fig. 1 Schematic representation of the structures of the CotB1/CotB1p fusion proteins constructed in this study. *Arrowheads* indicate SUMO protease cleavage sites

E. coli cells expressing GFP-CotB1, GFP-CotB1p, or GFP as a control were mixed with silica particles for 15 min at room temperature. Silica particles with bound protein were collected by centrifugation and washed three times with 25 mM Tris-HCl buffer (pH 8.0) containing 0.5 % (v/v) Tween 20. Proteins remaining bound to the particles were released by boiling in Laemmli sample buffer (Laemmli 1970) and then analyzed by SDS-PAGE. Densitometric analysis of the CBB-stained gel showed that 65 % of the GFP-CotB1 and 60 % of the GFP-CotB1p fusion proteins bound to the silica particles, whereas GFP alone did not bind to silica particles under the experimental conditions used (data not shown). These results clearly indicate that both CotB1 and CotB1p function as silica-binding fusion tags.

We then evaluated the silica-binding affinity of GFP-CotB1 and GFP-CotB1p. Adsorption data for the purified proteins mixed with silica particles were fitted to the Langmuir isotherm (Fig. 2). The silica-binding K_d values for GFP-CotB1 and GFP-CotB1p were 2.09 and 1.24 nM, respectively. The maximum amount of GFP-CotB1 and GFP-CotB1p bound was 44.6 and 25.1 $\mu\text{g}/\text{mg}$ dry weight of silica particles (corresponding to 0.91 and 0.82 nmol/mg of silica), respectively.

Optimization of silica-binding conditions

In the strategy we adopted for development of a silica-based affinity purification method using CotB1/CotB1p, silica

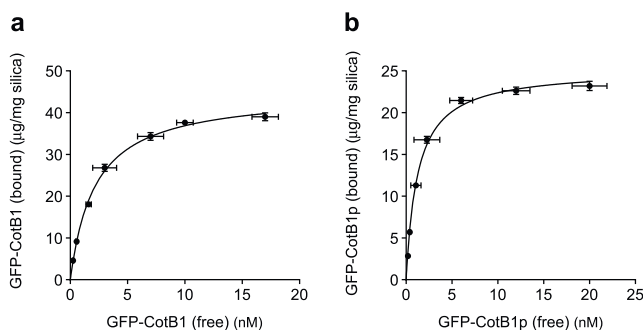


Fig. 2 Binding of GFP-CotB1 (**a**) and GFP-CotB1p (**b**) to silica particles. Data were fitted to the Langmuir isotherm (solid line) to determine the K_d value

particles were used as an adsorbent for the CotB1/CotB1p fusion proteins. To release the target protein from the adsorbed fusion proteins using this approach, we introduced a protease recognition site between the N-terminal CotB1/CotB1p tag and the C-terminal target protein. Addition of the appropriate protease would then result in cleavage of the silica-bound fusion protein and release of the tagless target protein into the liquid phase, with the tag region remaining bound to the solid phase. In the following experiments, we used CotB1/CotB1p, SUMO, and mCherry fusion proteins (designated CotB1-SC and CotB1p-SC; Fig. 1) as models to evaluate the affinity purification method. The fluorescent protein mCherry was selected as the model target protein, and SUMO, the C-terminal end of which is selectively cleaved by SUMO protease, was introduced as the protease recognition site.

To maximize the yield of our affinity purification method, we determined the optimal silica-binding conditions for CotB1/CotB1p fusion proteins using cleared lysates of recombinant *E. coli* cells expressing CotB1-SC or CotB1p-SC. Lysates of cell pellets harvested from 1-mL cultures (typically 10 mg wet weight of cells) were mixed with silica particles in a total volume of 1 mL, and the amount of protein bound to the silica particles was determined by SDS-PAGE as described in the “Materials and methods” section.

We first determined the optimal pH for silica binding, examining the pH range 6.0–9.0. Both the CotB1 and CotB1p fusion proteins bound to silica over a wide pH range, with slightly different optimal pH values (Fig. 3a). In contrast, SUMO-mCherry (without CotB1 nor CotB1p) did not bind to silica particles at any pH examined (data not shown), confirming that CotB1 (particularly the C-terminal CotB1p region) mediates silica binding. Because over 90 % of both CotB1-SC and CotB1p-SC bound to silica at pH 8.0, the following experiments were performed in 25 mM Tris-HCl buffer at pH 8.0.

Next, we determined the optimal silica concentration. The amount of the bound protein increased proportionally to the amount of silica particles added, reaching a plateau of >90 % binding of the fusion proteins with addition of >25 mg dry weight of silica particles in the 1-mL cleared lysate solution typically containing 10 mg wet weight of cells (Fig. 3b). At a silica concentration of 25 mg dry weight/mL, approximately 85 % of both fusion proteins adsorbed to the silica particles during the first minute of the incubation, and the amount of protein adsorbed reached a plateau within 15 min (Fig. 3c).

Finally, we investigated the effect of adding detergent to the binding buffer because nonionic detergents (e.g., Tween 20 and Triton X-100) have been used in other studies to reduce nonspecific binding of host proteins to silica surfaces (Bolivar and Nidetzky 2012; Castelletti et al. 2000). Although we also found that addition of Tween 20 or Triton X-100 did reduce the degree of nonspecific binding of host proteins to the silica particles (data not shown), these detergents also reduced the

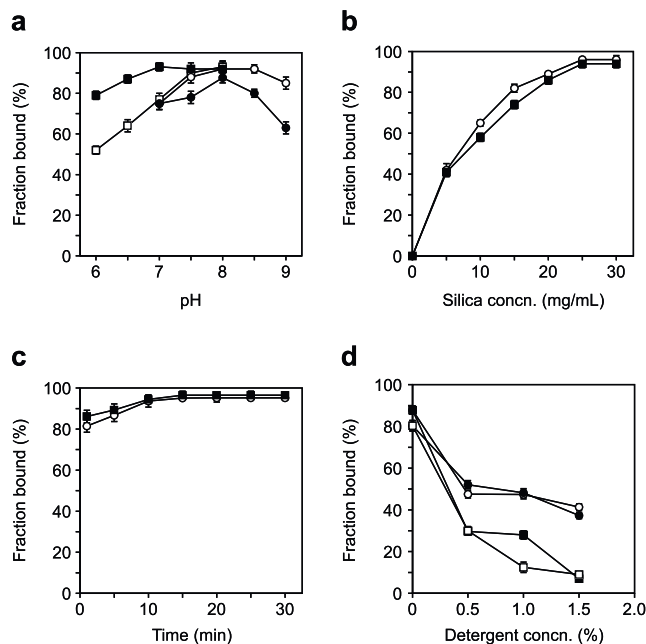


Fig. 3 Effect of buffer conditions and incubation time on silica binding of CotB1-SC and CotB1p-SC. **a** Effect of pH. *Open circles and squares* CotB1-SC in 25 mM Tris-HCl buffer and CotB1-SC in 25 mM phosphate buffer, respectively. *Closed circles and squares* CotB1p-SC in 25 mM Tris-HCl buffer and CotB1p-SC in 25 mM phosphate buffer, respectively. **b** Effect of silica concentration. *Circles* CotB1-SC, *squares* CotB1p-SC. **c** Effect of incubation time. *Circles* CotB1-SC, *squares* CotB1p-SC. **d** Effect of nonionic detergents. *Open circles and squares* CotB1-SC with Tween 20 and Triton X-100, respectively. *Closed circles and squares* CotB1p-SC with Tween 20 and Triton X-100, respectively

binding of CotB1-SC and CotB1p-SC (Fig. 3d). Therefore, no detergents were added to the binding buffer in the subsequent experiments.

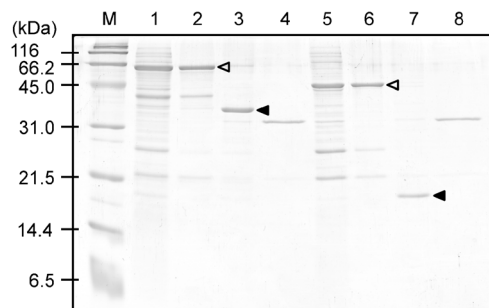


Fig. 4 SDS-PAGE analysis (15 %) of the affinity purification of mCherry using silica particles as an adsorbent. CotB1 (lanes 1–4) or CotB1p (lanes 5–8) was used as a silica-binding tag. Lanes 1 and 5 cell lysate, lanes 2 and 6 silica-bound fraction, lanes 3 and 7 silica-bound fraction after SUMO protease treatment, lanes 4 and 8 proteins released from solid phase after SUMO protease treatment, lane M molecular mass markers. For lanes 2, 3, 6, and 7, proteins bound to silica particles were released by boiling in Laemmli sample buffer (Laemmli 1970). Proteins were stained with CBB R-250. *Open arrowheads* indicate the expressed CotB1-SC and CotB1p-SC fusion proteins. *Closed arrowheads* indicate the CotB1-SUMO and CotB1p-SUMO fragments after SUMO protease treatment

Table 2 Purification of mCherry from *E. coli* using CotB1 as a silica-binding tag^a

Step	Total protein (mg)	Fusion protein (mg) ^b	Target protein (mg)	Purity (%) ^b	Purification (-fold)	Yield (%)
Cell lysate	9.28	1.42	(0.66) ^c	15	1.0	100 ^{b,c}
Silica-binding fraction	4.50	1.35	(0.63) ^c	30	2.0	95 ^{b,c}
SUMO protease elution	0.60	ND	0.56 ^b	93	6.2	84 ^b

ND not detected

^a Starting material was approximately 0.1 g wet weight of cells

^b Determined by densitometric analysis of SDS-PAGE protein bands

^c Calculated by multiplying the amount of fusion protein by the ratio of the molecular mass of mCherry (26.7 kDa) to the molecular mass of the fusion protein (57.5 kDa)

Affinity purification of mCherry using CotB1/CotB1p as silica-binding tags

Using the optimized conditions described above, CotB1-SC (57.5 kDa) and CotB1p-SC (39.9 kDa) were isolated from cleared cell lysates by immobilization on silica particles and analyzed by SDS-PAGE (Fig. 4, lanes 2 and 6, open arrowheads). Some host proteins also adsorbed onto and remained adsorbed to the silica particles even after washing. To recover the tagless mCherry protein from the bound fusion proteins, we added SUMO protease to the suspension of CotB1-SC- or CotB1p-SC-bound silica particles. SDS-PAGE analysis revealed that most of each of the recombinant proteins was cleaved after 3 h of incubation and that the CotB1-SUMO and CotB1p-SUMO fragments (30.8 and 13.2 kDa, respectively) remained bound to the silica particles (Fig. 4, lanes 3 and 7, closed arrowheads). The mCherry fragment (26.7 kDa) was released into the supernatant (Fig. 4, lanes 4 and 8). Because we used much less SUMO protease compared with the recombinant proteins (less than 0.1 % [w/w]), the SUMO protease band (~26 kDa) was not visible on SDS-PAGE (Fig. 4, lanes 4 and 8). The discrepancies between the calculated molecular masses and pattern of band migration on the gel could be ascribed to aberrant migration of the SUMO band (Marblestone et al. 2006) as well as the mCherry band (the mCherry parental protein mRFP1 [25.4 kDa] migrates as a

>30-kDa band on SDS-PAGE [Campbell et al. 2002]). Densitometric analysis of the CBB-stained protein bands showed that the purity of the released tagless mCherry was approximately 95 %.

Typical results for the affinity purification of mCherry using the CotB1-SC and CotB1p-SC fusion proteins are summarized in Tables 2 and 3, respectively. The mCherry recovery rate was approximately 85 %, with yields of 0.60±0.06 and 1.13±0.13 mg (mean ± standard deviation from three independent experiments) per 10-mL culture for CotB1-SC and CotB1p-SC, respectively. The 2-fold higher yield obtained with CotB1p-SC compared to CotB1-SC was due to higher expression of CotB1p-SC in *E. coli* (Tables 2 and 3).

Discussion

In this study, we found that the *B. cereus* spore coat protein CotB1 and its C-terminal 14-aa peptide CotB1p bind to silica surfaces. We demonstrated that both proteins function as silica-binding tags when fused to other proteins at either the N- or C-terminus. The resulting fusion proteins can be easily immobilized on silica surfaces by mixing the proteins in a solution with silica materials.

Our results strongly suggest that the 14-aa CotB1p region of CotB1 plays a crucial role in binding to silica because both

Table 3 Purification of mCherry from *E. coli* using CotB1p as a silica-binding tag^a

Step	Total protein (mg)	Fusion protein (mg) ^b	Target protein (mg)	Purity (%) ^b	Purification (-fold)	Yield (%)
Cell lysate	8.54	1.90	(1.27) ^c	22	1.0	100 ^{b,c}
Silica-binding fraction	5.56	1.68	(1.13) ^c	30	1.4	89 ^{b,c}
SUMO protease elution	1.13	ND	1.09	95	4.3	85 ^b

ND not detected

^a Starting material was approximately 0.1 g wet weight of cells

^b Determined by densitometric analysis of SDS-PAGE protein bands

^c Calculated by multiplying the amount of fusion protein by the ratio of the molecular mass of mCherry (26.7 kDa) to the molecular mass of the fusion protein (39.9 kDa)

CotB1p and full-length CotB1 showed comparable affinity for silica (Fig. 2). The amino acid sequence of CotB1p (SGRA RAQRQSSRGR) is rich in positively charged arginine residues. CotB1p therefore has a high net positive charge, with a theoretical isoelectric point of 12.6. In contrast, the surface of silica is negatively charged under either neutral or basic conditions (Iler 1979), suggesting that electrostatic attraction is a major driving force behind the binding of CotB1p (and also CotB1) to silica. This is also supported by the fact that the binding of CotB1p was inhibited at high ionic strength; in the presence of 1.0 M NaCl, only 15 % of CotB1p-SC bound to the silica particles (data not shown). Although the CotB1/CotB1p fusion proteins constructed in this study have a net negative charge, with theoretical isoelectric points of 5.3–6.8, these proteins bound to silica surfaces via CotB1/CotB1p. These results suggest that the positive charges in the CotB1p region of the fusion protein are capable of interacting with the negatively charged silica surface even though the net charge of the overall protein molecule is negative.

Although both CotB1 and CotB1p bind to silica, we believe that the latter is a more promising silica-binding tag because of its small size. The CotB1p fusion protein was expressed more efficiently in *E. coli* than was the CotB1 fusion protein (Tables 2 and 3). In addition, the CotB1 fusion proteins (i.e., GFP-CotB1 and CotB1-SC) tended to form insoluble inclusion bodies in *E. coli* when expressed at 37 °C, whereas both the CotB1p fusions (i.e., GFP-CotB1p and CotB1p-SC) and tagless proteins (i.e., GFP and SUMO-mCherry) were expressed in the soluble form in *E. coli* at 37 °C (data not shown). These differences could be attributed to the larger molecular mass of CotB1, as increasing molecular mass tends to negatively affect the expression of fusion proteins.

To use the CotB1/CotB1p tags for silica-based affinity purification of target proteins, we employed SUMO technology to cleave the target protein from the silica-bound fusion protein. Using mCherry as a model target protein, we demonstrated that our novel affinity purification method is highly efficient. The purity and yield obtained using our method are as high as the values reported by Lichty et al. (2005) for conventional affinity tags. One of the advantages of our method is that it enables the removal of the affinity tag and recovery of a tagless target protein with an authentic N-terminus. Fused affinity tags that remain after purification may affect the intrinsic activity of the target protein and/or interfere with downstream analyses, such as determination of protein structure. The presence of a tag on a target protein is particularly unsuitable for therapeutic applications. Therefore, many approaches (most of which involve protease cleavage at the junction) have been developed to remove affinity tags from recombinant proteins (Arnau et al. 2006; Waugh 2011). However, the endoproteases that are commonly employed in these approaches have several disadvantages, for example,

nonspecific cleavage of the target protein at locations other than the designed site and/or retention of nonnative amino acid(s) in the sequence of the protein of interest (Arnau et al. 2006; Jenny et al. 2003; Waugh 2011). In contrast to commonly used endoproteases, which recognize short, linear sequences (generally 4–8 aa), SUMO protease specifically recognizes the tertiary structure of SUMO and cleaves the polypeptide chain at the C-terminal end of the SUMO sequence, enabling the release of peptides or proteins with any desired N-terminal residue except proline (Malakhov et al. 2004). Therefore, our affinity purification method can be used to recover a wide variety of tagless proteins at high purity. Another advantage of our method is that protein elution does not require the addition of any harsh chemicals that could adversely affect protein activity.

Although the amount of SUMO protease used in this study for the release of the target protein was much less than the amount of the recombinant proteins used (see the “Results” section), further purification of the eluted, cleaved target protein necessitates removal of the SUMO protease from the solution. Because most commercially available SUMO proteases contain a His-tag, they can be easily removed by immobilized metal ion affinity chromatography (Panavas et al. 2009). Albeit beyond the scope of this study, construction of CotB1/CotB1p-fused SUMO proteases might also be useful because these proteins would be retained on silica surfaces along with the CotB1/CotB1p-SUMO fragments after cleavage of the fusion protein.

Because of its small size and high affinity for silica, the CotB1p tag should be a powerful tool not only for the affinity purification application reported in this paper but also for enzyme immobilization on silica supports and for developing silicon-based biomaterials, as has been reported for other silica-binding peptides and proteins (Bolivar and Nidetzky 2012; Choi et al. 2011; Fukuyama et al. 2010, 2011; Hnilova et al. 2012; Pamirsky and Golokhvast 2013; Yamatogi et al. 2009). We are currently developing silicon-based biomaterials using this promising tag as an interface.

Acknowledgments This work was supported in part by the Grant-in-Aid for Young Scientists (A) from the Japan Society for the Promotion of Science (No. 25712009 to T. Ikeda), the Industrial Technology Research Grant Program in 2009 from the New Energy and Industrial Technology Development Organization (NEDO) of Japan (No. 09C46130a to T. Ikeda), and a research grant from the Institute for Fermentation, Osaka (to T. Ikeda).

References

- Arnau J, Lauritzen C, Petersen GE, Pedersen J (2006) Current strategies for the use of affinity tags and tag removal for the purification of recombinant proteins. *Protein Expr Purif* 48:1–13. doi:10.1016/j.pep.2005.12.002

- Bolivar JM, Nidetzky B (2012) Positively charged mini-protein Z_{basic2} as a highly efficient silica binding module: Opportunities for enzyme immobilization on unmodified silica supports. *Langmuir* 28:10040–10049. doi:10.1021/la3012348
- Bradford MM (1976) A rapid and sensitive method for quantitation of microgram quantities of protein utilizing principle of protein-dye binding. *Anal Biochem* 72:248–254. doi:10.1016/0003-2697(76)90527-3
- Butt TR, Edavettal SC, Hall JP, Mattem MR (2005) SUMO fusion technology for difficult-to-express proteins. *Protein Expr Purif* 43:1–9. doi:10.1016/j.pep.2005.03.016
- Campbell RE, Tour O, Palmer AE, Steinbach PA, Baird GS, Zacharias DA, Tsien RY (2002) A monomeric red fluorescent protein. *Proc Natl Acad Sci U S A* 99:7877–7882. doi:10.1073/pnas.082243699
- Castelletti L, Verzola B, Gelfi C, Stoyanov A, Righetti PG (2000) Quantitative studies on the adsorption of proteins to the bare silica wall in capillary electrophoresis III: effects of adsorbed surfactants on quenching the interaction. *J Chromatogr A* 894:281–289. doi:10.1016/S0021-9673(00)00664-6
- Choi O, Kim B-C, An J-H, Min K, Kim YH, Um Y, Oh M-K, Sang B-I (2011) A biosensor based on the self-entrapment of glucose oxidase within biomimetic silica nanoparticles induced by a fusion enzyme. *Enzyme Microb Technol* 49:441–445. doi:10.1016/j.enzmictec.2011.07.005
- Fukuyama M, Yamatogi S, Ding H, Nishida M, Kawamoto C, Amemiya Y, Ikeda T, Noda T, Kawamoto S, Ono K, Kuroda A, Yokoyama S (2010) Selective detection of antigen-antibody reaction using Si ring optical resonators. *Jpn J Appl Phys* 49:04DL09. doi:10.1143/JJAP.49.04DL09
- Fukuyama M, Nishida M, Abe Y, Amemiya Y, Ikeda T, Kuroda A, Yokoyama S (2011) Detection of antigen-antibody reaction using Si ring optical resonators functionalized with an immobilized antibody-binding protein. *Jpn J Appl Phys* 50:04DL07. doi:10.1143/JJAP.50.04DL07
- Green MR, Sambrook J (2012) *Molecular cloning: a laboratory manual*, 4th edn. Cold Spring Harbor Laboratory Press, New York
- Henriques AO, Moran CP Jr (2007) Structure, assembly, and function of the spore surface layers. *Annu Rev Microbiol* 61:555–588. doi:10.1146/annurev.micro.61.080706.093224
- Hirota R, Hata Y, Ikeda T, Ishida T, Kuroda A (2010) The silicon layer supports acid resistance of *Bacillus cereus* spores. *J Bacteriol* 192:111–116. doi:10.1128/JB.00954-09
- Hnilova M, Khatayevich D, Carlson A, Oren EE, Gresswell C, Zheng S, Ohuchi F, Sarikaya M, Tamerler C (2012) Single-step fabrication of patterned gold film array by an engineered multi-functional peptide. *J Colloid Interface Sci* 365:97–102. doi:10.1016/j.jcis.2011.09.006
- Ikeda T, Kuroda A (2011) Why does the silica-binding protein “Si-tag” bind strongly to silica surfaces? Implications of conformational adaptation of the intrinsically disordered polypeptide to solid surfaces. *Colloids Surf B: Biointerfaces* 86:359–363. doi:10.1016/j.colsurfb.2011.04.020
- Ikeda T, Ninomiya K, Hirota R, Kuroda A (2010) Single-step affinity purification of recombinant proteins using the silica-binding Si-tag as a fusion partner. *Protein Expr Purif* 71:91–95. doi:10.1016/j.pep.2009.12.009
- Ikeda T, Motomura K, Agou Y, Ishida T, Hirota R, Kuroda A (2011) The silica-binding Si-tag functions as an affinity tag even under denaturing conditions. *Protein Expr Purif* 77:173–177. doi:10.1016/j.pep.2011.01.012
- Iler RK (1979) *The chemistry of silica*. Wiley, Inc., New York
- Jenny RJ, Mann KG, Lundblad RL (2003) A critical review of the methods for cleavage of fusion proteins with thrombin and factor Xa. *Protein Expr Purif* 31:1–11. doi:10.1016/S1046-5928(03)00168-2
- Laemmli UK (1970) Cleavage of structural proteins during the assembly of the head of bacteriophage T4. *Nature* 227:680–685. doi:10.1038/227680a0
- Lee C-D, Sun H-C, Hu S-M, Chiu C-F, Homhuan A, Liang S-M, Leng C-H, Wang T-F (2008) An improved SUMO fusion protein system for effective production of native proteins. *Protein Sci* 17:1241–1248. doi:10.1110/ps.035188.108
- Lichty JJ, Malecki JL, Agnew HD, Michelson-Horowitz DJ, Tan S (2005) Comparison of affinity tags for protein purification. *Protein Expr Purif* 41:98–105. doi:10.1016/j.pep.2005.01.019
- Malakhov MP, Mattem MR, Malakhova OA, Drinker M, Weeks SD, Butt TR (2004) SUMO fusions and SUMO-specific protease for efficient expression and purification of proteins. *J Struct Funct Genomics* 5:75–86. doi:10.1023/B:JSFG.0000029237.70316.52
- Malhotra A (2009) Tagging for protein expression. *Methods Enzymol* 463:239–258. doi:10.1016/S0076-6879(09)63016-0
- Marblestone JG, Edavettal SC, Lim Y, Lim P, Zuo X, Butt TR (2006) Comparison of SUMO fusion technology with traditional gene fusion systems: enhanced expression and solubility with SUMO. *Protein Sci* 15:182–189. doi:10.1110/ps.051812706
- Pamirsky IE, Golokhvast KS (2013) Silaffins of diatoms: from applied biotechnology to biomedicine. *Mar Drugs* 11:3155–3167. doi:10.3390/md11093155
- Panavas T, Sanders C, Butt TR (2009) SUMO fusion technology for enhanced protein production in prokaryotic and eukaryotic expression systems. In: Ulrich HD (ed) *Methods in molecular biology: SUMO protocols*. Humana Press, New York, pp 303–317
- Schneider CA, Rasband WS, Eliceiri KW (2012) NIH Image to ImageJ: 25 years of image analysis. *Nat Methods* 9:671–675. doi:10.1038/nmeth.2089
- Shaner NC, Campbell RE, Steinbach PA, Giepmans BNG, Palmer AE, Tsien RY (2004) Improved monomeric red, orange and yellow fluorescent proteins derived from *Discosoma* sp. red fluorescent protein. *Nat Biotechnol* 22:1567–1572. doi:10.1038/nbt1037
- Taniguchi K, Nomura K, Hata Y, Nishimura T, Asami Y, Kuroda A (2007) The Si-tag for immobilizing proteins on a silica surface. *Biotechnol Bioeng* 96:1023–1029. doi:10.1002/bit.21208
- Terpe K (2003) Overview of tag protein fusions: from molecular and biochemical fundamentals to commercial systems. *Appl Microbiol Biotechnol* 60:523–533. doi:10.1007/s00253-002-1158-6
- Waugh DS (2005) Making the most of affinity tags. *Trends Biotechnol* 23:316–320. doi:10.1016/j.tibtech.2005.03.012
- Waugh DS (2011) An overview of enzymatic reagents for the removal of affinity tags. *Protein Expr Purif* 80:283–293. doi:10.1016/j.pep.2011.08.005
- Yamatogi S, Amemiya Y, Ikeda T, Kuroda A, Yokoyama S (2009) Si ring optical resonators for integrated on-chip biosensing. *Jpn J Appl Phys* 48:04C188. doi:10.1143/JJAP.48.04C188

Article title

Affinity purification of recombinant proteins using a novel silica-binding peptide as a fusion tag

Journal name

Applied Microbiology and Biotechnology

Authors names

Mohamed A. A. Abdelhamid, Kei Motomura, Takeshi Ikeda, Takenori Ishida, Ryuichi Hirota, and Akio Kuroda

Corresponding author

Takeshi Ikeda

Department of Molecular Biotechnology, Graduate School of Advanced Sciences of Matter, Hiroshima University, 1-3-1 Kagamiyama, Higashi-Hiroshima, Hiroshima 739-8530, Japan

e-mail: ikedatakeshi@hiroshima-u.ac.jp

Supplementary Material

Fig. S1 Nucleotide and amino acid sequences of the CotB1-SUMO fusion

Fig. S2 Nucleotide and amino acid sequences of the CotB1p-SUMO fusion

